NOTE TO USERS

This reproduction is the best copy available.

UMI®

uOttawa

L'Université canadienne
Canada's university

FACULTÉ DES ÉTUDES SUPÉRIEURES ET POSTOCTORALES

u Ottawa

L'Université canadienne
Canada's university

FACULTY OF GRADUATE AND POSDOCTORAL STUDIES

Lisa Anne Vandermeer
AUTEUR DE LA THÈSE / AUTHOR OF THESIS

M.Sc. (Cellular and Molecular Medicine)
GRADE / DEGREE

Department of Cellular and Molecular Medicine
FACULTÉ, ÉCOLE, DÉPARTEMENT / FACULTY, SCHOOL, DEPARTMENT

Evaluation of *c-KIT* in Ovarian Surface Epithelial Cells and Ovarian Tumours

TITRE DE LA THÈSE / TITLE OF THESIS

D. Vanderhyden
DIRECTEUR (DIRECTRICE) DE LA THÈSE / THESIS SUPERVISOR

CO-DIRECTEUR (CO-DIRECTRICE) DE LA THÈSE / THESIS CO-SUPERVISOR

EXAMINATEURS (EXAMINATRICES) DE LA THÈSE / THESIS EXAMINERS

C. Addison

K. Turksen

Gary W. Slater
LE DOYEN DE LA FACULTÉ DES ÉTUDES SUPÉRIEURES ET POSTDOCTORALES /
DEAN OF THE FACULTY OF GRADUATE AND POSTDOCORAL STUDIES

EVALUATION OF *c-KIT* IN OVARIAN SURFACE EPITHELIAL CELLS AND OVARIAN TUMOURS

By

Lisa Anne Vandermeer

Thesis submitted to the Faculty of Graduate and Postdoctoral Studies at the University of Ottawa in partial fulfillment for the requirements for the degree of

Master of Science (Cellular and Molecular Medicine)

Department of Cellular and Molecular Medicine
Faculty of Medicine
Ottawa, Canada

January 2005

© Lisa Vandermeer, Ottawa, Canada, 2005

Library and Archives Canada

Published Heritage Branch

395 Wellington Street
Ottawa ON K1A 0N4
Canada

Bibliothèque et Archives Canada

Direction du Patrimoine de l'édition

395, rue Wellington
Ottawa ON K1A 0N4
Canada

Your file Votre référence
ISBN: 0-494-11440-1
Our file Notre référence
ISBN: 0-494-11440-1

NOTICE:
The author has granted a non-exclusive license allowing Library and Archives Canada to reproduce, publish, archive, preserve, conserve, communicate to the public by telecommunication or on the Internet, loan, distribute and sell theses worldwide, for commercial or non-commercial purposes, in microform, paper, electronic and/or any other formats.

The author retains copyright ownership and moral rights in this thesis. Neither the thesis nor substantial extracts from it may be printed or otherwise reproduced without the author's permission.

AVIS:
L'auteur a accordé une licence non exclusive permettant à la Bibliothèque et Archives Canada de reproduire, publier, archiver, sauvegarder, conserver, transmettre au public par télécommunication ou par l'Internet, prêter, distribuer et vendre des thèses partout dans le monde, à des fins commerciales ou autres, sur support microforme, papier, électronique et/ou autres formats.

L'auteur conserve la propriété du droit d'auteur et des droits moraux qui protège cette thèse. Ni la thèse ni des extraits substantiels de celle-ci ne doivent être imprimés ou autrement reproduits sans son autorisation.

In compliance with the Canadian Privacy Act some supporting forms may have been removed from this thesis.

While these forms may be included in the document page count, their removal does not represent any loss of content from the thesis.

Conformément à la loi canadienne sur la protection de la vie privée, quelques formulaires secondaires ont été enlevés de cette thèse.

Bien que ces formulaires aient inclus dans la pagination, il n'y aura aucun contenu manquant.

Canada

TABLE OF CONTENTS

ACKNOWLEDGMENTS

There are many people that I would like to thank for their contribution in the completion of this thesis.

Firstly, thanks to my supervisor, Dr Barbara Vanderhyden, for taking me on as an Honours student 4 years ago and introducing me to the world of research. Thank you for your encouragement, your praise, and your contagious excitement about science. You are a great mentor and have created a wonderfully positive environment to work in. I am going to miss it!

I'd also like to thank the many members of the Vanderhyden lab, who have helped me along the way. I have been really lucky to work with such a wonderful group of people and I thank you all for the many contributions you have given me at our wiplets. Thanks to Liz Macdonald for all her help and suggestions on troubleshooting the *c-KIT* PCR for the clinical trial and for her perseverance when I was ready to give up on it. Thanks also to Colleen Crane for being the best histo-tech ever and for helping me with all my immunos. A big thank you to Olga Collins for her expertise in the culture of MOSE cells, for answering all of my technical questions, and for our chats about Gilmore Girls.

A special thanks to the graduate students in the lab, Tanya Shaw, Katherine Clark and David Pepin. Thanks for working beside me during this part of my life and for your never-ending offers to help! Thanks to Tanya for inspiring me and always making me smile, to Katherine for being my LTS partner in crime and for the great lunch talks about keeping things in perspective, and to David for keeping my brain working and for making us laugh! Thanks for everything guys!

I would also like to thank my family, who have supported me unconditionally and encouraged me always. To my Mom, for sharing with me her love of science and learning and to my Dad for teaching me to do my best and for being so proud of my posters! To Jess and Sarah, the best sisters a girl could ask for. Thanks for helping me take such fun breaks and for being around when I needed you. To Nicolas, for being my big-little brother, for your visits home, and for being so good at making your sisters laugh! Thanks to Gran and Grandad for always being so proud of me and for hosting such delicious Sunday dinners.

I'd also like to thank my family in law, Harold, Bea, and Tim Vandermeer, for all the quick suppers, for listening (with interest!) to what I do at work and for all the wishes of providence!

Finally, thanks to Brent, my husband and my best friend. I couldn't have finished this degree without him. Thank you for encouraging me, supporting me, and feeding me throughout this season, and for giving such great hugs when they were needed most.

ABSTRACT

Ovulation is a putative risk factor for ovarian cancer, and may be attributed to proliferating ovarian surface epithelial (OSE) cells interacting with the extracellular matrix (ECM) during ovulatory wound repair. We investigated the effects of ECM and cellular density on OSE cell morphology, proliferation, and expression of c-*Kit*, a proto-oncogene expressed in 70% of ovarian tumours. Fibrillar collagen I caused significant changes in morphology and proliferation but monomeric ECM had no effect. Normal human ovaries co-expressed KIT, collagen I and fibronectin in 75% of abnormal OSE structures. At increased cellular densities, rat OSE cells expressed increased levels of Kit. Retrovirus-mediated expression of c-*Kit* in OSE caused a significant increase in proliferation. Additionally, sequence analysis of *c-KIT* in 21 ovarian tumours revealed no mutations. These results suggest a relationship between KIT and collagen I in OSE and that cellular density in the OSE regulates KIT, which increases cell proliferation and may contribute to transformation.

LIST OF FIGURES

LIST OF TABLES

LIST OF ABBREVIATIONS

α-MEM	alpha minimum essential medium
bp	base pairs
BSA	bovine serum albumin
CML	chronic myelogenous leukemia
DAB	diaminobenzidine
dbcAMP	dibutyryl adenosine 3',5'-cyclic monophosphate
DBS	donor bovine serum
D-MEM	Dulbecco's minimum essential medium
DMSO	dimethylsulfoxide
DNA	deoxyribonucleic acid
DTT	dithiothreitol
ECM	extracellular matrix
EDTA	ethylenediaminetetraacetic acid
EGF	epidermal growth factor
FCS	fetal calf serum
FSH	follicle stimulating hormone
GIST	gastrointestinal stromal tumour
hCG	human chorionic gonadotropin
HGF	hepatocyte growth factor
HRP	horseradish peroxidase
IgG	immunoglobulin
ITSS	insulin transferrin sodium selenite
kDa	kilo Daltons
KGF	keratinocyte growth factor
KL	kit ligand
LH	luteinizing hormone
MAPK	mitogen activated protein kinase
MOSE	mouse ovarian surface epithelium

mRNA	messenger ribonucleic acid
nm	nanometre
OSE	ovarian surface epithelium
PAGE	polyacrylamide gel electrophoresis
PBS	phosphate buffered saline
PCR	polymerase chain reaction
PDGF-R	platelet-derived growth factor receptor
PI3K	phosphoinositol-3-kinase
RNA	ribonucleic acid
RNase	ribonuclease
ROSE	rat ovarian surface epithelium
rpm	revolutions per minute
RT	reverse transcription
SDS	sodium dodecyl sulphate
SEM	standard error of the mean
S-PBS	Stockholm's phosphate buffered saline
TBS/T	Tris-buffered saline, Tween-20
TE	Tris-EDTA
TGF-β	transforming growth factor-beta
Tyr	tyrosine
W	White-spotting locus
X-gal	X-galactosidase

INTRODUCTION

1. Basic Features of the Ovary

1.1. Ovarian Structure

The ovaries are paired organs that are located on either side of the uterus near the fimbriae of the fallopian tubes. They are dual purpose organs, responsible for the growth and release of the female germ cells and the production of steroid hormones. The ovary is composed of many cell types including ovarian surface epithelium (OSE), stromal cells, granulosa cells, and oocytes (see Figure 1). The surface epithelium covers the entire outer surface of the ovary and is separated from the stromal cells by a basal lamina and a tunica albuginea. The basal lamina is a very thin structure that is composed of type IV collagen, laminin, and other glycoproteins (Rodgers, R.J. and Irving Rodgers, H.F., 2002). It provides structural attachment for the epithelial cells as well as acts as a selective filtration barrier and induces cell polarity (Rodgers, R.J. *et al.*, 2003). The tunica albuginea is a dense collagenous connective tissue layer that gives the ovary its whitish colour. It is thought to provide a partial barrier to the diffusion of bioactive agents between the ovarian stroma and the OSE (Auersperg, N. *et al.*, 2001). The ovarian cortex is richly vascularized and contains stromal cells and granulosa cell-encircled follicles at various stages of development.

Figure 1 – Diagram of the mammalian ovary.

The ovary is covered with a single layer of ovarian surface epithelial cells (OSE). The OSE are separated from the stromal cells by the basal lamina and the tunica albuginea which are composed of specific extracellular matrix proteins.

ovarian surface epithelium

stroma

basement membrane

granulosa

oocyte

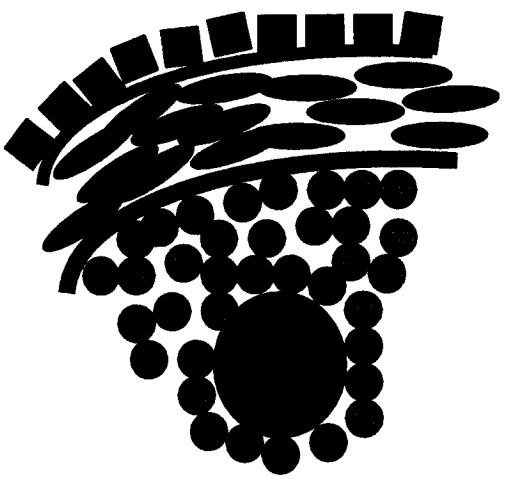

1.2. Description of the Normal OSE

The OSE vary in shape from squamous, to cuboidal and cobblestone, to low pseudostratified columnar (Papadaki, L. and Beilby, J.O., 1971; Blaustein, A. and Lee, H., 1979). OSE cells are embryonically derived from the mesodermal epithelium of the gonadal ridges (Moore, K.L., 1992). In the adult ovary, OSE cells are continuous with the flattened mesothelium of the peritoneum and are separated from the ovarian stroma by a basement membrane. Unlike all other epithelia the OSE cells are loosely attached to the basement membrane and can easily be removed by gently scraping the surface of the ovary. OSE cells are also unlike other epithelia, in that they behave like generative stem cells. With each mitotic division, one OSE cell produces two pluripotent daughter cells with continued growth potential (Hamilton, T.C., 1992; Dyck, H.G. *et al.*, 1996). OSE cells maintain intercellular contact and epithelial integrity by desmosomes, tight junctions, several integrins (Kruk, P.A. and Auersperg, N., 1994; Cruet, S. *et al.*, 1999), and N-cadherin (Sundfeldt, K. *et al.*, 1997; Davies, B.R. *et al.*, 1998; Wong, A.S. *et al.*, 1999). It has been shown that OSE cells express low-molecular weight cytokeratins, transforming growth factor-α, epidermal growth factor (EGF), hepatocyte growth factor (HGF), keratinocyte growth factor (KGF; Czernobilsky, B. *et al.*, 1985; Isola, J. *et al.*, 1990; Rodriguez, G.C. *et al.*, 1991; Jindal, S.K. *et al.*, 1994; Parrott, J.A. and Skinner, M.K., 2000; Parrott, J.A. *et al.*, 2000a), and Kit Ligand (KL; Ismail, R.S. *et al.*, 1999; Parrott, J.A. *et al.*, 2000b) as well as receptors for progesterone, estrogen, luteinizing hormone (LH), and follicle stimulating hormone (FSH; Isola, J. *et al.*, 1990; Parrott, J.A. *et al.*, 2001).

It is commonly reported that OSE cells have morphological plasticity. *In vivo*, they are typically cuboidal or cobblestone in appearance yet after passaging under standard tissue culture conditions, primary human OSE cells tend to flatten out and become more atypical and fibroblastic (Auersperg, N. *et al.*, 1984; Siemens, C.H. and Auersperg, N., 1988). This epithelial-mesenchymal transition includes a switch from apicobasal to anterioposterior polarity, a loss of intercellular contacts and loss of expression of the epithelial marker keratin, as well as a gain of expression of the mesenchymal marker vimentin. Also while in culture, OSE cells produce both epithelial (laminin and collagen IV) and mesenchymal (collagen I and III) components of the extracellular matrix (Auersperg, N. *et al.*, 1994). Factors such as LH, FSH, and human chorionic gonadotropin (hCG) have been shown to stimulate proliferation of bovine OSE cells in culture as well as alter gene expression of EGF, HGF, and KGF (Parrott, J.A. *et al.*, 2001), however treatment of human and rat OSE cells with steroid hormones such as estrogen, progesterone, and testosterone did not influence cell proliferation despite the continued presence of receptors for these hormones (Karlan, B.Y. *et al.*, 1995; Prevost, M., 1999).

1.3. Ovulation

The process of follicle maturation begins at puberty, when a signal from the hypothalamus stimulates the pituitary's production of LH and FSH. These hormones initiate the process of ovulation as well as stimulate the ovary to produce the steroid hormones, progesterone and estrogen. FSH stimulates growth and development of follicles as well as production of estrogen by the ovarian granulosa cells. When estrogen

levels peak, the pituitary secretes a surge of LH, which induces ovulation of the follicle. Once the follicle ruptures a corpus luteum develops at the wound site and secretes progesterone, which maintains the thickness of the uterine endometrium for implantation. If fertilization does not occur, the corpus luteum ceases production of hormones and the uterine lining breaks down, causing menses. If fertilization of the oocyte occurs, the zygote will begin production of hCG, which stimulates the ovary to continue production of progesterone and maintain a nourishing endometrium for the developing embryo. Prior to puberty, the surface of the ovary is very smooth, however it becomes rough and scarred after repeated ovulations.

Ovulation results in the release of a mature oocyte from the ovary into the fallopian tube and represents the time around which a female is able to become pregnant. It is a complex process involving approximately 70 genes and multiple layers of the ovary (Espey, L.L. *et al.*, 2004). OSE cells play an active role in the process of ovulation. The OSE cells directly above the point of rupture release proteolytic enzymes from cytoplasmic granules which degrade and disrupt the dense tunica albuginea, the basal lamina, as well as the theca externa which surrounds the pre-ovulatory follicle (Bjersing, L. and Cajander, S., 1974). The OSE also undergo apoptosis to allow release of the follicle (Ackerman, R.C. and Murdoch, W.J., 1993). Following ovulation, surface epithelial cells on the periphery of the rupture site must then rapidly proliferate to repair the ovulatory wound (Osterholzer, H.O. *et al.*, 1985). These peripheral OSE cells also flatten out, assume a mesenchymal phenotype, and become migratory to help repair the ovary (Nicosia, S.V. *et al.*, 2004). As well, OSE cells are capable of depositing and restructuring the extracellular matrix of the tunica albuginea following ovulation (Kruk,

P.A. and Auersperg, N., 1992; Kruk, P.A. and Auersperg, N., 1994). The importance of the OSE in ovulation has been well demonstrated in frogs (Schuetz, A.W. and Lessman, C., 1982), sheep (Colgin, D.C. and Murdoch, W.J., 1997) and pigs (Hall, J.A. *et al.*, 1993) which shows that when the ovarian surface epithelium is surgically removed or disrupted by handling, ovulation is blocked.

1.4. Formation of Invaginations and Inclusion Cysts

During the repetitive process of ovulatory wound repair, OSE cells and the underlying stroma rapidly proliferate to reconstruct the ovarian epithelium. It is during this proliferative phase that OSE can undergo epithelial-stromal rearrangements, assume a columnar histology, and form multiple cell layers. Sometimes, the OSE will start to migrate into the ovarian stroma forming invaginations and these invaginations can eventually become sealed off to form inclusion cysts of epithelial cells within the stroma (Figure 2). These structures are more prevalent in postmenopausal women (Nicosia, S.V., 1987) as well as in aging mice (Clow, O.L. *et al.*, 2002). Although inclusion cysts are fairly common in women, these structures are thought to be precursor lesions to ovarian cancer (Hutson, R. *et al.*, 1995; Salazar, H. *et al.*, 1996; Aoki, Y. *et al.*, 2000). Histopathological examination suggests that early malignant changes (including neoplasia, dysplasia, and expression of CA125 and HER-2 neu) frequently occur in these OSE lined invaginations and inclusion cysts rather than on the ovarian surface (Young, R.H. *et al.*, 1989). These structures can also arise as a consequence of follicular attrition or from inflammation caused by carcinogens or chemical irritants such as talc (Hamilton, T.C., 1992).

FIGURE 2 - Invagination and inclusion cyst formation in the mammalian ovary. Following ovulation, ovarian surface epithelial (OSE) cells must rapidly proliferate to repair the wound in the ovarian surface. During this process, OSE cells can invade into the stroma of the ovary forming invaginations (A). These invaginations can penetrate into the tunica albuginea and pinch off to form inclusion cysts (B) lined with OSE cells within the ovary. These structures are often seen as precursor lesions of ovarian cancer. Taken from (Ghahremani, M. *et al.*, 1999).

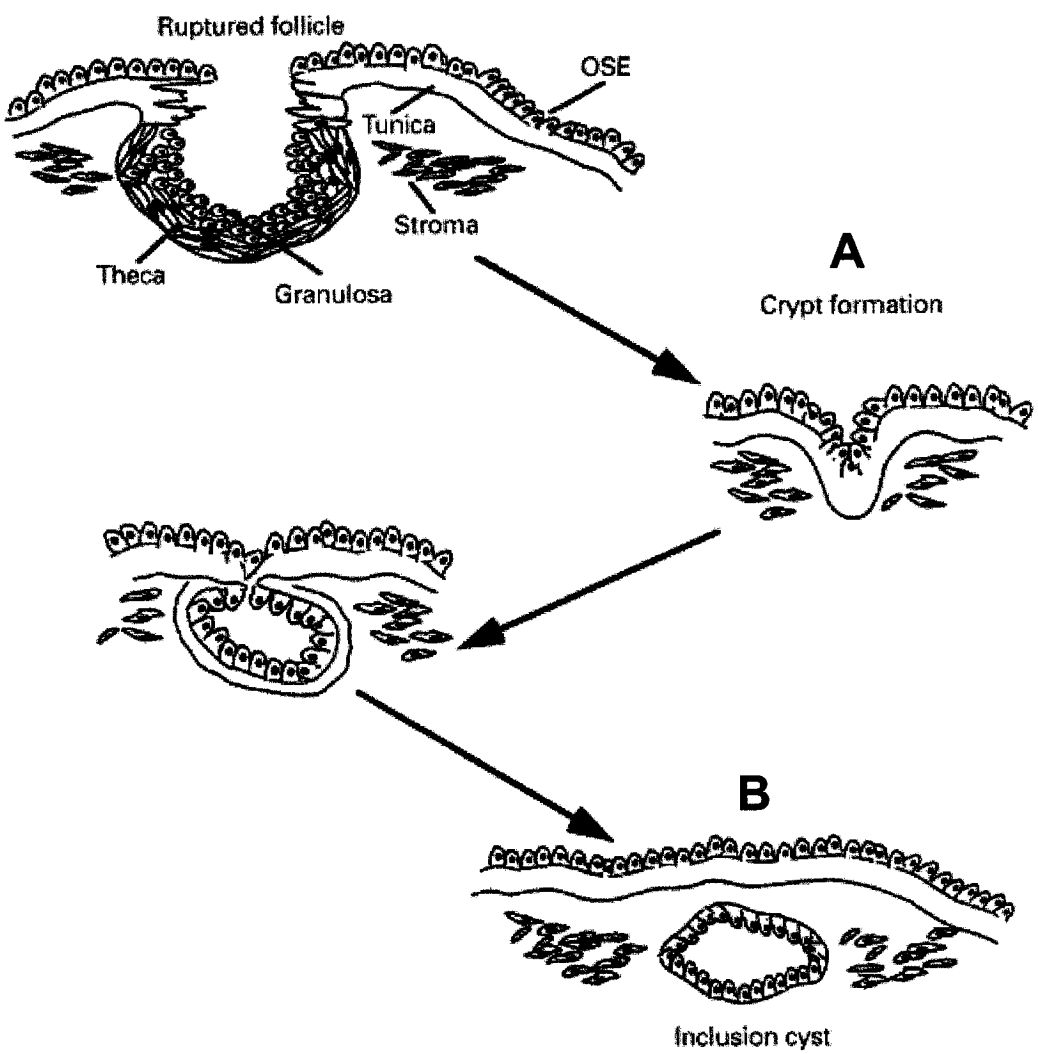
Ruptured follicle
OSE
Tunica
Stroma
Theca
Granulosa
A
Crypt formation
B
Inclusion cyst

Analysis of the OSE in inclusion cysts revealed frequent expression of E-cadherin, HOXA7 and KIT expression, which are all absent in cells located on the ovarian surface (Sundfeldt, K. *et al.*, 1997; Maines-Bandiera, S.L. and Auersperg, N., 1997; Davies, B.R. *et al.*, 1998; Tonary, A.M. *et al.*, 2000; Naora, H. *et al.*, 2001). Expression of E-cadherin and KIT are also found in human cutaneous melanoma (Baldi, A. *et al.*, 2001). As E-cadherin, HOXA7, and KIT are overexpressed in the majority of epithelial ovarian cancers (Sundfeldt, K. *et al.*, 1997; Tonary, A.M. *et al.*, 2000; Naora, H. *et al.*, 2001) the induction of their expression in the preneoplastic inclusion cysts suggests a potential role for these factors in early ovarian tumourigenesis however the mechanism of induction of expression is not unknown.

2. Ovarian Cancer

2.1. Incidence Rates, Symptoms, and Treatment

Ovarian cancer is the leading cause of death from gynecological malignancies in the western world. It is estimated that if diagnosed and treated in the early stage, the five year survival rate is 90% (Murdoch, W.J., 1996) however, ovarian cancer is commonly diagnosed in late stage, due to the lack of obvious symptoms. In Canada this year, 2300 new cases will be diagnosed and 1500 women will die from the disease within 5 years (National Cancer Institute of Canada: Canadian Cancer Statistics, 2004). Symptoms of ovarian cancer may include abdominal swelling, gastrointestinal cramps, nausea, indigestion, and abnormal vaginal bleeding; however some women may have no symptoms at all. It is therefore common that ovarian cancer is typically diagnosed once the disease has spread past the confines of the ovary. It is at this stage that ascites fluid

can begin to accumulate in the abdomen and women notice sudden weight gain. Once the cancer has spread outside of the ovaries, the 5-year survival of advanced stage ovarian cancer is approximately 15% (Teneriello, M.G. and Park, R.C., 1995; Landis, S.H. *et al.*, 1998). Despite improved knowledge and research on the development and progression of the disease, as well as combination chemotherapy and aggressive surgery, there has been little change in the ovarian cancer survival rate over the past 30 years. There are currently no reliable screening methods to detect ovarian cancer and the only significant risk factors determined thus far are uninterrupted ovulation (Fathalla, M.F., 1971) and germline mutations in the BRCA1 or BRCA2 genes (Takahashi, H. *et al.*, 1995; Lancaster, J.M. *et al.*, 1996). Although ovarian cancer can arise from any of the cell types found in the ovary, over 90% of ovarian tumours are derived from the ovarian surface epithelium (Weiss, N.S. *et al.*, 1977). Treatment for ovarian cancer depends on the type and stage of the disease, however the standard treatment regimen for patients is surgical debulking of the tumour followed by chemotherapy treatment with Carboplatin and Paclitaxel.

2.2. Risk Factors – Ovulation

There are two major theories describing the development of ovarian cancer. The first is the gonadotropin theory which hypothesizes that the elevated LH and FSH concentrations in post-menopausal women, as a result of reduced estrogen levels, contribute to the development of ovarian tumours (Cramer, D.W. and Welch, W.R., 1983). It is based on the original observation that transplantation of ovaries onto the splenic pulp of adult rats led to the development of ovarian tumours (Biskind, M. and

Biskind, G., 1944). The tumorigenesis was attributed to the inactivation of estrogen in the liver, and the consequent elevation of gonadotropin levels due to the lack of steroid feedback on the pituitary. Numerous models of ovarian cancer characterized since that time have demonstrated that the development of tumours could be prevented by blocking the secretion of gonadotropins (Matzuk, M.M. *et al.*, 1992; Nilson, J.H. *et al.*, 2000; Keri, R.A. *et al.*, 2000; Danilovich, N. *et al.*, 2001).

The "incessant ovulation hypothesis" states that uninterrupted ovulation, with its repeated surface rupture followed by rapid proliferation of the epithelial cells, increases the chance of mutations and transformation (Fathalla, M.F., 1971; Murdoch, W.J., 1996). Studies in sheep show ovulation-induced DNA damage (accumulation of 8-oxoguanine and internucleosomal DNA fragmentation) in the OSE cells near the ovulatory rupture site (Murdoch, W.J. *et al.*, 2001). The domestic hen model also supports the hypothesis of ovulation being a risk factor for ovarian cancer. These animals are laying eggs daily and frequently develop peritoneal cancer of epithelial origin (Fredrickson, T.N., 1987). As well, Godwin *et al.* (1992) showed that when rat OSE cells are repeatedly subcultured to mimic continued growth stress, the cells gain features of transformation such as loss of contact inhibition, substrate-independent growth, and the ability to form tumours in nude mice.

Epidemiological evidence also links ovarian cancer with ovulation (Gross, T.P. and Schlesselman, J.J., 1994; Vessey, M.P. and Painter, R., 1995). Conditions which decrease a woman's total number of ovulations such as the use of oral contraceptives, pregnancy, and the length of the lactation period all decrease the risk of ovarian cancer (Chen, Y. *et al.*, 1992; Hankinson, S.E. *et al.*, 1993; Obermair, A. *et al.*, 1998; Narod,

S.A. *et al.*, 2001). As well, conditions which increase the number of ovulatory cycles such as "fertility drugs" can increase the risk for developing ovarian cancer (Burmeister, L. and Healy, D.L., 1998) as can long menstrual intervals consisting of early menarche and late menopause (Cramer, D.W. and Welch, W.R., 1983; Cramer, D.W. *et al.*, 1983).

3. c-*KIT*

3.1 c-*KIT* Structure, Function and Expression

The c-*KIT* proto-oncogene is the normal cellular homologue of v-kit, the transforming gene of the Hardy-Zuckerman 4 strain of feline sarcoma virus (Besmer, P. *et al.*, 1986). The c-*KIT* gene is distributed over 21 exons and encodes a 5.1kb transcript in humans (Vandenbark, G.R. *et al.*, 1992). The KIT locus, also known as *W* locus for *White-spotting*, is located on human chromosome 4q11-13 (Yarden, Y. *et al.*, 1987) and encodes the KIT protein. KIT is a class III transmembrane tyrosine kinase receptor that is structurally similar to the receptors for colony-stimulating factor-1 and platelet-derived growth factor (Chabot, B. *et al.*, 1988). The KIT protein consists of an extracellular domain which contains five immunoglobulin-like repeats, a transmembrane domain, and an intracellular kinase domain (Figure 3) (Yarden, Y. and Ullrich, A., 1988). The KIT protein can be 125, 145, or 160 kDa in size depending on the amount of post-translational modification (Yarden, Y. *et al.*, 1987; Reith, A.D. *et al.*, 1991; Matsuda, R. *et al.*, 1993). An alternatively spliced form of the KIT protein also exists. This c-*KIT* isoform contains a 12bp insertion in the c-*KIT* gene, which creates an alternative splice donor site in exon 9. This insertion codes for a 4 amino acid proteolytic cleavage site in the juxtamembrane domain of the receptor which translates into a protein in which the extracellular domain

FIGURE 3 – The KIT receptor.

Linear representation of the domain structure of KIT, showing the transmembrane domain (TM), juxtamembrane domain (JM), and the two tyrosine kinase domains (TK1 and TK2). The arrows show the sites where activating mutations have been found in gastrointestinal stromal tumours and mast cell leukemia; the juxtamembrane domain (550-560), the SHP-1 binding site (569), and the PI3K binding site (719).

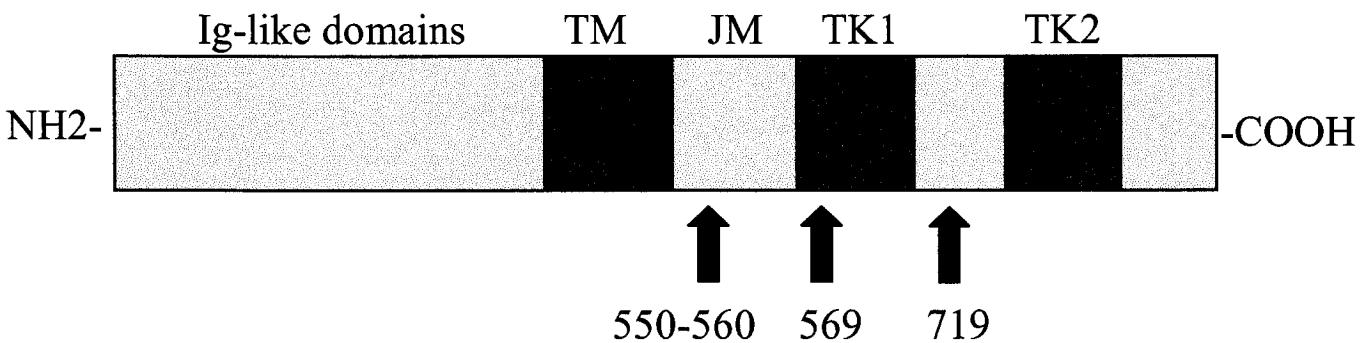
Ig-like domains
TM
JM
TK1
TK2
NH2-
-COOH
550-560
569
719

can be cleaved to become soluble (Reith, A.D. *et al.*, 1991; Vandenbark, G.R. *et al.*, 1992; Giebel, L.B. *et al.*, 1992). Soluble KIT is 95kDa and is reported to act as an antagonist to the membrane bound KIT receptor by competing for the ligand (Turner, A.M. *et al.*, 1995; Dahlen, D.D. *et al.*, 2001). The KIT receptor is activated by the binding of its ligand, Kit Ligand (KL). KL is encoded by the Steel locus, which maps to human chromosome 12 (Geissler, E.N. *et al.*, 1991; Baldi, A. *et al.*, 2001). The KL mRNA transcript is generated from 9 exons and as with c-KIT, there are two splice variants of KL. The larger mRNA transcript includes exon 6 and is proteolytically cleaved in the extracellular domain to release soluble KL. Translation of the shorter mRNA transcript that does not contain exon 6 results in a protein that is more stably associated with the membrane (Flanagan, J.G. *et al.*, 1991; Baldi, A. *et al.*, 2001). Specific roles for each isoform in follicle growth and maturation and in stimulation of mast cells by Sertoli cells have been reported (Tajima, Y. *et al.*, 1991; Thomas, F.H. *et al.*, 2004). The KL protein is 25-40kD and has extensive glycosylation of the extracellular domain (Huang, E. *et al.*, 1990) .

Upon binding, the receptors dimerize and catalytic activation of the kinase domain occurs via autophosphorylation of tyrosine (Tyr) 568 and 570 (Lennartsson, J. *et al.*, 1999). Activated KIT receptor is known to interact with, and phosphorylate a variety of downstream signalling molecules including phosphatidyl inositol 3'-kinase (PI3K), $p21^{ras}$, $p21^{ras}$ GTPase-activating protein, src kinase, and members of the Ras/mitogen activated protein kinase family (MAPK; (Lev, S. *et al.*, 1991; Herbst, R. *et al.*, 1991; Lev, S. *et al.*, 1992; Duronio, V. *et al.*, 1992; Blume-Jensen, P. *et al.*, 1994; Lennartsson, J. *et al.*, 1999). Activity of the KIT receptor is negatively regulated by protein tyrosine

phosphatases, SHP-1 and SHP-2, which inactivate KIT by dephosphorylation (Paulson, R.F. *et al.*, 1996; Kozlowski, M. *et al.*, 1998). Protein kinase C (PKC) can also negatively regulate KIT by phosphorylating the receptor's active serine residues (Blume-Jensen, P. *et al.*, 1993).

In adults, expression of KIT can be found in many cell types, including germ cells, mast cells, melanocytes, and bone marrow cells (Lammie, A. *et al.*, 1994). Depending on the cell type, KIT has been shown to play a role in proliferation, migration, differentiation, and survival (Metcalf, D. and Nicola, N.A., 1991; Tsai, M. *et al.*, 1991; Matsui, Y. *et al.*, 1991; Godin, I. *et al.*, 1991). Mutations resulting in reduced expression or function of KIT can lead to anemia, mast cell deficiency, decreased fertility, decreased gastrointestinal motility, and impairment of learning (Chian, R. *et al.*, 2001). There are a number of growth factors, hormones, and second messengers that have been shown to regulate KIT expression in normal and cancer cells. Transforming growth factor-β (TGF-β) has been shown to decrease growth by inhibiting c-*KIT* expression in murine and human hematopoietic progenitor cells (Dubois, C.M. *et al.*, 1994) as well as to decrease expression of KL in rat OSE cells (Ismail, R.S. *et al.*, 1999). Tumour necrosis factor-α downregulates the c-*KIT* transcript in CD34+ hematopoietic progenitor cells which causes an inhibition of KL-induced proliferation (Rusten, L.S. *et al.*, 1994; Khoury, E. *et al.*, 1994). Interleukin-1 can upregulate c-*Kit* expression in murine bone marrow cells (Neta, R. *et al.*, 1994) and human leukemia cells (Tomeczkowski, J. *et al.*, 1998), while interleukin-4 and -10 can downregulate Kit protein expression in murine mast cells (Mirmonsef, P. *et al.*, 1999). C-*Kit* can also be upregulated by compounds such as dibutyryl adenosine 3',5'-cyclic monophosphate (dbcAMP) in hematopoetic cells

(Ogawa, K. *et al.*, 1995) as well as in ovarian cancer cell lines (Shaw, T.J. *et al.*, 2002). DbcAMP also stimulates increased expression of KL in rat OSE cells (Ismail, R.S. *et al.*, 1999).

Co-expression of KIT and KL has been found in many types of cancer including breast (Hines, S.J. *et al.*, 1995; Hines, S.J. *et al.*, 1999), cervix (Inoue, M. *et al.*, 1994), lung (Hibi, K. *et al.*, 1991), melanoma (Papadimitriou, C.A. *et al.*, 1995), and ovary (Matsui, Y. *et al.*, 1991). Expression of KIT was also detected in mast cells of leukemia patients (Wang, C. *et al.*, 1989; Ikeda, H. *et al.*, 1991) as well as in gastrointestinal stromal tumours (GISTs) (Hassan, S. *et al.*, 1998; Shinomura, Y., 2000), however in these cancers, KIT was found to be constitutively active and signalling without stimulation from the ligand. Further analysis revealed gain-of-function point mutations in the c-*KIT* DNA coding sequence in both cancers rendering KIT protein phosphorylated and constitutively activated (Furitsu, T. *et al.*, 1993; Hirota, S. *et al.*, 1998). In GISTs, activating mutations were found in the highly conserved juxtamembrane domain of the c-*KIT* sequence (Hirota, S. *et al.*, 1998) while in mast cell leukemia, activating mutations were found in the SHP-1 binding site (Chian, R. *et al.*, 2001) and the PI3K binding site (Furitsu, T. *et al.*, 1993). The juxtamembrane domain may contain inhibitory factors, which are suppressed when the region is mutated rendering KIT constitutively active, thus promoting proliferation and antiapoptotic signalling (Eisenberg, B.L., 2003). Since SHP-1 negatively regulates KIT receptor activity by dephosphorylation, mutations to the SHP-1 binding site would prevent c-*KIT* from being inactivated. PI3K is part of a family of lipid products, which act as second messengers in a variety of signalling cascades. Of interest to us is the ability of KL to stimulate PI3K to bind to KIT and activate Akt and

Jnk kinases (Chian, R. *et al.*, 2001). Mutations to the PI3K binding site render PI3K constitutively associated with KIT and constantly activating the signalling pathway. It has been reported that forced expression of murine c-*Kit* in NIH 3T3 mouse fibroblasts resulted in increased proliferation rates, as well as invasion into Matrigel, and tumorigenicity in nude mice (Lev, S. *et al.*, 1990; Caruana, G. *et al.*, 1998). These observations confirm the ability of KIT to act as an oncogene, but also suggest that overexpression of KIT is a sufficient event to initiate tumourigenesis.

3.2 KIT Expression in the Ovary and Ovarian Cancer

KIT receptors have been detected in oocytes and theca cells in human, mouse and rat ovaries (Manova, K. *et al.*, 1990; Horie, K. *et al.*, 1993; Ismail, R.S. *et al.*, 1997) while KL has been shown to be produced by granulosa cells in humans, mice, and rats (Manova, K. *et al.*, 1993; Laitinen, M. *et al.*, 1995; Ismail, R.S. *et al.*, 1996) and by rat ovarian surface epithelium (Ismail, R.S. *et al.*, 1999). Interaction between KL produced by the granulosa cells and the KIT receptor on the oocytes is required for normal oocyte growth and development (Driancourt, M.A. *et al.*, 2000; Reynaud, K. *et al.*, 2000; Kissel, H. *et al.*, 2000). KIT is not expressed in the normal human ovarian surface epithelium however, KIT expression can be detected in the OSE that form invaginations and inclusion cysts (see Figure 4) as well as in 70% of ovarian tumours (Tonary, A.M. *et al.*, 2000). Since these cells normally express KL, there exists potential for autocrine stimulation of the OSE that have gained expression of KIT. Few experiments have been performed to examine the role of KIT in ovarian cancer, and there is little published on the subject. KIT expression in the OSE appears to coincide with developing pre-

FIGURE 4 –Expression of KIT in the human ovary and ovarian tumours.

Expression of KIT can be seen in the human oocytes (o; D), in the ovarian surface epithelial (OSE) cells lining the inclusion cysts (ic; B) and invaginations (E) as well as in the ovarian carcinomas (C). There is no KIT expression in the normal OSE (A, D). Taken from (Tonary, A.M. *et al.*, 2000).

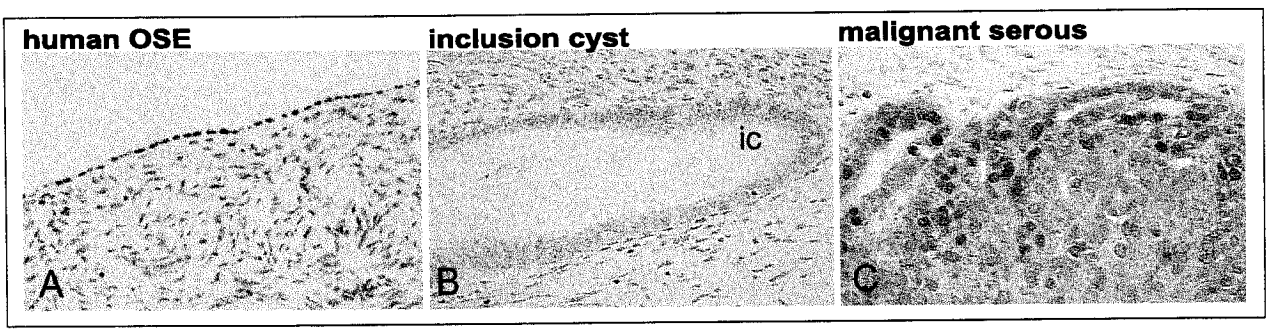
human OSE
inclusion cyst
malignant serous
ic
A
B
C

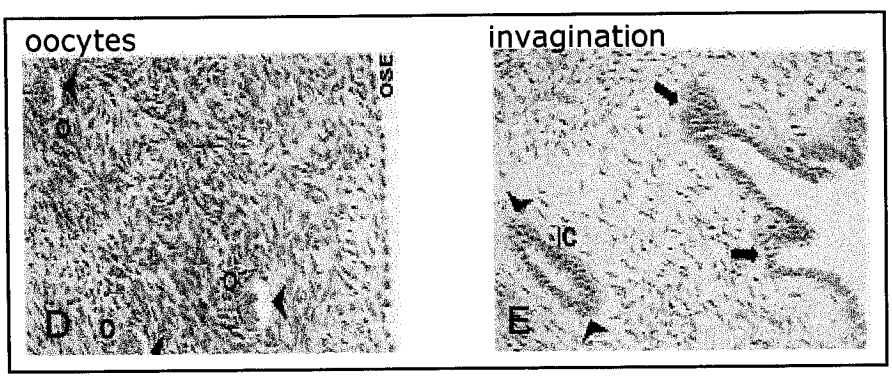
oocytes
invagination
OSE
o
o
o
ic
D
E

malignant lesions, yet ovarian cancer patients whose tumours express KIT have a better prognosis than patients whose tumours do not express KIT (Tonary, A.M. *et al.*, 2000). To date, no activating mutations have been identified in ovarian cancer cells or ovarian tumours (Singer, G. *et al.*, 2003), however, only one study has been reported. The function of KIT and its role in the development of ovarian cancer requires more research and is one of the main projects in our lab.

3.3 Gleevec Clinical Trials

Gleevec or STI571 is a specific small molecule tyrosine kinase inhibitor. It inhibits activity of the KIT receptor, as well as platelet-derived growth factor receptor (PDGF-R), Abl, and Bcr-Abl. It functions by competitively binding to the ATP binding site on the tyrosine kinase receptor, thus preventing it from becoming phosphorylated and active. Gleevec is currently being used to treat patients with chronic myelogenous leukemia (CML) by inhibiting Bcr-Abl; and in patients with GIST, Gleevec inhibits KIT or PDGF-R signalling (Heinrich, M.C. *et al.*, 2003; Jiang, H. *et al.*, 2003). Inhibition of both receptors with this drug has shown dramatic efficacy in slowing tumour progression in GIST and CML patients (Radford, I.R., 2002; Joensuu, H., 2002; Croom, K.F. and Perry, C.M., 2003). Recent studies have shown that Gleevec is capable of inhibiting growth of ovarian cancer cells by targeting KIT and/or PDGF-R (Matei, D. *et al.*, 2004; Shaw, T.J. and Vanderhyden, B.C., 2005). Gleevec is currently in a Gynecologic Oncology Group Phase II clinical trial for treatment of patients with persistent or recurrent epithelial ovarian or primary peritoneal carcinoma. While the primary goals of the trial are to determine the efficacy of this drug in ovarian cancer patients, secondary objectives

include the determination of expression levels of KIT, KL, PDGF-R, PDGF, AKT2 and phospho-AKT2 in primary ovarian tumours collected prior to initiation of first-line chemotherapy as well as the presence or absence of c-*KIT* mutations in these tumours. The patients' responses to Gleevec will then be correlated with the expression of KIT, mutant KIT, PDGF-R and/or activated AKT2. The results of this ongoing study will be very interesting as targeted therapeutics for ovarian cancer are currently lacking and existing treatments are often ineffective on recurrent disease.

4. Extracellular Matrix

4.1. Extracellular Matrix Signalling

Extracellular matrix (ECM) is defined as a complex mixture of proteins, proteoglycans, and adhesive glycoproteins that provide structural support to cells and tissues (Pupa, S.M. *et al.*, 2002). Every cell type has specific surface receptors for the matrices in its environment and interacting with these ECM components affects cell shape, behaviour and the response to soluble molecules such as cytokines and growth factors (Lin, C.Q. and Bissell, M.J., 1993). Numerous studies have shown how ECM components play a role in regulating cellular processes such as proliferation, apoptosis, adhesion, migration, differentiation, and gene expression, which in turn affect physiological processes such as embryonic development, angiogenesis, and also transformation and metastasis (Ingber, D.E. and Folkman, J., 1989; Yurchenco, P.D. and Schittny, J.C., 1990; Damsky, C.H. and Werb, Z., 1992; Juliano, R.L. and Haskill, S., 1993; Assoian, R.K. and Marcantonio, E.E., 1996). ECM can exist as a monomeric matrix consisting of one helix or a fibrillar matrix which is a trimeric complex of one or

more matries. Epithelial cells receive signals through their attachment with the basement membrane, which is highly organized and controls signalling to the cells by altering its ECM composition.

Adhesion of the cells to the ECM components of the basement membrane is mediated through members of the integrin family of transmembrane receptors (Gumbiner, B.M., 1996; Brown, N.H. *et al.*, 2000). Integrins consist of heterodimers of one α and one β-subunit, which are type 1 transmembrane glycoproteins. Integrins are described as being "2-faced receptors"; one face, the large extracellular domain that is oriented towards the extracellular space and interacts with the ECM protein or other transmembrane protein ligands and the other face, which is oriented to the cell interior, is interactive with cytoplasmic proteins (Xiong, J.P. *et al.*, 2002; Shattil, S.J. and Newman, P.J., 2004). The activation and signalling of integrins are bidirectional. Inside-out signalling involves the binding of an intracellular ligand with the integrins cytoplasmic tail, which leads to a conformational change in the extracellular domain and an increase or decrease in the extracellular domain's affinity for an ECM ligand. Outside-in signalling describes an extracellular ligand such as an ECM protein irreversibly binding to the extracellular domains of multiple integrins causing them to cluster and undergo a conformational change, which is transmitted to the cytoplasmic tails. This results in recruitment or activation of enzymes, adaptors, and effectors to form integrin based signalling complexes (Schwartz, M.A. and Ginsberg, M.H., 2002; Shattil, S.J. and Newman, P.J., 2004).

Integrins share many common elements in their signalling pathway with growth factor receptors and can intersect pathways such as the MAPK pathway at multiple

points. This crosstalk means that adhesion of cells to certain extracellular matrices can activate integrins and in turn signal to pathways normally activated by growth factors. Cells could therefore, mistake signalling from integrins as signalling from growth factors and this confusion could lead to inappropriate cell growth (Schwartz, M.A. and Ginsberg, M.H., 2002). Specifically, stimulation of integrins by extracellular cues such as ECM can cause ligand-independent trans-activation of tyrosine kinase growth factor receptors, which if uncontrolled, can result in tumourigenesis. Tumour cells want to encourage proliferation and avoid apoptosis so in turn; they remodel the matrix by changing the ECM composition to escape control by the microenvironment. Cell-adhesion molecules such as E-cadherin also play a very important role in maintaining tissue integrity. E-cadherin is a 120kDa calcium-dependent transmembrane protein. Adhesion is initiated by the homologous binding of the E-cadherin extracellular domains between adjacent cells. Internal stability is maintained by the binding of the intracellular domain to α, β, or γ-catenins, which form functional adherent junctions by linking with F-actin (Auersperg, N. *et al.*, 1999; Ong, A. *et al.*, 2000). E-cadherin expression is not detected in the normal surface OSE of the ovary but is detected in the OSE forming invaginations and inclusion cysts as well as in ovary carcinomas (Sundfeldt, K. *et al.*, 1997; Davies, B.R. *et al.*, 1998; Wong, A.S. *et al.*, 1999).

4.2. Presence of Extracellular Matrix in the Ovary

Normal ovarian function is dependent upon continuous and cyclical remodelling of the extracellular matrix. These functions include formation, growth and atresia of the follicle, ovulation, as well as formation and regression of the corpus luteum (Smith, M.F.

et al., 2002). The components of the ECM can modulate cellular activities such as proliferation and differentiation as well as serve as a reservoir for growth factors and cytokines within the ovary due to its aility to bind and sequester growth factors (Logan, A. and Hill, D.J., 1992). Ovulation involves the localized breakdown of extracellular matrix at the apex of the preovulatory follicular wall. When the ECM is degraded (eg. by matrix metalloproteinases and collagenases), sequestered growth factors and cytokines are liberated into the cell which can alter the microenvironment (Logan, A. and Hill, D.J., 1992). For example, it is thought that differentiation of granulosa cells into steroidogenic luteal cells after ovulation, requires sequential exposure to different ECM environments (Smith, M.F. *et al.*, 2002).

Numerous studies have been performed to determine which specific ECM proteins are expressed in the ovary prior to and after ovulation. Standard epithelial basement membranes express laminin and collagen IV, and epithelial stroma express collagen I and III (Kruk, P.A. *et al.*, 1994). Before ovulation, dense collagen can be found in the theca cell layer as well as in the tunica albuginea. The basal lamina which separates the theca cells from the granulosa cells contains primarily collagen IV (Silvester, L.M. and Luck, M.R., 1999), and collagen IV can also be detected in the basement membranes around capillaries located in the ovary. After ovulation, collagen IV and laminin have been localized to the luteinizing granulosa layer (Matsushima, T. *et al.*, 1996), while expression of collagen I and fibronectin is abundant in the outer regions of the corpus luteum (Silvester, L.M. and Luck, M.R., 1999) where new tissue is being formed. Studies have also shown that initiation of collagen synthesis within the ovary appears to be an early event that is associated with follicle rupture (Nagai, R. *et al.*, 1998).

Ovulation has often been termed an inflammatory process, followed by the wound repair process of luteinisation (Espey, L.L., 1980). Wound healing is a very well understood pattern of tissue remodelling that involves a specific sequence of ECM deposition. During early stages, healing tissue is rich in fibronectin, however this is slowly replaced by increases in fibrillar collagen I which is then replaced by collagen I (Bailey, A.J. *et al.*, 1975; Gay, S. *et al.*, 1978; Grinnell, F. *et al.*, 1981; Sottile, J. and Hocking, D.C., 2002). It is interesting that a similar process takes place in the ovary with the development of the corpus luteum after ovulation.

4.3. OSE and ECM Interactions

The OSE are usually in contact with the basal lamina which consists mainly of collagen IV and laminin, however during ovulation or during the formation of cysts, ovarian surface epithelial cells interact directly with the collagen-dense tunica albuginea and other stromal ECM (Kruk, P.A. and Auersperg, N., 1994). Epithelial-mesenchymal transitions are often mediated by components in the extracellular matrix (Kruk, P.A. and Auersperg, N., 1994); therefore it is possible that the transition of OSE lining invaginations and inclusion cysts from a cuboidal phenotype to a more squamous fibroblastic-like cell is caused by direct interactions with stromal ECM components such as collagen I during ovulation. An excellent study done by Kruk *et al.*, (1994) shed some light on this possible relationship by culturing early passage rat OSE on various substrates to mimic the ovarian environment. Cells were cultured on Matrigel to simulate the basement membrane, on collagen gels to simulate the tunica albuginea or stromal ECM, and fibrin clots to simulate the post ovulatory follicle. They looked at cellular

morphology, proliferation, production of ECM, expression of integrins, and production of proteases. Results showed that OSE cells cultured on collagen I have characteristics similar to epithelial-mesenchymal transition, including loss of cell-cell contacts, spindle shaped morphology and loss of integrin expression. The OSE cells did not proliferate on collagen gels compared to plastic control plates. They showed that OSE cells are capable of producing matrix components of both the basement membrane and the stroma as well as capable of secreting proteases to break down matrix. This suggests that there is a significant relationship between the ovarian surface epithelium and the adjacent ECM, which may contribute to the epithelial-mesenchymal plasticity of these cells as well as their propensity for neoplastic transformation. A more recent study examined benign, low-grade, and metastatic ovarian tumours and found that the basement membranes (made of collagen IV and laminin) are absent in almost all cases and the ovarian surface epithelial cells are in direct contact with other ECM components in the extracellular environment (Capo-chichi, C.D. *et al.*, 2002). This suggests a model where changes to the extracellular environment such as loss of basement membrane occur before the transformation of the OSE.

5. ROSE 199 Cell Line and Primary MOSE Cells

5.1 ROSE 199 Cell Line

The ROSE 199 cell line is a spontaneously immortalized rat ovarian surface epithelial (ROSE) cell line that was generated in the laboratory of Dr. Nelly Auersperg. Cultured ROSE 199 cells have been shown to retain their epithelial morphology in subconfluent cultures, however ROSE 199 at higher confluencies and after repeated passage exhibit

tumourigenic behaviour such as loss of contact inhibition, production of collagen layers, and formation of papillary structures but do not form tumours in immunodeficient mice (Adams, A.T. and Auersperg, N., 1985; Testa, J.R. *et al.*, 1994). ROSE 199 cells express extracellular matrix proteins similar to normal human OSE, such as collagen I, III, laminin, and fibronectin (Kruk, P.A. and Auersperg, N., 1994) when in culture. These cells can also produce their own stromal matrix (collagen I and fibronectin) which suggests that intact OSE within the rat ovary could participate in post-ovulatory wound repair (Kruk, P.A. and Auersperg, N., 1994).

It has been shown by Northern blotting that ROSE 199 cells like human OSE, do not express c-*Kit* mRNA but do express the ligand, KL (Ismail, R.S. *et al.*, 1999). This laboratory has recently detected c-*Kit* mRNA expression in ROSE 199 and in primary cultures of ROSE by reverse transcription-polymerase chain reaction (RT-PCR).

5.2 Primary MOSE Cells

Although human OSE cultures are the most appropriate system to study cell transformation leading to ovarian cancer, they are very difficult to obtain, are more sensitive to damage caused by handling, and have very limited growth potential *in vitro*. Primary cultures of mouse OSE (MOSE) are more routinely used because they can be obtained in greater number and can sometimes be cultured indefinitely. There currently exist many methods to isolate and culture primary MOSE (Quirk, S.M. *et al.*, 1997; Roby, K.F. *et al.*, 2000; Flesken-Nikitin, A. *et al.*, 2003). Observations from our lab have shown that maintaining the primary MOSE at higher density (rather than sparsely) appears to increase the success of expanding the culture. After repeated passaging of

MOSE, spontaneous immortalization can occur (Roby, K.F. *et al.*, 2000), however, this behaviour can be avoided if experiments are done with early passage (less than 5 passages) MOSE. Unfortunately, MOSE that are still at early passage have a slower growth rate, and do not handle manipulations very well thus limiting experimental approaches. Our lab has found that early passage MOSE cells do not express the KIT receptor.

5.3 Primary ImmortoMOSE Cells

The ImmortoMouse is a transgenic mouse strain that carries a temperature-sensitive mutant of SV40 large T antigen under the control of the ubiquitous H-2K^b promoter. It has been used to derive a variety of cell lines, including many of epithelial origin such as the surface epithelium of the ovary (Jat, P.S. *et al.*, 1991; Jiang, F. *et al.*, 2003). Ovarian surface epithelial cells isolated from the female ImmortoMouse (ImmortoMOSE) express large T-antigen only when cultured at 32°C. Under normal culture conditions at 37°C, there is no detectable large T-antigen protein expression and the cells are unable to form tumours in immunodeficient mice. Since ImmortoMOSE are immortalized but not transformed, they have a predictable growth rate and can handle procedures such as transfection.

6. Rationale

The purpose of this thesis project was twofold. 1) To investigate the role of extracellular matrices in ovarian surface epithelial cell behaviour in *vitro*, specifically looking at cellular morphology, cellular proliferation, and expression of the proto-

oncogene c-*KIT,* as well as determine if expression of any particular ECM in the ovary correlates with KIT expression in the OSE cells. 2) To analyse ovarian tumours for mutations in the c-*KIT* gene.

Knowing that uninterrupted ovulatory cycles and invaginations and inclusion cysts are indications of increased risk of ovarian cancer, and that expression of KIT is often detected in these structures, we wanted to investigate if there was an association between the changes in extracellular matrix composition at ovulation and the induction of KIT expression in the OSE cells. Specifically, we wanted to determine if any ECM component, such as collagen I or fibronectin which are known to be involved in wound repair after ovulation, is capable of altering OSE cell behaviour *in vitro*. To make these studies relevant *in vivo*, it was of interest to determine the expression level of extracellular matrix components (collagen I, laminin, fibronectin, collagen III, collagen IV) in normal human pre- and post-menopausal ovaries by immunohistochemistry, specifically looking at expression in the OSE forming invaginations and inclusion cysts. It was hypothesized that expression of ECM will be different in and around the OSE cells forming invaginations and inclusion cysts vs. underlying normal surface epithelium and that expression of specific ECM components will correlate with expression of KIT, indicating a possible cause and effect relationship.

We also wanted to determine if cellular density of OSE cells affected expression levels of c-*Kit*. Ovarian surface epithelial cells that are forming invaginations and inclusion cysts are at a higher cellular density than normal, therefore it is possible that the increase in cell-cell communication at this time is causing genetic changes within the cell. This may provide further insight into why incessant ovulation is associated with

increased risk of ovarian cancer and potentially explain a method of regulating KIT expression *in vivo*. Previously in the lab, growth factors and stromal cell factors such as TGF-α, EGF, hCG, FSH, and ovarian stromal cell-conditioned medium were examined for their potential role in regulating KIT expression in primary OSE. Because no such regulation was found, it was hypothesized that perhaps it is not the stromal cell factors but the ECM produced by the stroma that is causing the induction of KIT in the OSE cells.

For the *in vitro* studies, we used two types of ovarian surface epithelial cells. ROSE 199 is an immortalized rat ovarian surface epithelial cell line. Because immortalized cell lines are not always the most clinically relevant, we also used primary mouse ovarian surface epithelial cell cultures. ROSE 199 expressed basal levels of c-*Kit* mRNA detectable only by PCR, therefore quantitative RT-PCR (Q-RT-PCR) was used to measure changes in expression. In preliminary experiments, we showed that early passage MOSE cells do not express Kit and this provided us with an excellent opportunity to study the effects of the introduction of the c-*Kit* gene via retroviral infection. The hypothesis was that forced expression of c-*Kit* in early passage MOSE cells will increase cellular proliferation and survival of the cells.

It was also of interest to us to determine if ovarian tumours possessed the same activating mutations in the c-*KIT* gene as seen in gastrointestinal stromal tumours. Knowing the mutation status of KIT in patients with ovarian cancer would allow the use of a targeted therapeutic such as Gleevec.

The specific objectives of the project were the following:

- To determine if any ECM components (collagen I, laminin, fibronectin, collagen IV) affect morphology, proliferation, and c-*Kit* expression in mouse and rat OSE cells *in vitro.*
- To determine if culturing OSE cells at increasing density affects expression of c-*Kit* *in vitro.*
- To examine the expression of ECM components and KIT in OSE cells forming the invaginations and inclusion cysts in normal human pre- and post-menopausal ovaries by immunohistochemistry, and to determine if there is a correlation between ECM expression and KIT expression *in vivo.*
- To determine if forced expression of murine c-*Kit* by retroviral infection of MOSE cells affects cellular behaviours such as morphology, proliferation, and survival.
- To identify c-*KIT* mutations in human ovarian tumours by sequencing and Southern blot analysis.

MATERIALS AND METHODS

7. Tissue Culture

7.1. Cell Maintenance

The following cell lines were used in this project: ROSE 199 cells received from Dr. N. Auersperg (Vancouver, BC; (Adams, A.T. and Auersperg, N., 1985), NIH 3T3 (ATCC, Mannassas, VA), and Phoenix Eco cells (ATCC). ROSE 199 cells were cultured in α-minimum essential medium with phenol red dye (α-MEM; HyClone, Logan, UT) and NIH 3T3 and Pheonix cells were cultured in Dulbecco's minimum essential media (D-MEM; HyClone), all supplemented with 10% heat-inactivated 3:1 donor bovine serum:fetal bovine serum (DBS:FCS; CanSera, Rexdale, ON). Cell cultures were maintained in an incubator at 37°C equilibrated with 5% CO_2. Cells were passaged prior to reaching confluency, first by rinsing with phosphate-buffered saline (PBS; 9g/L NaCl, 0.08g/L Na_2PO_4 and 0.14g/L KH_2PO_4) and then by incubating at 37°C in 0.05% trypsin (HyClone). Once cells had detached from the dish, trypsin was inactivated with media, and cells were centrifuged at 4000 rotations per minute (rpm) for 3 min. The cell pellet was resuspended in fresh media and cell number was determined using a Coulter counter (Beckman Coulter Inc., St-Laurent, QC).

Cells were aliquoted for long-term storage into cryovials (Nalge Co., Rochester, N.Y.) with 10% dimethylsulfoxide (DMSO; Sigma-Aldrich., Oakville, ON) at a density of $1x10^6$ cells/mL. Cells were frozen at -80°C for temporary storage and transferred to liquid nitrogen for storage longer than one month. Cells were thawed in a 37°C waterbath and transferred immediately to a 100mm dish containing α-MEM and D-MEM + 10% DBS:FCS.

7.2. Isolation of Primary MOSE

Primary MOSE cells were isolated from ovaries surgically removed ovaries from 6-8 week old female CD-1, FVB/N, and ImmortoMouse mice (Charles River Laboratories, Wilmington, MA) and were housed with free access to food and water. All animals were cared for according to the Guidelines for the Care and Use of Animals established by the Canadian Council on Animal Care. Animals were euthanized by carbon dioxide asphyxiation and the ovaries were removed aseptically, with complete removal of the bursal membrane. Ovaries were placed in PBS and washed three times, then transferred to 15mL Falcon tubes (Nalge Company) containing 0.25% trypsin in PBS (Hyclone) and placed in a 37°C incubator for 40 min. Tubes were inverted three times to mechanically remove any surface epithelial cells remaining on the ovary and the supernatant containing the cells was centrifuged at 1000rpm for 10 min. The cell pellet was resuspended in fresh MOSE media [α-MEM (Hyclone) supplemented with 4% FCS (CanSera), insulin transferrin-sodium selenite (ITSS; 5 ug/ml insulin, 5 ug/ml transferrin, 5 ng/mL sodium selenite, Roche Applied Science, Laval, QC), 2.1 ng/mL epidermal growth factor (EGF, Roche), 1.05 ug/mL gentamicin (Invitrogen, Burlington, ON), and 5.2 U/mL penicillin/streptomycin (Invitrogen)].

7.3. Culture of MOSE cells

Primary MOSE cells were maintained in an incubator at 37°C equilibrated with 5% CO_2. For maintenance and experiments, MOSE cells were cultured in 6-well plates (35mm Nalge Nunc, International, Denmark) in MOSE culture medium supplemented with 4% FCS until passage 4. Cells were routinely passaged every 7-10 days upon

reaching confluence and cultured in 10% FCS once they reached passage 5. Early passage MOSE refers to less than 6-8 passages. Late passage MOSE refers to more than 10 passages.

8. Experimental Procedures

8.1. Preparation of Matrices

Multiwell plates coated with a monolayer of collagen I (rat tail), collagen IV (lathrytic mouse tumour), laminin (Engelbreth-Holm-Swarm tumour), fibronectin (human plasma), and poly D lysine (synthetic) (BD Bioscience, San Jose, CA) were washed twice with PBS and allowed to equilibrate at 37°C with fresh media for a minimum of one hour.

Fibrillar collagen I coated plates were made by coating 35mm dishes with 1mL of bovine dermal collagen consisting of 95-98% collagen I and the remainder collagen III. The fibrillar collagen I was prepared using 8 parts Vitrogen 100 (Cohesion Technologies, Palo Alto, CA), 1 part 10X sterile PBS, 0.8 parts 0.1M NaOH, and 0.2 parts sterile H_20. All components, except Vitrogen were filter sterilized with a 0.2μM filter and all components were kept on ice prior to and during mixing. The solution was adjusted to pH 7.2 using 0.1M NaOH. The collagen I was dispensed into 35mm wells using sterile plastic pipettes and incubated at 37°C overnight to allow gelation to occur. Prior to seeding of cells, the plates were equilibrated with fresh media for a minimum of 1hour at 37°C.

8.2. Culture of OSE Cells on Matrices

To study the effects of extracellular matrix components on ovarian surface epithelial cells, all experiments followed a standard experimental protocol. ROSE 199 cells were seeded on all matrices (monomeric collagen I, laminin, and fibronectin, and collagen IV) plus plastic and poly D lysine at a density of $5x10^3$ cells/35 mm well and on fibrillar collagen I at a density of $5x10^4$ cells/35 mm well. Early passage MOSE were seeded on monomeric collagen I and plastic at a density of $1x10^4$ cells/35mm well and on fibrillar collagen I at a density of $2x10^4$ cells/35 mm well. Cells were incubated at 37°C for 96 hours for ROSE 199 and 120 hours for MOSE and fresh media was supplied after 48 hours. Control (plastic) and matrix-coated dishes were handled in the same manner and all experimental groups were plated in triplicate (ROSE 199) or duplicate (MOSE) and repeated a minimum of three times. After the culture period, cells were trypsinized, resuspended in growth media and counted.

The fibrillar collagen I gels were washed twice with PBS and then digested with warmed (37°C) 2.5 mg/mL collagenase (Sigma). The collagen I was disrupted using sterile plastic pipettes and the plates were rocked twice at room temperature for 10 min with gentle pipetting in between. The ROSE 199 and MOSE cells were washed with PBS, pelleted and resuspended in 1mL of PBS to count. All cells were then pelleted at 3000 rpm for 4 min, resuspended in 350μL of RLT buffer (RNeasy Kit, Qiagen, Mississauga, ON) and frozen at -80°C until RNA extraction was performed.

8.3. Assessment of Morphology

Cells cultured on matrices were assessed daily for changes in morphology compared with cell cultured on plastic. Cells were observed for epithelial characteristics (cuboidal shape, formation of cell rafts) or mesenchymal characteristics (fibroblastic projections). Cells were photographed using a PixeLink digital imaging system (Vitana Corporation, Ottawa, ON) mounted on an inverted light microscope (Leica Microsystems Inc., Richmond Hill, ON).

8.4. Culture of Cells at Increasing Density

OSE cells were cultured at increasing cell density to determine if confluency of cells affected expression of c-*Kit* mRNA and protein. ROSE 199 cells were seeded at $1x10^3$, $5x10^3$, $10x10^3$, and $20x10^3$ cells/35mm dish for 72 hours. The confluency of the ROSE 199 cells after 72 hours was 50-55%, 70-75%, 90-95% and 100%+ respectively. Early passage MOSE cells were seeded at $27x10^3$, $35x10^3$, and $42x10^3$ cells/35mm dish for 120 hours. Confluency of MOSE cells after 120 hours was approximately 40%, 70%, and 95% respectively. Media was changed every 48 hours and following the culture period, cells were collected by trypsinization, inactivated with media, and counted. Cells were then pelleted at 3000 rpm for 4 min, resuspended in 350μLof RLT buffer and frozen at -80°C until RNA extraction was performed. Experiments were performed in triplicate (ROSE 199) or in duplicate (MOSE).

To determine if confluency affected KIT protein expression, ROSE 199 cells were seeded in six dishes at a density of $5x10^3$ cells/60mm dish and cultured for 48, 72, 96, and 120 hours. Confluency of the cells at each timepoint was approximately 30-35%, 50-

60%, 75-80% and 95-100% respectively. Following incubation, three dishes of cells at each density were washed twice in PBS and protein was extracted directly from the plates. The remaining three dishes were used for cell counts to ensure that cells were proliferating over the incubation period.

8.5. Proliferation Assay

Quantitative assessments of cell number for all culture experiments were completed using a Coulter counter. The mean number of cells was determined by calculating the average of two independent cell counts for each well. Briefly, 40μL of a 1mL cell suspension was mixed with 20mL of Isoton II (Beckman Coulter) in a counting vial. The vial was capped and inverted prior to counting to ensure mixing of the cells. The sample was then counted twice with a 6μm-18μm filter size.

9. RNA Analysis

9.1 Extraction and Quantification of RNA

Total RNA was extracted from frozen cell pellets using the RNeasy Mini-Kit (Qiagen). Cell pellets frozen at -80°C in RLT buffer were thawed at 37°C for 15 min to dissolve salts. Samples were then homogenized using a 20 gauge (0.9mm) needle and a 1mL syringe to shear contaminating DNA. Samples were processed through multiple wash/spin cycles according to the RNeasy protocol and total RNA was eluted from the silica column using 50μL of RNase free water. The RNA was then treated with DNase (Ambion, Austin, TX) to eliminate all remaining traces of contaminating DNA and incubated at 37°C for 30 min. After inactivation of the DNase enzyme, the concentration

of RNA was quantified by diluting 1μL of RNA in 49μL of RNase-free water and reading the optical density using a spectrophotometer (Eppendorf BioPhotometer). RNA samples were frozen at -80°C until needed.

9.2 Quantitative RT-PCR

9.2.1 TaqMan Quantitative RT-PCR

Taqman Q-RT-PCR was done with RNA from ROSE 199 cells cultured on ECM and at increasing densities. Reverse transcription (RT) reactions were performed using 150ng of total RNA. The RNA was reverse-transcribed and PCR amplified using the Taqman EZ RT-PCR kit (PE Applied Biosystems, Foster City, CA). All RT-PCR steps were performed on an ABI Prism 7700 Sequence Detector (PE Applied Biosystems), quantified using the cycle threshold (Ct) method, and normalized to GAPDH mRNA levels using PE-ABI supplied (rodent) primers and probe (VIC-labelled). The c-*Kit* forward (caa ggc gat ggc gtt cc) and reverse (tga tcc gcc cgt gag tg) primers and fluorescent probe (6-Fam-cgc ctc caa gaa ttg tat tca cag aga ttt -tamra.) were designed to amplify an 86bp region of exon 16. Primers and probes were used at concentrations of 600 and 200nM, respectively. The probe was designed to overlap the corresponding intron-exon boundary to block measurement of any possible genomic DNA contamination. The thermal cycling conditions for the RT-PCR step were as follows: 50°C for 2 min, 60°C for 30 min, and 95°C for 5 min, then followed by 45 cycles of PCR at 94°C for 20 sec and 60°C for 1 min.

9.2.2 Light Cycler Quantitative RT-PCR

Light Cycler Q-RT-PCR was done using RNA from experiments with MOSE cells with ovarian cancer cell lines. The RT reactions were performed using 100 ng of RNA. RNA was first incubated at 65°C for 5 min, followed by 4°C for 1 minute with 15 ng/μL random primers (Invitrogen; all components from Invitrogen unless otherwise indicated), 0.1 mM of each dNTP (Boerhringer Mannheim), and RNAse free water to a total volume of 13 μL. The sample was brought to a total volume of 20 μL with 1X First Strand Buffer, dithiothreitol (DTT), RNase inhibitor, and 200 U Superscript RT II and incubated at 25°C for 5 min, 50°C for 50 min, and 70°C for 15 min. Genomic DNA contamination was excluded in each PCR reaction using a control for each sample that was generated in the absence of reverse transcriptase.

Oligonucleotide primers for PCR were designed to amplify c-*Kit* and custom ordered from Sigma Genosys. The housekeeping genes β-actin was amplified as references for mRNA quantification. The primer sequences were as follows: c-*Kit* (5'-AGG AGA TAA ATG GAA ACA ATT ATG T-3' and 3'-TTG AGC ATC TTT ACA GCG ACA GTC A-5') and β-actin (5'-GTG GGC CGC CCT AGG CAC CAG-3' and 3'-CTC TTT GAT GTC ACG CAC GAT TTC-5'). For the PCR, 2 μl of cDNA was amplified in a reaction mixture (total volume 20 μl) containing 2 μl 5x reaction buffer, 0.6 μl $MgCl_2$ (1.5 mM), 0.4 μl dNTP mix (0.2 mM), 0.4 μl each of forward and reverse primers (0.5 μM each primer), 0.4 μl BSA (25 mg/ml), 0.33 μl SYBR Green 1 (1/60,000; Molecular Probes, Eugene, OR), 0.2 μl temperature-release Taq DNA polymerase (Platinum Taq Polymerase) and 13.27 μl ddH_2O.

Real-time PCR was carried out using LightCycler technology (Roche Diagnostics). The reaction conditions were as follows: pre-denaturation (95°C for 30 sec), 35 PCR cycles consisting of denaturation (95°C for 30 sec), annealing (58°C for 10 sec for β-actin and 52°C for 10 sec for c-*Kit*), extension (72°C for 22 sec for β-actin and 72°C for 8 sec for c-*Kit*). Fluorescence data was acquired after the extension phase of each cycle, during an additional step at approximately 3°C below the melting temperature of each product (see Figure 5A). This excluded quantification of any non-specific products. In order to quantify mRNA levels, a standard curve was generated for each transcript by amplifying serial dilutions (1, 1/5, 1/10, 1/20, 1/30) of control cDNA known to express the gene of interest (see Figure 5B). Samples of mouse oocyte, MOSE RNA, and negative controls containing RNA and no reverse transcriptase enzyme were amplified using Light Cycler RT-PCR and samples were separated on a 1% agarose gel at 100V to confirm product size (195bp for Kit, 540bp for β-actin). DNA ladder (100bp; Invitrogen) was included to determine band size (see Figure 5C). There is no detectable Kit or GAPDH band in lanes 3 and 5 indicating no genomic DNA contamination in the reaction. Kit and GAPDH bands can be seen in all other lanes which confirm that the RT-PCR reaction is correctly amplifying the genes of interest.

10. Protein Analysis

10.1 Extraction and Quantification of Protein

Cells were prepared for protein extraction when 70-90% confluent by washing twice in PBS. Protein was extracted by lysing cells in RIPA buffer (50mM TrisHCl pH7.4, 150mM NaCl, 1mM phenyl methyl sulfonyl fluoride, 1mM sodium orthovanadate,

FIGURE 5 – Q-RT-PCR graphs and control curve

Real time quantitative RT-PCR was done on RNA samples to measure changes in expression of c-*Kit* mRNA. Panel A shows a sample melting curve for the c-*Kit* reaction. The corresponding control curve is seen in B. RT-PCR samples were separated on a 1% agarose gel to confirm fragment size. Panel C shows samples from a KIT (195 bp) and B-actin (540 bp) Q-RT-PCR analysis. Lanes 3 and 5 have no detectable Kit or GAPDH bands indicating no genomic DNA contamination in the reaction. Kit and GAPDH bands can be seen in all other lanes which confirm that the RT-PCR reaction is correctly amplifying the genes of interest.

A

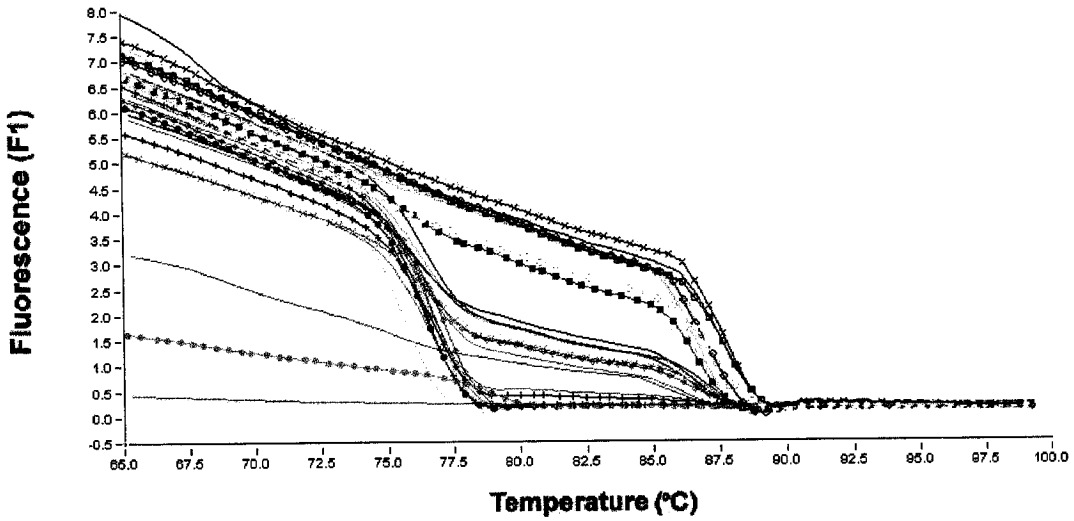

B

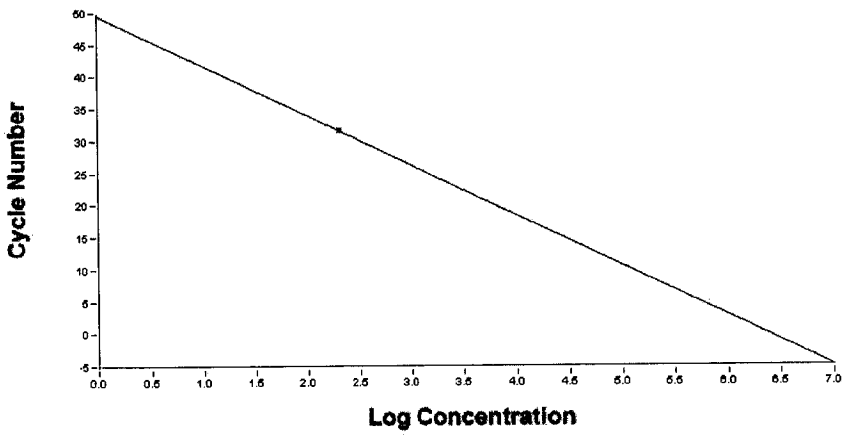

C

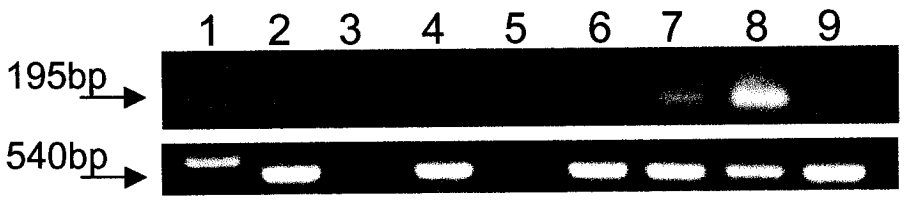

1- 100 bp marker

2- oocyte RNA

3- oocyte no RT

4- MOSE RNA (low density)

5- MOSE no RT

6- MOSE (moderate density)

7- MOSE (moderate density)

8- MOSE (high density)

9- MOSE (high density)

10mM sodium pyrophosphate, 10mM sodium fluoride, 1 μg/mL aprotinin, 1 μg/ml leupeptin). Cells were scraped with a rubber policeman into a microfuge tube. Samples were incubated on ice for 10 min with frequent vortexing, and centrifuged at 14000rpm for 10 min at 4°C. The protein supernatant was removed and quantified using the BioRad protein assay kit (BioRad, Mississauga, ON) and the absorbance was read at a wavelength of 595nm with a Beckman DU40 spectrophotometer. Protein was kept at -80°C for storage.

10.2 SDS-Page and Western Blotting

Protein samples (50 μg) were separated on a one-dimensional NuPage Novex Bis-Tris acrylamide gel with a 4-12% gradient (Invitrogen) in a vertical electrophoresis system containing 1X NuPage MOPS running buffer (1M MOPS, 1 M Tris, 69.3mM SDS, 20.5mM NaEDTA; all components from BioShop, Burlington, ON). Samples were loaded with 10% 1.0 M DTT. The gels were then transferred to a nitrocellulose membrane (Hybond C Extra, Amersham Biosciences, Arlington Heights, IL) in circulating 1X NuPage transfer buffer (500mM Bicine, 500mM Bis-Tris, 20.5mM NaEDTA; BioShop). All immunoblotting steps were performed in a humidified chamber with constant shaking at the temperature indicated. Membranes were first blocked for 1 hour at room temperature in 5% skim milk in TBS/T (180mM NaCl, 10mM Tris, 0.05% Tween-20, pH 7.4) then incubated overnight at 4°C with the following primary antibodies diluted in blocking solution at the concentration indicated: 1) rabbit polyclonal human KIT (Santa Cruz Biotechnology, Santa Cruz, CA) at 1:500, 2) mouse polyclonal E-cadherin (Santa Cruz) at 1:500, 3) mouse monoclonal GAPDH (Abcam, Cambridge,

UK) at 1:2000 or 4) mouse monoclonal α-tubulin (Oncogene Research Products, San Diego, CA) at 1:500. Blots were washed in TBS/T three times for 5 min prior to incubating with the appropriate horseradish peroxidase (HRP) conjugated IgG secondary antibody (anti-mouse; KPL, Gathersburg, MD and anti-rabbit; Cedarlane Laboratories, Hornby, ON) at a dilution of 1:4000 for 1 hour at room temperature. Blots were washed in TBS/T three times for 10 min and protein bands were visualized using a chemiluminescence detection kit (ECL plus western blotting detection kit; Amersham Biosciences, Piscataway, NJ). Blots were then developed onto Kodak X-Omat Blue XB-1 film (Rochester, NY).

10.3 Immunohistochemistry

Immunohistochemistry for extracellular matrix components, KIT, and inhibin was done on serial sections from formalin-fixed paraffin-embedded human ovaries to determine location and level of expression in ovaries. Five micron sections were cut from pre- and post-menopausal ovaries removed prophylactically. Sections were all deparaffinized in xylene and rehydrated in decreasing concentrations of ethanol. Every fifth slide was stained with hemotoxylin (Fisher Scientific International, Ottawa, ON) and eosin (Shandon Scientific, Cheshire, UK). Heat induced antigen retrieval using citrate buffer was done on sections stained for KIT, collagen type I, fibronectin, collagen type IV, and inhibin (slides incubated in pre-heated 10mM sodium citrate pH 6.0 for 20 minutes at 100°C using a pressure cooker). Proteolytic induced epitope retrieval using pepsin buffer was used for sections stained for laminin and collagen type III (slides incubated in pre-heated 0.5% pepsin in 10mM HCl for 30 minutes at 37°C). All

incubations were done in a humidified chamber at room temperature unless otherwise stated. All slides were blocked for endogenous peroxidase activity in 3%H_2O_2 (Sigma) for 10 min at room temperature, washed in Stockholm-PBS (S-PBS) three times for 5 min, and incubated in serum-free protein block (DakoCytomation; Missassauga, ON) for 10 min. Samples were then incubated with the following antibodies at the indicated time and concentration; 1) rabbit anti-human KIT (DakoCytomation), 1:10, overnight; 2) rabbit anti-human collagen type I (Cedarlane Laboratories), 1:50, overnight; 3) monoclonal mouse anti-human collagen type III (BioGenex, San Ramon, CA), 1:50, 30 min; 4) monoclonal mouse anti-human collagen type IV (DakoCytomation), 1:25, overnight; 5) monoclonal mouse anti-human laminin (Novocastra Laboratories, Newcastle, UK), 1:50, 1 hour; 6) rabbit anti-human fibronectin (DakoCytomation), 1:400, overnight; and 7) monoclonal mouse anti-inhibin (DakoCytomation), 1:50, overnight. Following incubation with the primary antibody, the slides were washed in S-PBS three times for 5 min and then incubated in EnVision Dual Link HRP Labelled Polymer (rabbit/mouse, DakoCytomation) for 30 min. Sections were washed in S-PBS three times for 5 min and developed in diaminobenzidine (DAB) as a substrate (0.2% DAB, 0.001%H_2O_2) for 5 min with stirring. After rinsing in distilled water, slides were counter stained in hematoxylin for 1 minute, rinsed in running tap water, dipped five times in ammonia water, and rinsed in water. Slides were then dehydrated and mounted for analysis and photography. Control tissue for each antibody was also stained (KIT in breast tumour tissue; collagen I in skin tissue; laminin in basement membrane of ovary; fibronectin in tonsil tissue; collagen III in skin tissue; collagen IV in breast tumour tissue).

Serial sections from each ovary were assessed on a Zeiss Axioskop2 (Carl Zeiss International, Thornwood, NY) for expression and intensity of expression in (KIT) or around (ECM) the ovarian surface epithelial cells forming invaginations and inclusion cysts. Invaginations were counted if more that 5 OSE deep. All abnormal structures within the slides were counted and assessed for positive staining. Intensity of positive expression was scored on a scale of 1(+) to 4 (++++) where + represents mild positive staining, ++ represents moderate staining intensity, +++ represents staining intensity similar to positive control tissues, and ++++ represents more intense staining than the positive control.

11. Retroviral Infection

11.1 Retroviral Constructs

Constructs for pRuf neo and pRuf murine c-*Kit* were obtained from Dr. L. Ashman (Callaghan, New South Wales, Australia). The pHIT 111 construct which expresses the lacZ gene and is used as a control to determine transfection or infection efficiency was obtained from Dr. J. Bell (Ottawa, ON).

11.2 Infection of Retroviral c-*Kit* into MOSE cells

Recombinant viruses of the pRuf murine c-*Kit*, pRuf neo, or pHIT111 vectors were generated by transfecting the ecotropic packaging cell line, Phoenix Eco using Fugene 6 (Roche Molecular Biochemicals). Phoenix cells were plated in 100mm plates and when 50% confluent, were transfected with 18 μL of Fugene 6 and 6 μg of DNA. Media was replenished after 24 hours. At this time, MOSE and NIH 3T3 cells were seeded in 6 well

plates at approximately 2 x 10^5 cells/35 mm well. Medium containing released virus produced from near-confluent populations of Phoenix cells was collected after 24 hours, filtered (0.45μm) and used to infect MOSE and NIH 3T3 cells. Growth media was removed from the target cells and 2 mL of retroviral media was mixed with 20 μL of hexadimethrine bromide (polybrene 0.8 mg/mL; Sigma) and added to the cells. The plates were incubated in a 32°C incubator for 12 min and then centrifuged at 2500rpm for 30 min at 32°C. Retroviral media was then aspirated and replaced with fresh growth media and the cells were incubated at 37°C. The infection process was repeated 18 hours later.

Expression of β-galactosidase was determined 24 hours after transfection (Phoenix Eco cells) or infection (MOSE or NIH 3T3) with pHIT111 by washing cells twice with PBS, fixing cells with 0.4% glutaraldehyde, and staining for β -galactosidase activity with X-gal staining solution [8mM $K_3Fe(CN)_6$, 8mM $K_4Fe(CN)_6 \cdot 3H_2O$, 2mM $MgCl_2$, 0.4mg/mL of X-Gal (5-bromo-4-chloro-3-indolyl-β-D-galactopyranoside (BioWorld, Dublin, OH)]. Efficiency of transfection or infection was determined 24 hours later by counting the percentage of blue cells. Transfection efficiency of the Phoenix cells was 100%. Infection efficiency for the NIH 3T3 cells and MOSE cells (early and late passage) cells was 100% and 70%, respectively.

11.3 Proliferation Assays

Rate of proliferation was determined by seeding MOSE or NIH 3T3 cells infected with pRuf murine c-*Kit* or mock infected in 24 well plates at a density of $2x10^4$ cells/well. Assays were done for late passage MOSE in 4% and 0.2% FCS, for early

passage MOSE in 10% or 1% FCS, and for 3T3 cells in either 10% or 0% DBS:FCS (3:1). Cell number was determined using a Coulter counter at 24, 48, 72 and 96 after plating. Experiments were performed twice in duplicate, with each sample being counted twice.

11.4 Confirmation of construct expression

Expression of the murine c-*Kit* gene in the infected cells was confirmed using western blotting techniques as described in section 10. Protein was extracted from confluent 35 mm dishes of MOSE or NIH 3T3 cells using 35 μL of RIPA buffer. SDS-PAGE gels were loaded with 50 μg of protein and immunoblotted using the polyclonal human KIT and monoclonal human GAPDH antibodies described in section 10.2.

12. Mutation Analysis – Large Mutations

12.1 Isolation of Tumour DNA

Frozen tumour sections were obtained from the Ovarian Cancer Tumour Bank and 1cm^2 pieces were used for the extraction. The tissue was digested overnight at 58°C in 500μL of DNA lysis buffer (10mM Tris HCl pH 8.3, 17mM KCl, 3.5mM $MgCl_2$, 20mM DTT, 1.7μM SDS and 0.05 mg/mL Proteinase K). An equal volume of phenol:chloroform (1:1, Sigma-Aldrich) was added to the sample and incubated at room temperature for 5 min with frequent vortexing. Following centrifugation at 12000 rpm for 5 min at 4°C, the aqueous layer was removed from all samples, transferred to new microfuge tubes, and two volumes of isopropanol was added. Samples were centrifuged at 14000 rpm for 20 min at 4°C. Following the spin, the supernatant was decanted and

the pellet was washed in 70% ethanol and centrifuged at 14000 rpm for 15 min at 4°C. The ethanol was decanted and the pellets were air dried for 5 min and vacuum dried for 10 min on medium speed. The DNA pellet was resuspended in 250μL of TE (10 mM TrisHCl pH 8.0 and 0.1mM EDTA) and quantified using an Eppendorf BioPhotometer and stored at 4°C until needed.

12.2 Restriction Digest and Gel Electrophoresis of DNA samples

DNA was digested with restriction enzyme BamHI (New England Biolab). Five μg of DNA was digested overnight at 37°C with 1unit of enzyme, 10% of the appropriate buffer and supplemented with 10% BSA (New England BioLabs). Digested DNA samples were loaded with 4 μL of loading dye onto a 1% agarose gel containing ethidium bromide. 20 μL of 100bp and 1Kb ladder (Invitrogen) were also loaded. Gels were run at 80V for 2 hours and DNA smears were visualized and captured with a UV transilluminator and a thermal printer (DiaMed, Missassauga, ON). The gels were denatured in buffer (1.5M NaCl, 0.5M NaOH) for 40 min and rinsed and neutralized in buffer (1.0M Tris pH 8, 1.5M NaCl) for 40 min.

12.3 Southern Transfer and Hybridization

DNA was transferred overnight to Hybond N nylon membrane (Amersham) using capillary action in 4X saline sodium citrate (35.06g sodium chloride and 17.64g sodium citrate in 1L of water). Following transfer, membranes were cross-linked at 125mJ by UV irradiation and dried. When ready to probe, membranes were prehybridized (2 hours) at 42°C in 30 mL of prehybridization buffer (100 mL solution consisting of 30 ml

of 20X SSC, 2.5 ml of 20% SDS, 50 ml of formamide, 5 ml of 100X Denhardts, and 12.5 ml of H_2O) that was warmed to 55°C.

The full length human c-*KIT* fragment was digested from pTRE-c-*KIT*, excized from the agarose gel and resuspended in 225 μL of TE. 25ng of cDNA was labeled with [^{32}P] and the Megaprime Probe Labelling Kit (Amersham) and incubated at 37°C for 45 min. The probe was diluted 1:2 in TE, cleaned by passing it through 900 μL of Sephadex G-50 in a spin column, boiled at 100°C for 5 min and quenched on ice for 2 min. The probe was then added to the prehybridisation tube containing the membranes and incubated overnight in a rotating 42°C chamber. The blots were washed twice for 10 min in 2% SSC + 1% SDS and then washed twice for 10 min in warmed (55°C) 0.5% SSC + 0.1% SDS at 65°C. All washes were done with shaking. Washed blots were then exposed to phosphor screens overnight and scanned using a PhosphorImager SI (version 4.0, Molecular Dynamics, Sunnyvale, CA) and analysed using ImageQuaNT software (version 4.2a, Molecular Dynamics).

13. Mutation Analysis – Small Mutations

13.1 Laser Capture Microscopy

Gleevec is currently in a Gynecologic Oncology Group Phase II clinical trial for treatment of patients with persistent or recurrent epithelial ovarian or primary peritoneal carcinoma. One of the goals of the study is to determine the presence or absence of c-*KIT* mutations in these tumours. Tumour samples for this trial were obtained with full consent from the patients. Using the Arcturus Laser Capture Microscopy System and CapSure HS caps, approximately 1000 tumour cells were isolated from 10 micron

sections of paraffin embedded formalin-fixed tissue. Prior to isolation, the tissue had been deparaffinized in xylene and rehydrated in ethanol. Two sections were obtained for every patient and analysed twice.

13.2 Isolation of Tumour DNA

DNA was extracted using the Picopure DNA extraction kit (Arcturus, Mountain View, CA), incubated overnight at 58°C, and eluted in 10μL of resuspension buffer. When unable to obtain sufficient quantities of DNA from the laser dissected section, DNA was isolated from the entire 10 micron tissue section. The slides were first deparaffinized and rehydrated, the tissue section was covered in 100μL of DNA Extraction Buffer (10mM Tris-Cl, 50mM KCl, 2M $MgCl_2$) with proteinase K (60 μg/100μL) and scraped using a yellow tip. The solution was incubated at 58°C overnight. The DNA was isolated, precipitated, and resuspended in 100 μL of EB buffer (Qiagen). All DNA samples were stored at 4°C.

13.3 PCR

PCR reactions for exon 10-11 and exon 14 of the c-*KIT* gene were performed using the Advantage 2 Polymerase Kit and 2μL of tissue sample DNA in a 10μL reaction (1X Advantage 2 buffer, 1mM dNTPs, 0.4pM primers, and 1X Advantage 2 Polymerase). The forward (exon 10, 5'-ggt ttc gta atc gta gct ggc-3' and exon 14, 5'-atg gcc atg acc acc ctt ggg-3') and reverse (exon 10-11, 5'-gcc tgt ttc tgg gaa act ccc-3' and exon 14, 5'-att gca aac cct tat gac ccc-3') primers were ordered from Sigma Genosys. Cycling parameters for all reactions were an initial 3 minute denaturation at 94°C, followed by 5

cycles of 94°C for 5 sec and 72°C for 1 minute, followed by 5 cycles of 94°C for 5 sec and 70°C for 1 minute, then 30 cycles of 94°C for 5 sec and 68°C for 1 minute and a final elongation at 72°C for 10 min. Samples were loaded on a 1% agarose gel and separated at 100V for approximately 1 hour. Bands were stained with ethidium bromide and visualized using a UV transilluminator.

13.4 Sequence Analysis

PCR products were sent for sequencing according to the requirements provided by the Ottawa Genome Centre DNA Sequencing Facility. Sequences for each PCR product were aligned to the c-*KIT* gene sequence (L04143; (Vandenbark, G.R. *et al.*, 1992) using Vector NTI 8.0 (University of North Carolina Centre for Bioinformatics; Chapel Hill, NC) and aligned chromatograms were printed and analysed to identify any mutations.

14. Statistical Analyses

All cell counts are duplicate counts from at least 2 replicates of 3 independent experiments and are expressed as mean count ± standard error of the mean (SEM). Multiple culture groups were statistically compared using analysis of variance (1-way ANOVA). When whole group differences were determined by ANOVA, a Bonferroni's post t test was used to determine significance ($p<0.05$) between culture groups.

Expression levels of c-*Kit* mRNA determined by Q-RT-PCR are expressed as fold change ± SEM of c-*Kit* mRNA relative to control mRNA (β-actin or GAPDH). These fold changes represent duplicate measurements from 3 replicates of 2 (MOSE) or 3 (all other cell types) independent experiments. Treatment groups were statistically compared

using analysis of variance (1-way ANOVA). When whole group differences were determined by ANOVA, a Bonferroni's post test was used to determine significance ($p<0.05$) between culture groups.

For growth curves of cells infected with murine c-*Kit*, cell counts are done twice for 2 experiments done in triplicate and represent the mean count ± standard error of the mean. To compare between groups at each timepoint, a 2-way ANOVA test was performed with significance inferred at $p<0.05$

Two-tailed chi-squared tests were done to determine if a significant association between expression of individual ECM components and KIT expression existed. Statistical significance was set at $p<0.05$. All statistical tests were performed using GraphPad Prism software (Version 3.2m GraphPad Software, San Diego, CA).

RESULTS

The purposes of this research project were to examine the effects that extracellular matrices have on OSE cell morphology, proliferation and expression of c-*Kit* as well as to determine if cellular density of OSE cells affects c-*Kit* expression. The rat ovarian surface epithelial cell line ROSE 199 and early passage MOSE cells were cultured on various ECM components and at various densities. Proliferation, mRNA, and protein expression levels were assessed using cell counts, Q-RT-PCR for c-*Kit*, and Western blotting for Kit. Normal human ovary sections were also analysed for co-expression of KIT and ECM components by immunohistochemistry. We also analysed human ovarian tumours for mutations in the c-*KIT* gene by sequencing and Southern blot analysis.

15. Effect of extracelluar matrices on OSE cell morphology, proliferation, and c-*Kit* expression.

ROSE 199 and early passage MOSE cells were cultured on various extracellular matrices and changes in cellular morphology, proliferation, and expression of c-*Kit* mRNA were analysed. Figure 6 shows the effect of monomeric extracellular matrices: collagen I (B), laminin (C), fibronectin (D), and collagen IV (E) on ROSE 199 cell morphology compared to plastic (A) and poly D lysine (F) controls. There were no significant changes in cellular morphology while cultured on matrices. ROSE 199 cells maintained a cobblestone appearance. Proliferation of ROSE 199 cells cultured on matrices was also not affected (Figure 7A) as compared to control (both plastic and poly D lysine) and there was no affect on expression level of c-*Kit* mRNA detectable by Q-RT-PCR (Figure 7B).

FIGURE 6 – ECM has no effect on ROSE 199 cell morphology.

ROSE 199 cells were seeded in triplicate at a density of $5x10^3$ and cultured on extracellular matrix-coated plates; collagen I (B), laminin (C), fibronectin (D) and collagen IV (E); as well as plastic (A) and poly D lysine (F) control plates for 96 hours. Live cells were photographed at 100X magnification.

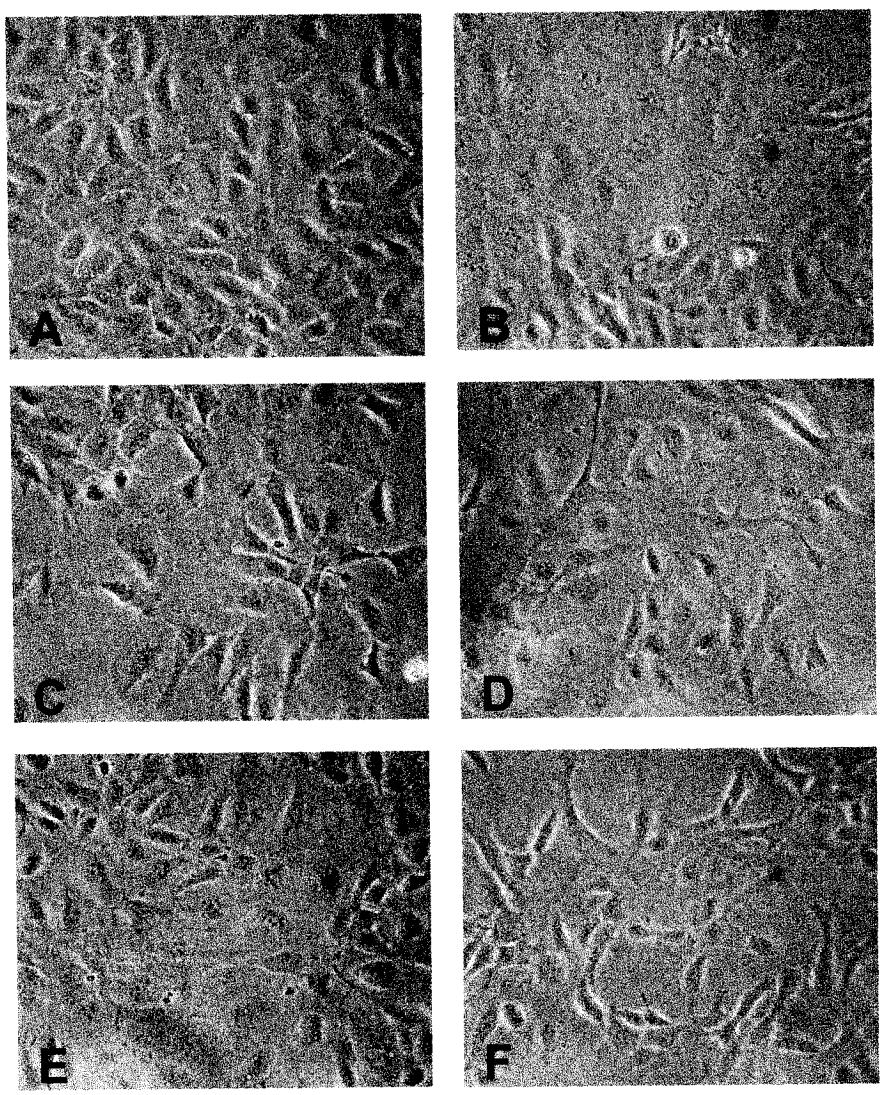
A
B
C
D
E
F

FIGURE 7 – ECM has no effect on ROSE 199 cell proliferation or expression of c-*Kit* mRNA.

A) ROSE 199 cells were seeded at a density of $5x10^3$ and cultured on extracellular matrix-coated plates as well as plastic control plates for 96 hours. Cells were counted in duplicate and were calculated as mean counts relative to the control ± SEM where each data point represents 3 experiments done in triplicate. The control group was set to 100 for comparison.

B) After 96 hours of culture, RNA was collected and used for Q-RT-PCR analysis for c-*Kit*. Changes in c-*Kit* mRNA expression were calculated as fold change relative to control mRNA (GAPDH). Values are presented as mean ± SEM where each data point was derived from duplicate Q-PCR analysis of 3 individual experiments done in triplicate.

A

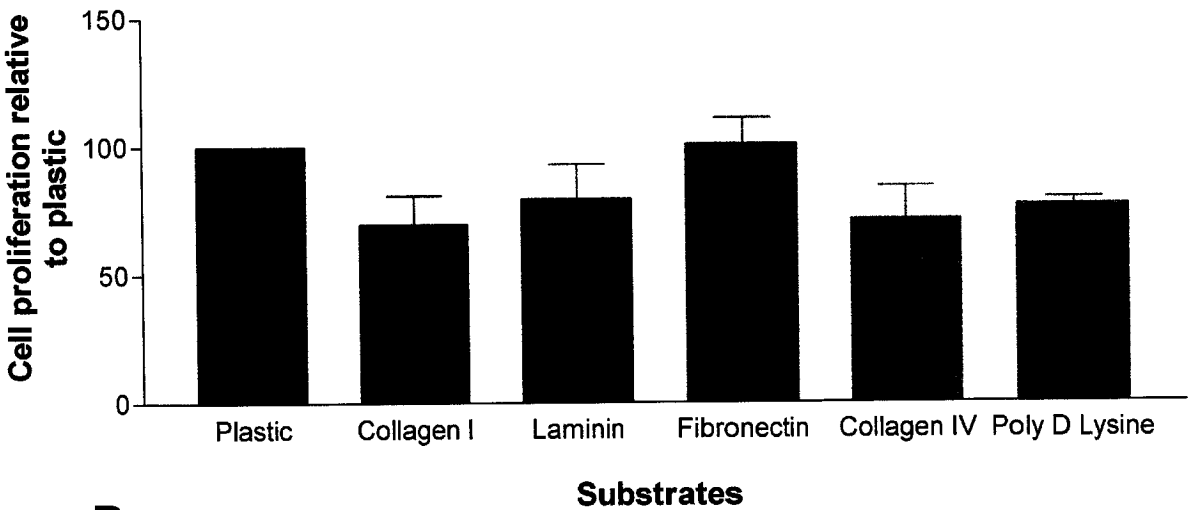
Cell proliferation relative to plastic
150
100
50
0
Plastic
Collagen I
Laminin
Fibronectin
Collagen IV
Poly D Lysine
Substrates

B

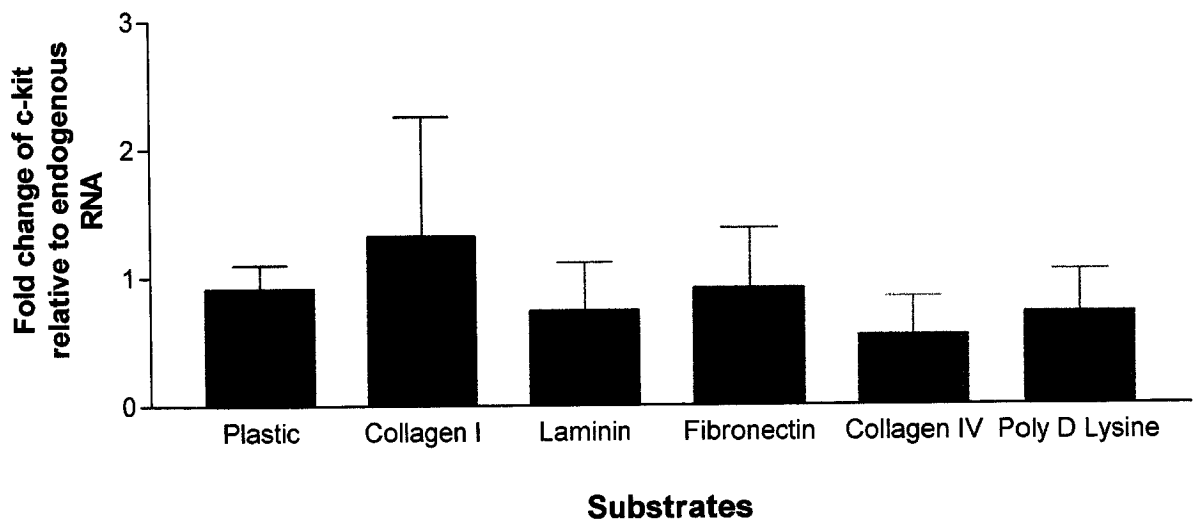
Fold change of c-kit relative to endogenous RNA
3
2
1
0
Plastic
Collagen I
Laminin
Fibronectin
Collagen IV
Poly D Lysine
Substrates

Due to the possible implications arising from the immortalized nature of the ROSE 199 cell line, the experiments were repeated with early passage MOSE cells as perhaps they represent a better model of normal OSE. Since MOSE cells are very difficult to isolate and culture, cells were only cultured on monomeric collagen I and this had a significant effect on proliferation (Figure 8A). Cells proliferated significantly more slowly on collagen I compared to plastic. After 96 hours, the total number of MOSE cells on collagen was 31% less than the number of MOSE on plastic. Q-RT-PCR for c-*Kit* mRNA revealed no change in expression level (Figure 8B). ROSE 199 and MOSE were then cultured on fibrillar collagen I to better simulate the extracellular matrix present in the ovarian stroma. Figure 9A shows the drastic morphological changes seen in the MOSE cells when cultured on fibrillar collagen I compared to plastic. The same changes can be seen in the ROSE 199 cells cultured on the fibrillar matrix (Figure 9B). The cells lost their epithelial phenotype and became much more fibroblastic in shape. The fibrillar collagen I also caused a significant decrease in proliferation of MOSE (Figure 10A) and ROSE 199 (Figure 10B). To assure that cells were plating onto the fibrillar collagen I and plastic at equal rates and not undergoing apoptosis, floating cells were counted in the media after 24 hours. This showed that 98% of cells were plating and less than 2% were found floating in the media on both collagen I and plastic. RNA was collected from the MOSE cells cultured on plastic and collagen I and analysed for expression of c-*Kit* by RT-PCR. Figure 11 shows a 195bp c-*Kit* band in the positive control lane, but not in the MOSE cultured on plastic or fibrillar collagen I.

FIGURE 8 – Collagen I significantly decreases proliferation but does not affect expression level of c-*Kit* mRNA in early passage MOSE cells.

A) Early passage MOSE cells were seeded at a density of $1x10^4$ (dashed line) on monomeric collagen I coated and plastic (control) plates and cultured for 96 hours. Cells were counted in duplicate and were calculated as mean counts relative to the control ± SEM where each data point represents three experiments done in duplicate. The asterisk indicates statistical significance ($p<0.05$).

B) RNA was extracted and used for Q-RT-PCR for c-*Kit*. Changes in c-*Kit* mRNA expression were calculated as fold change relative to control mRNA (β-actin). Values are presented as mean ± SEM where each data point was derived from duplicate Q-PCR analysis of three experiments done in duplicate.

A

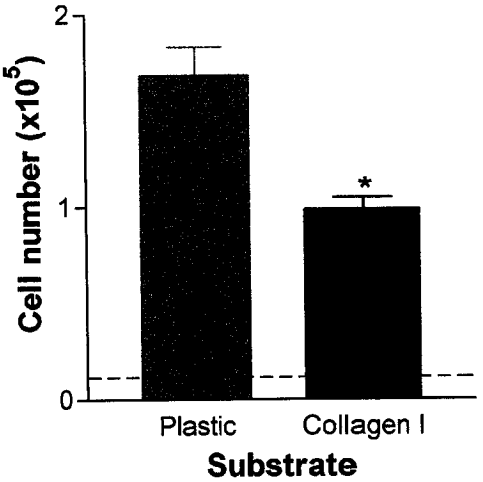
2
1
0
Cell number (x10^5)
*
Plastic
Collagen I
Substrate

B

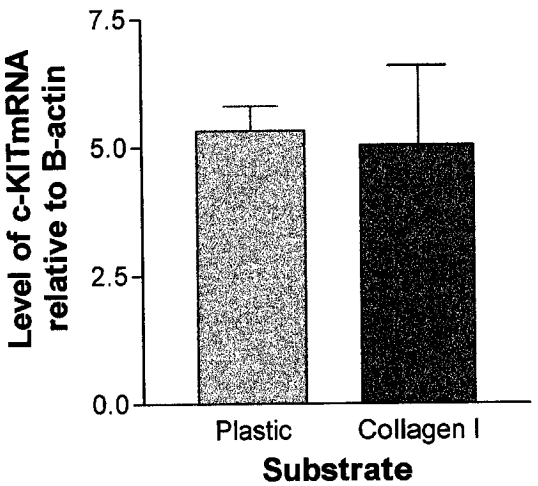
7.5
5.0
2.5
0.0
Level of c-KITmRNA relative to B-actin
Plastic
Collagen I
Substrate

FIGURE 9 – Fibrillar collagen I significantly affects morphology of ROSE 199 and early passage MOSE cells.

MOSE (A) and ROSE 199 (B) cells were seeded in duplicate on plastic or fibrillar collagen I coated plates at a density of $2x10^4$ (MOSE) cells and $5x10^4$ cells/35mm well (ROSE 199), respectively. The morphology of the cells was observed and photographed after 72 hours of culture. Magnification 100X.

A

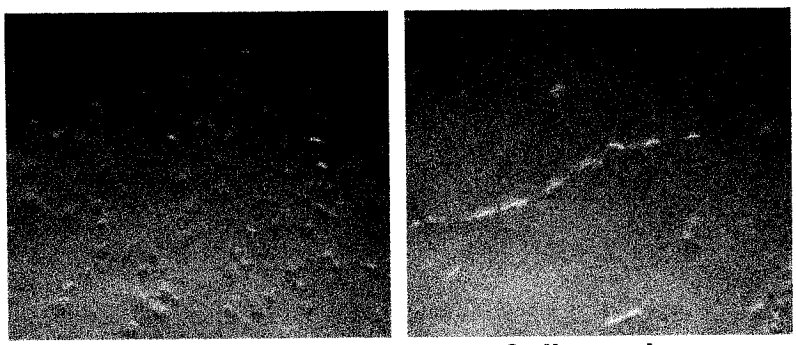

Plastic Collagen I

B

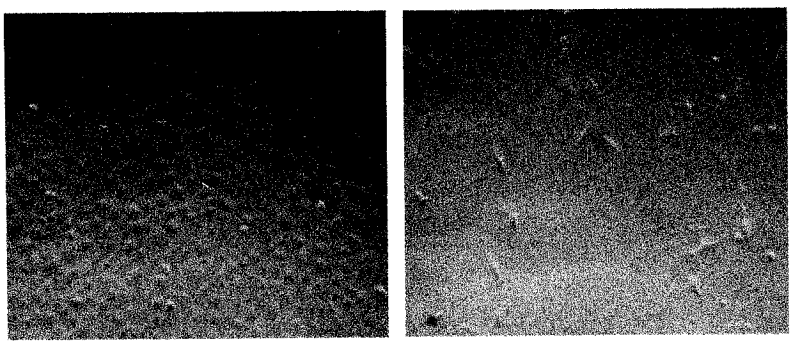

Plastic Collagen I

FIGURE 10 – Fibrillar collagen I significantly decreased proliferation of early passage MOSE and ROSE 199.

MOSE (A) and ROSE 199 (B) cells were seeded at a density of $2x10^4$ (MOSE - dashed line in A) and $5x10^4$ (ROSE 199 - dashed line in B) on fibrillar collagen I or plastic plates. Cells were counted in duplicate after 72 hours and counts were calculated as mean counts ± SEM where each data point represents two experiments done in duplicate (MOSE) or triplicate (ROSE 199). The asterisk indicates statistical significance ($p<0.05$).

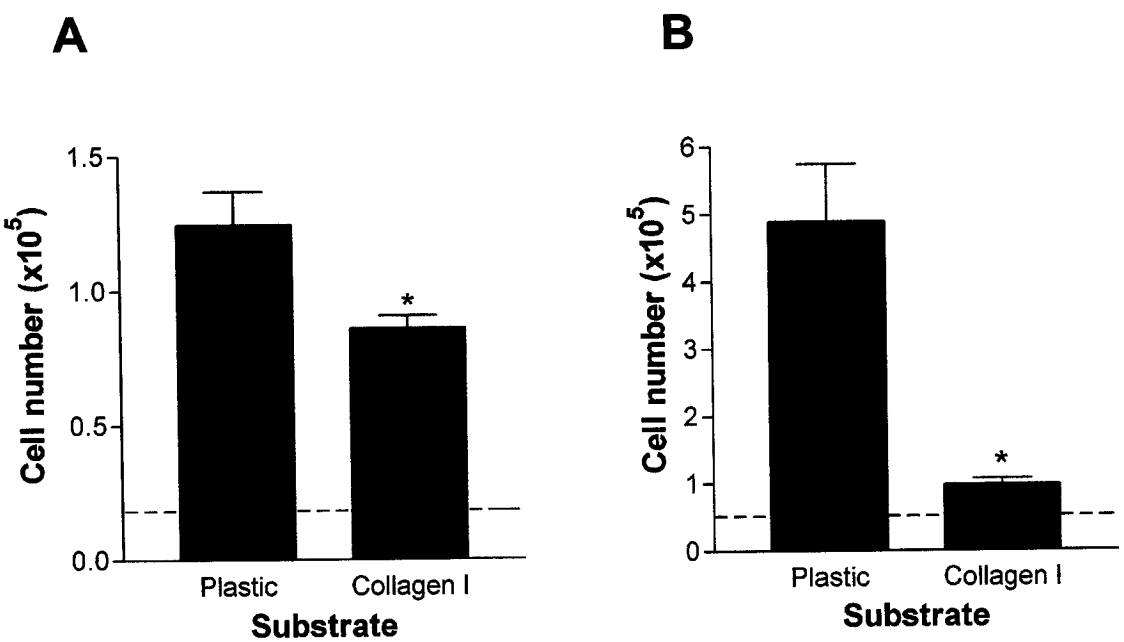
A
B
Cell number (x10^5)
1.5
1.0
0.5
0.0
6
5
4
3
2
1
0
*
*
Plastic
Collagen I
Substrate

FIGURE 11 – Culture on fibrillar collagen I does not induce expression of KIT in MOSE.

RNA was isolated from MOSE cells cultured on plastic or fibrillar collagen I for 72 hours and amplified by RT-PCR for c-*Kit*. RNA from the mouse cell line MC-9 was used as a positive control (C). A 195 bp c-*Kit* band can be seen in the positive control lane. C-*Kit* cannot be detected in the MOSE cells cultured on plastic or collagen I. Genomic DNA contamination was excluded in each PCR reaction using a control for each sample that was generated in the absence of reverse transcriptase (RT-).

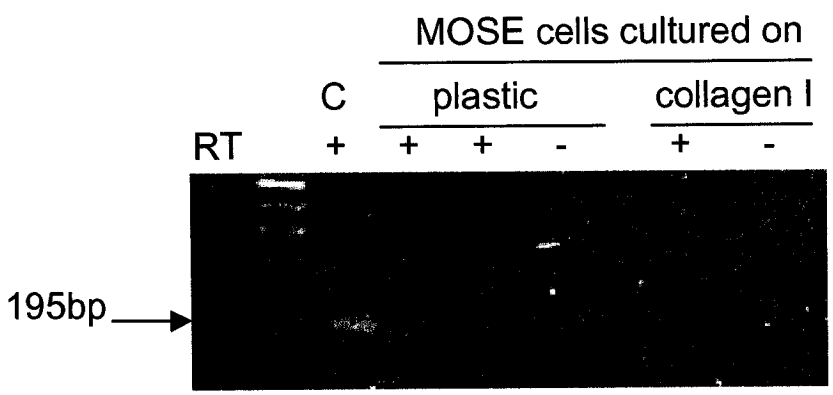
MOSE cells cultured on
C
plastic
collagen I
RT
+
+
+
-
+
-
195bp

16. Effect of cellular density on expression levels of c-*Kit* in OSE cells.

To assess whether cell confluency impacted the expression of c-*Kit*, two experiments were performed. First, ROSE 199 were cultured in their maintenance media at four different seeding densities for 96 hours. After 96 hours, cells were counted to assess proliferation and RNA was extracted for Q-RT-PCR. Cells were approximately 50-55% confluent when plated at $1x10^3$, 70-75% confluent when plated at $5x10^3$, 90-95% confluent when plated at $1x10^4$, and over 100% confluent when plated at $2x10^4$. Cell numbers for each of these estimated confluencies can be seen in Figure 12A. Q-RT-PCR results for c-*Kit* revealed that expression increased as cell density increased. At the lowest confluency, c-*Kit* mRNA is undetectable, despite abundant expression of the β-actin housekeeping gene (Figure 12B).

Secondly, ROSE 199 were seeded at $1x10^4$ cells /60 mm dishes and cultured for up to 120 hours. Proliferation and KIT protein expression level were quantified at 24 hour intervals. Cells were approximately 30-35% confluent after 48 hours, 50-60% confluent after 72 hours, 75-80% confluent after 96 hours, and 95-100% confluent after 120 hours. The actual cell numbers that correspond to these cell confluencies are shown in Figure 13A. Analysis of expression of Kit protein at the increasing confluencies revealed an interesting trend: expression of Kit in ROSE 199 cells increased as the confluency increased, albeit the levels were still very low compared to control (Mc-9 cells). In fact, Kit protein could not be detected in the ROSE 199 cells cultured at the lowest confluency (30-35%; Figure 13 B).

FIGURE 12 – Culture of ROSE 199 at increasing confluencies increases expression of c-*Kit* mRNA.

A) ROSE 199 cells were seeded at increasing densities in 35mm plates. After 96 hours of culture, cells were counted in duplicate and were calculated as mean ± SEM where each data point represents three individual experiments done in duplicate.

B) RNA was extracted from ROSE 199 cells cultured at increasing densities and analysed by Q-RT-PCR for c-*Kit*. Changes in c-*Kit* mRNA expression were calculated as fold change of c-*Kit* expression relative to control mRNA (β-actin). Values are presented as mean ± SEM where each data point was derived from duplicate Q-RT-PCR analysis of three individual experiments done in duplicate.

Different lowercase letters (a, b, c) above the bars indicate statistically significant differences ($p<0.05$) between the groups of that graph.

A

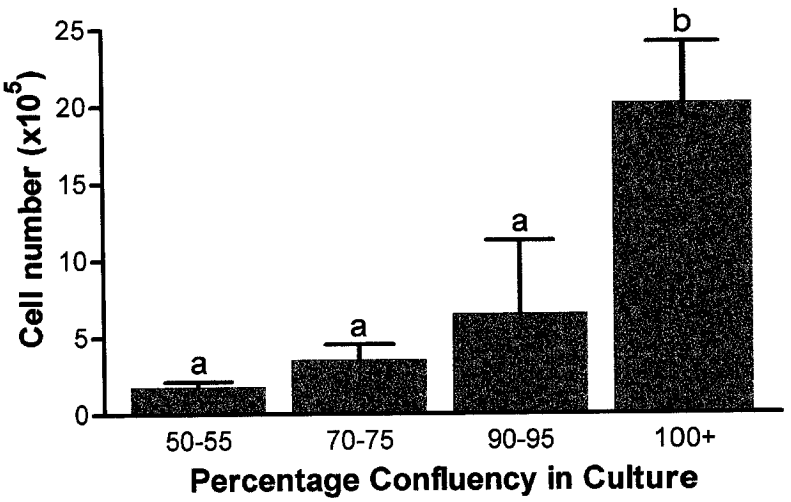
Cell number (x10^5)
25
20
15
10
5
0
a
a
a
b
50-55
70-75
90-95
100+
Percentage Confluency in Culture

B

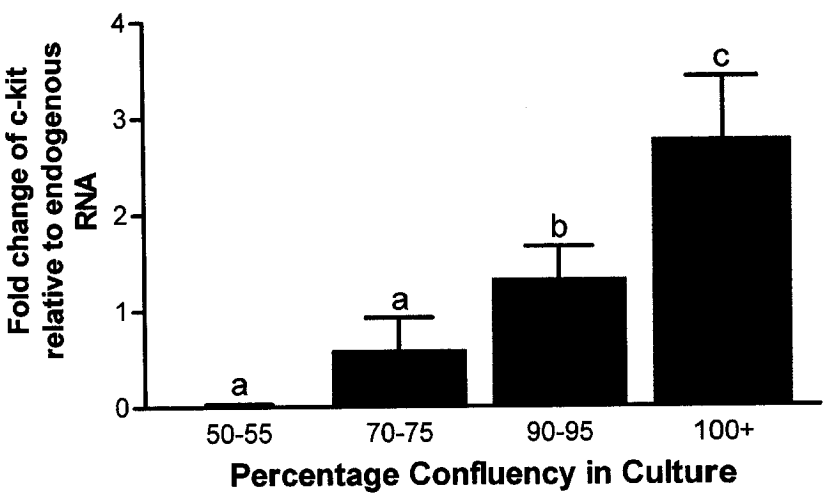
Fold change of c-kit relative to endogenous RNA
4
3
2
1
0
a
a
b
c
50-55
70-75
90-95
100+
Percentage Confluency in Culture

FIGURE 13 – Culture of ROSE 199 at increasing confluencies increases expression of KIT.

A) ROSE 199 cells were seeded at a density of $1x10^4$ cells (dashed line) in 60mm plates. After 48, 72, 96, and 120 hours of culture, cells were counted in duplicate and were calculated as mean counts ± SEM where each data point represents 3 individual experiments done in triplicate. Lowercase letters (a, b, c) above the bars indicate statistical significance ($p<0.05$) in the cell number between the groups of that graph.

B) Protein was isolated from ROSE 199 cells at each time point and 50 μg of protein was separated on an SDS gel and immunoblotted for Kit. Protein from the mouse mast cell line MC/9 cells was used as a positive control. ROSE 199 cultured at 50-55%, 75-80%, and 95-100% confluency express the 110kDa Kit protein as do the MC/9 cells. In contrast, ROSE 199 cultured at 30-35% confluency show no 110 kDa Kit protein. GAPDH was used as a loading control, and this indicates equal loading across all samples except for the first 30-35% confluency sample which is slightly underloaded.

A

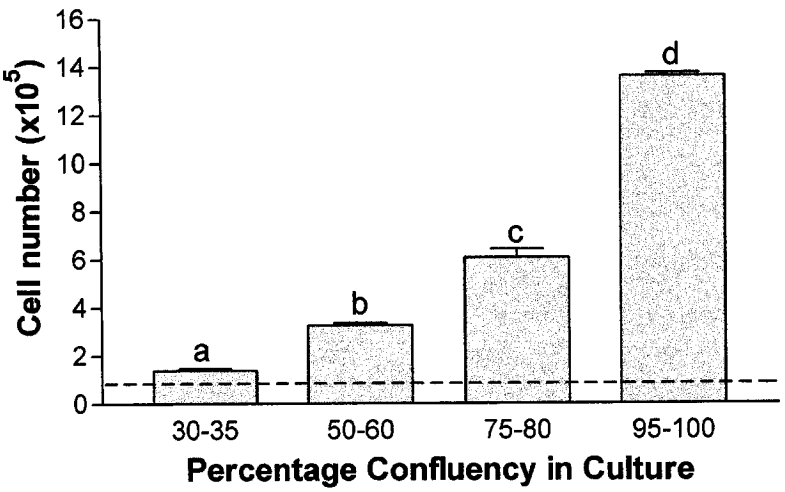
16
14
12
10
8
6
4
2
0
Cell number (x10^5)
a
b
c
d
30-35
50-60
75-80
95-100
Percentage Confluency in Culture

B

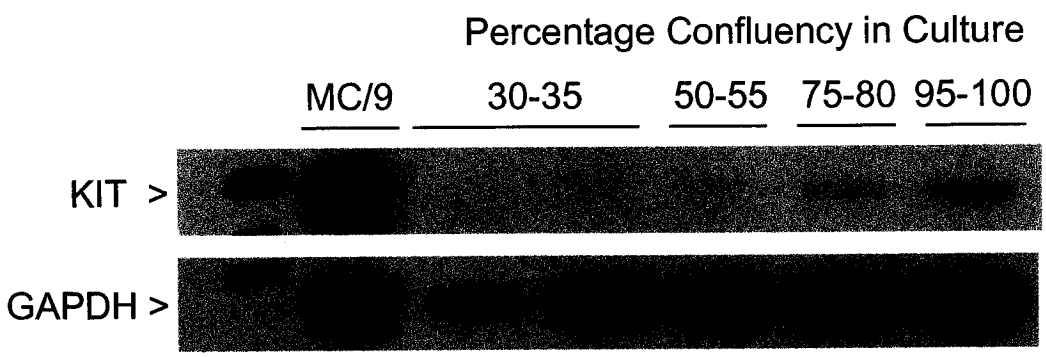
Percentage Confluency in Culture
MC/9
30-35
50-55
75-80
95-100
KIT >
GAPDH >

To determine if an increase in cell-cell contacts could be responsible for induction of Kit expression, we used an experimental model previously established in the lab. ImmortoMOSE are cells that express SV40 large T-antigen when cultured at 32°C, however at 37°C they do not express large T-antigen or Kit. ImmortoMOSE were stably transfected with E-cadherin and western blot analysis was performed to determine if the overexpression of the cell adhesion protein E-cadherin was capable of inducing Kit expression. These cells formed three-dimensional colonies in soft agar, which demonstrates an increase in cell-cell contacts, however the cells did not cause tumours in nude mice. Figure 14 shows that the ImmortoMOSE transfected with E-cadherin express more abundant E-cadherin than the control ImmortoMOSE however, they do not express KIT protein.

17. **Expression analysis of ECM components and KIT in invaginations and inclusion cysts in pre- and post-menopausal human ovaries.**

Serial sections from pre- and post-menopausal ovaries were stained for expression of KIT, collagen I, laminin, fibronectin, collagen III, and collagen IV. Sections were analysed for the number of invaginations and inclusion cysts and then assessed for staining intensity on a scale of 1-4 (+) for expression in and around the OSE forming those structures. Positive staining was assessed for staining intensity on a scale of 1-4 (+) based on control stains. All structures showing positive staining were included in the study. Photographs of a sample section of one side of a large ovarian inclusion cyst can be seen in Figure 15. Panel A shows expression of KIT in the OSE cells lining the inclusion cyst as well as in the stromal cells directly below the inclusion cyst. Panel B

shows abundant expression of collagen I in the OSE cells as well in the ovarian stroma. Panel C shows expression of laminin in the stromal cells and basement membrane of the ovary but not in the OSE cells lining the cyst. Intense fibronectin staining of the OSE and the ovarian stroma can be seen in Panel D. Panel E and Panel F show no expression of collagen III or IV in the entire section of the ovary. These photographs represent the trend seen in the study and all results are summarized in Table 1 (inclusion cysts) and Table 2 (invaginations). Immunohistochemical detection of KIT protein in four pre- and two post-menopausal ovaries revealed that surface OSE did not express KIT (Figure 16B), however KIT protein was readily detectable in oocytes (16A) and over 50% of invaginations (16E) and inclusion cysts in both pre- and post-menopausal ovaries (Table 3). Inhibin staining was used to distinguish inclusion cysts from collapsed follicles or follicular cysts (Figure 16C) and the follicles were not included in the study.

The frequency of extracellular matrix expression is presented in Table 4. Expression of collagen I was detected in 89% of inclusion cysts and 87% of invaginations. This is similar to the pattern of fibronectin expression (89% of inclusion cysts and 71% of invaginations), yet drastically different from the expression frequency of laminin, collagen III, and collagen IV which were all below 25%. When this data was correlated with KIT expression (Table 5A and B), very interesting trends were noted. Table 5A shows that of the invaginations and inclusion cysts that expressed KIT, 94% of both structures also expressed collagen I, and 100% of inclusion cysts and 78% of invaginations expressed fibronectin, however, less than 20% expressed laminin, collagen III, and collagen IV. Co-expression of ECM and KIT in the structures was also analysed by Chi-squared analysis (Table 5B) and revealed that the association between collagen I

FIGURE 14 – Expression of E-cadherin in ImmortoMOSE cells is not sufficient for induction of KIT expression.

MOSE cells stably transfected with E-cadherin (E-cad) were analysed for expression of KIT by western blot analysis. Protein was isolated and confirmation of over-expression of E-cadherin in the transfected cells was done by western blot. The human ovarian cancer cell line, SKOV3, was used as a positive control for E-cadherin. The blots were then probed for KIT. Protein from the human lung cancer cell line, LC-80, was used as positive control for KIT. KIT protein cannot be detected in the MOSE cells transfected with E-cadherin, but is seen in the LC-80 cells. α-tubulin was used as a loading control.

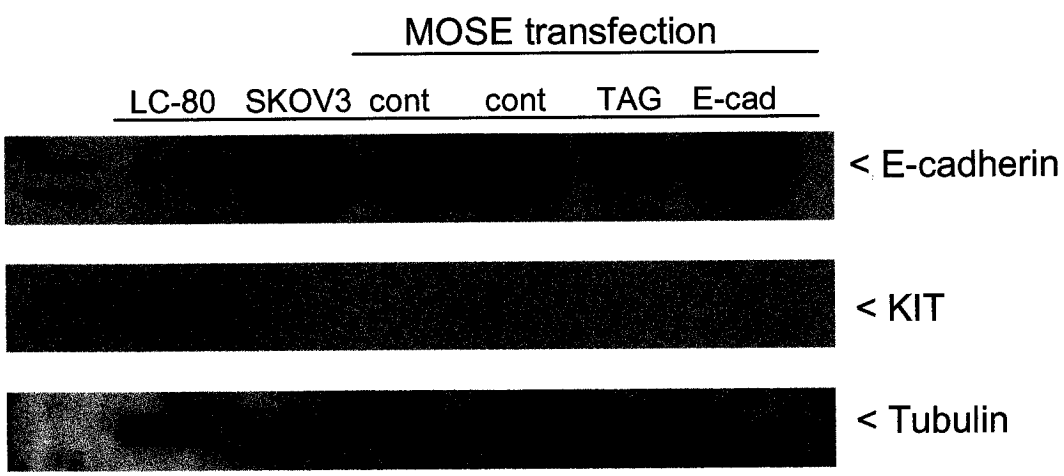
MOSE transfection
LC-80
SKOV3
cont
cont
TAG
E-cad
< E-cadherin
< KIT
< Tubulin

FIGURE 15 – Immunohistochemical detection of ECM components in an inclusion cyst.

Paraffin-embedded tissue sections were stained for KIT (A), collagen I (B), laminin (C), fibronectin (D), collagen III (E), and collagen IV (F), and counterstained using hematoxylin (blue). Positive immunoreactivity is seen as a brown reaction product. The OSE forming the large inclusion cyst showed KIT staining in the ovarian surface epithelial cells as well as in the stroma (A). The OSE and stromal cells also expressed abundant collagen I (B) and fibronectin (D) expression and lacked expression of collagen III (E) and IV (F). The basement membrane located below the surface shows expression of laminin (inset; C). Consecutive sections were also processed without the primary antibodies (KIT, inset A; collagen I, inset B; fibronectin, inset D) and all slides lacked staining indicating the specificity of the reaction. Positive controls were used for all stains and are shown for collagen III (inset E; skin tissue) and collagen IV (inset F; breast tumour). Magnification 200X.

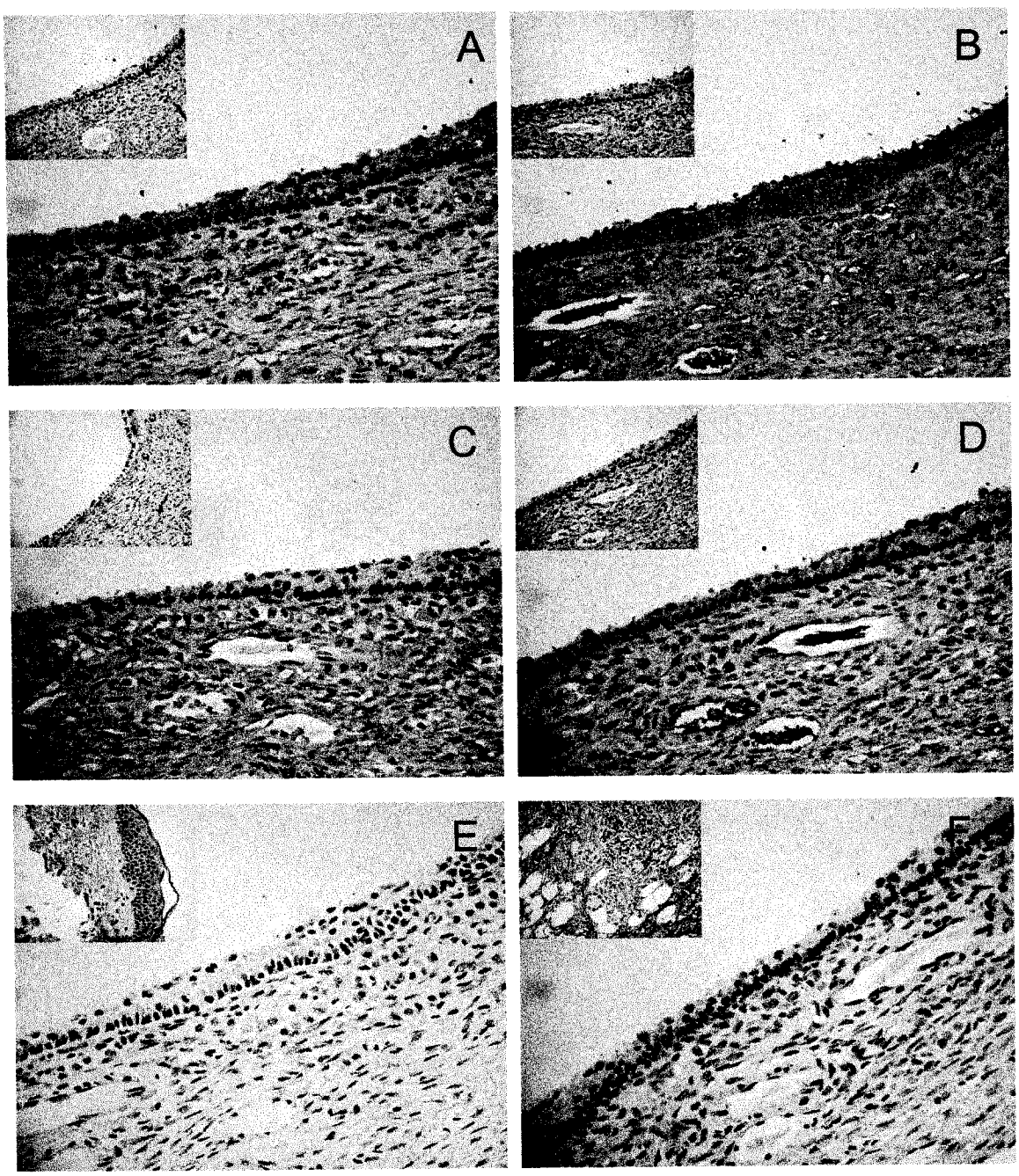
A
B
C
D
E
F

TABLE 1 – Expression of ECM and KIT in inclusion cysts of pre- and post-menopausal human ovaries.

INCLUSION CYSTS	KIT	Coll I	Laminin	Fibro-nectin	Coll III	Coll IV
Ovary 1						
1	++[a]	++++	-	+++	+	-
2	-	+	-	-	+	-
3	+	+++	-	++	+	-
Ovary 2						
1	+++	++	-	+++	-	-
2	+	+	+	++	-	+
3	-	+	-	n/a	-	+
4	+	+	-	n/a	-	+
Ovary 3						
1	+	+	-	++	-	-
2	++	+++	-	++	-	-
3	-	++	-	++	-	-
4	++	+++	-	++	-	-
5	-	-	-	++	-	+
6	-	++	-	++	-	-
7	+++	++++	-	+++	-	-
8	+++	+++	-	++++	-	-
9	+++	+	-	+++	-	+
Ovary 4						
1	-	+	-	++	n/a	-
2	-	+	-	++	-	+
3	+	++	-	++	-	-
4	++	n/a	-	+++	-	-
5	-	+++	-	++	-	++
6	++	++	-	++	-	-
Ovary 5						
1	-	-	-	+	-	-
Ovary 6						
1	++	++++	-	++++	-	-
2	+++	++++	-	++++	-	-
3	-	+	-	++	-	-
4	+++	++++	-	+++	-	-
5	+++	+++	-	++	-	-

[a] – grading scale for level of expression; + mild positive staining, ++ moderate staining intensity, +++ staining intensity similar to positive control tissues, ++++ intense staining than the positive control.

n/a – structure could not be found in the section and was not evaluated

TABLE 2 – Expression of ECM and KIT in invaginations of pre- and post-menopausal human ovaries.

INVAGINATION	KIT	Coll I	Laminin	Fibro-nectin	Coll III	Coll IV
Ovary 1						
1	+ [a]	++	-	+	-	-
2	+	++	-	+	-	-
3	+	+	-	+	+	-
4 [b]	-	++	-	+	+	-
5 [b]	-	-	-	+	++	-
6 [b]	-	+	-	+	-	-
Ovary 2						
1	-	+	-	-	-	-
2	-	+	-	-	-	-
3	-	-	-	-	-	-
4	-	+	-	-	-	-
5	-	+	-	+	-	-
6	-	+	-	+	-	+
Ovary 3						
1	+	+	-	+	-	-
2	+	++	-	+	-	-
3	+	+	-	+	-	-
Ovary 4						
1	++	++	-	++	+	-
2	++	++	-	++	+	-
3	++	++	-	++	-	-
Ovary 5						
1	+	+	-	-	-	-
2	+	-	-	-	-	-
3	-	-	-	-	-	-
4	++	++	-	-	-	-
5	+	++	-	-	-	-
6	++	+++	-	++	-	-
Ovary 6						
1 [b]	-	+	+	+	-	-
2 [b]	-	+	+	+	-	-
3	++++	++	-	++	-	-
4	++++	++	-	++	-	-
5	++++	++	-	++	-	-
6 [b]	-	++	+	+	-	-
7	+++	++	-	++	-	-

[a] – grading scale for level of expression; + mild positive staining, ++ moderate staining intensity, +++ staining intensity similar to positive control tissues, ++++ more intense staining than the positive control.

FIGURE 16 – Immunohistochemical detection of KIT, inhibin, and ECM components in human ovaries.

Paraffin-embedded tissue sections were stained for KIT (A, B, E), inhibin (C), laminin (D), and collagen I (F), and counterstained using hematoxylin (blue). Positive immunoreactivity is seen as a brown reaction product. Oocytes (A) were KIT positive, however, normal OSE (B) were KIT negative. Sections were stained with inhibin to distinguish between inclusion cysts and collapsed follicles and follicles were excluded from the study (C). Although most OSE cells forming invaginations and inclusion cysts were negative for laminin expression, basement membrane regularly stained laminin positive (D). As well, OSE lining surface invaginations often co-expressed KIT (E) and collagen I (F).

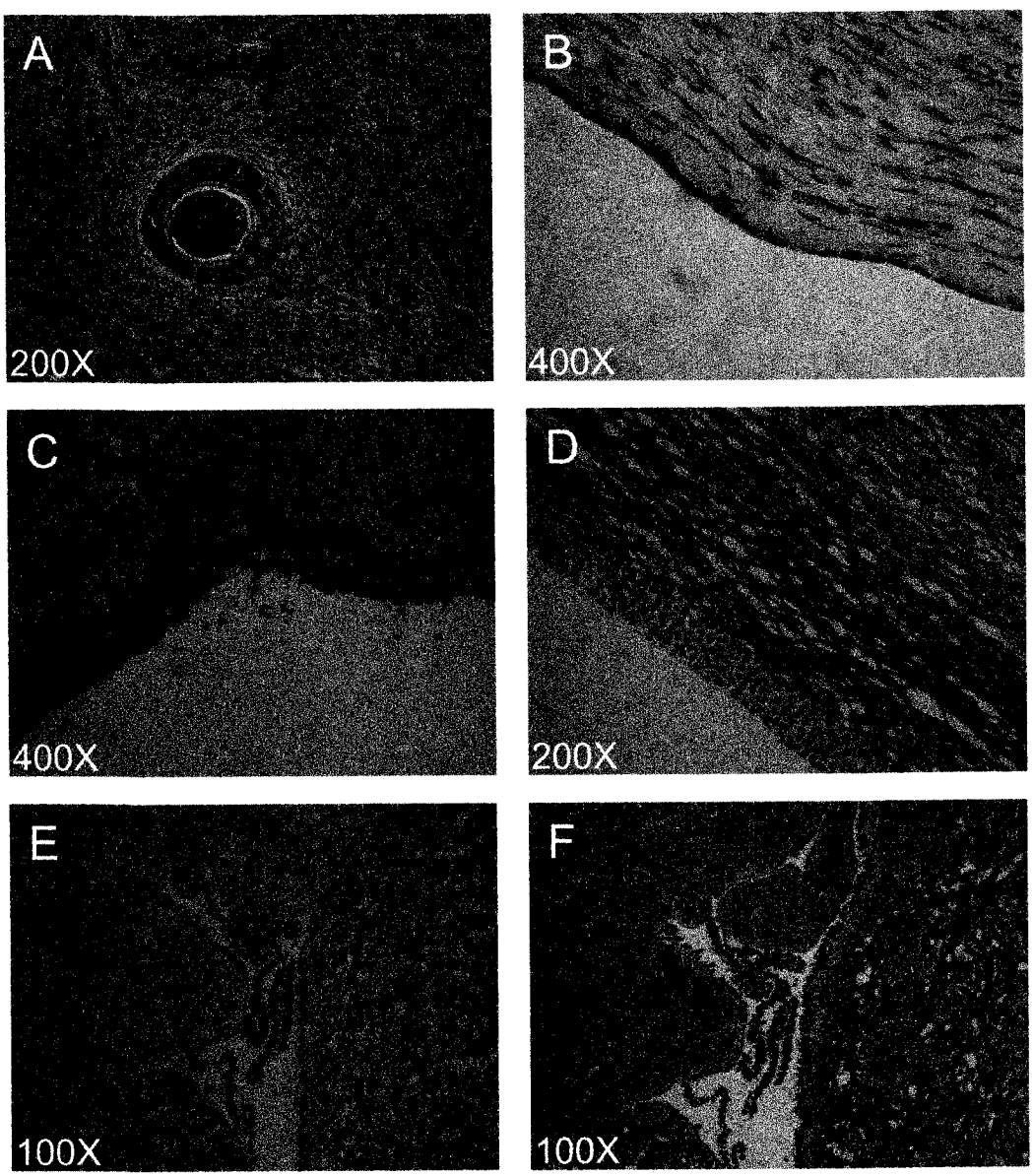
A
200X
B
400X
C
400X
D
200X
E
100X
F
100X

TABLE 3 – Frequency of expression of KIT in the OSE forming invaginations and inclusion cysts of healthy ovaries from pre- and post-menopausal women.

Ovary Status	N	Mean No. Inclusion Cysts ± SEM	% KIT+ Inclusion Cysts	Mean No. Invaginations ± SEM	% KIT+ Invaginations
Pre-menopausal	4	5.5 ± 1.3	74	4.5 ± 0.87	50
Post-menopausal	2	3 ± 2	67	6.5 ± 0.5	69

TABLE 4 – Frequency of expression of ECM in the OSE forming invaginations and inclusion cysts of healthy ovaries from pre- and post-menopausal women.

Structure (total)	Collagen I	Laminin	Fibronectin	Collagen III	Collagen IV
Inclusion Cysts (28)	89%	4%	89%	11%	25%
Invaginations (31)	87%	10%	71 %	16%	4%

TABLE 5 – Correlation of KIT and ECM component expression.

A

Inclusion Cysts	Collagen I +	Laminin +	Fibronectin +	Collagen III +	Collagen IV +
KIT + (18)	94%	6%	100%	11%	11%
Invaginations	**Collagen +**	**Laminin +**	**Fibronectin +**	**Collagen III +**	**Collagen IV +**
KIT + (18)	94%	0%	78%	17%	0%

B

	% KIT + inclusion cysts (n)	% KIT + invaginations (n)	x^2
Collagen I	68% (25)	63% (27)	9.753[a]
Laminin	100% (1)	0% (3)	0.4364
Fibronectin	68% (25)	64% (22)	8.752[a]
Collagen III	67% (3)	60% (5)	0.1222
Collagen IV	43% (7)	0% (1)	0.6982

[a] indicates statistical significance ($p<0.005$).

and KIT expression and fibronectin and KIT expression was significantly ($p<0.005$) related, however the association between KIT expression and expression of laminin, collagen III, and collagen IV was not significantly related.

18. Effect of forced expression of c-*Kit* in OSE cells.

To analyse the effect of exogenous c-*Kit* expression on MOSE cells, a retrovirus expressing murine c-*Kit* was created. NIH 3T3 cells, and late and early passage MOSE cells were infected and proliferation was assessed. A western blot analysis was performed with protein from the infected MOSE to ensure that the cells were expressing Kit (Figure 17). Kit protein can be detected in the positive control cell line MC/9 as well as in the late passage MOSE cells infected with Kit whereas control late passage MOSE cells do not express Kit protein. Cell count experiments were done to measure the rate of proliferation of cells infected with Kit compared to control (mock-infected). Cells were cultured in maintenance media supplemented with high or low concentrations of serum for 96 hours, and counted every 24 hours. The rate of proliferation in the NIH 3T3 cells was significantly increased after 72 hours in the Kit infected group compared to controls at both 10% (Figure 18A) and 0% (Figure 18B) serum. Figure 18B also shows that prolonged exposure to 0% serum slowed proliferation of NIH3T3 at the later timepoints. After 48 hours, late passage MOSE infected with Kit also proliferated significantly faster than controls when cultured in 0.2% serum (Figure 19B) however in 4% serum there was no significant difference in rate of proliferation (Figure 19A). A significant increase in proliferation of early passage MOSE infected with Kit was seen as early as 48 hours in both 10% serum and 1% serum (Figure 20).

FIGURE 17 – Expression of KIT in MOSE cells infected with retroviral murine c-*Kit*

Determination of the expression of murine c-*Kit* in late passage MOSE cells was done using SDS-PAGE and immunoblotting. Fifty μg of protein was separated on an SDS gel and immunoblotted for murine Kit. Protein from the mouse mast cell line MC-9 cells was used as a positive control. Late passage MOSE cells infected with retroviral murine c-*Kit* express the 110kDa Kit protein as do the MC-9 cells. In contrast, late passage MOSE cells that were mock infected (cont) show no 110 kDa Kit protein. GAPDH was used as a loading control.

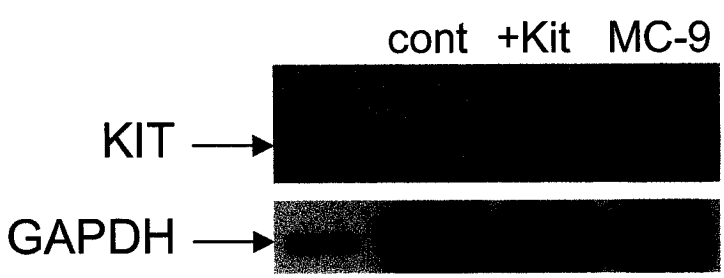
cont +Kit MC-9
KIT
GAPDH

FIGURE 18 – Proliferation of NIH 3T3 cells infected with retroviral murine c-*Kit*

NIH 3T3 cells were infected with retroviral murine, c-*Kit* (3T3 + Kit) and mock infected (3T3 control) and 48 hours later, seeded at a density of 20000 cells/24-well in triplicate in D-MEM supplemented with (A) or without (B) 10% FCS:DBS and cultured for 96 hours. Cell counts were done in duplicate at 24 hour intervals using a Coulter counter. Points represent the mean ± SEM of two experiments done in triplicate. Asterisks (*) indicate statistical significance between groups at that timepoint. NIH 3T3 cells infected with retroviral murine c-*Kit* proliferated significantly more rapidly than cells that were mock infected (control) when cultured in the presence or absence of 10% FCS:DBS, however the experiment done in 0% FCS:DBS shows a significant difference in proliferation rates as early as 48 hours.

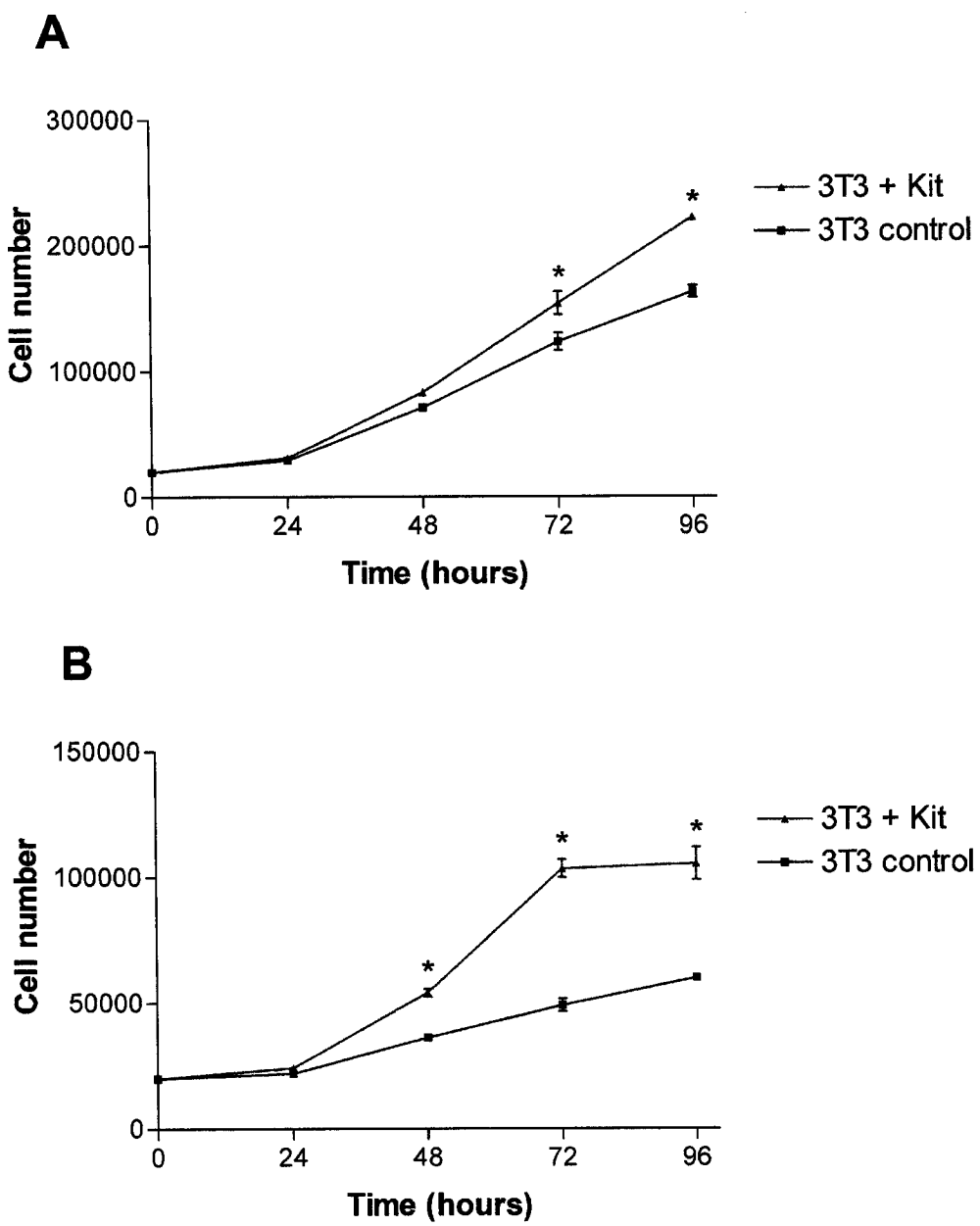
A
300000
200000
100000
0
Cell number
0
24
48
72
96
Time (hours)
3T3 + Kit
3T3 control
*
*
B
150000
100000
50000
0
Cell number
0
24
48
72
96
Time (hours)
3T3 + Kit
3T3 control
*
*
*

FIGURE 19 – Proliferation of late passage MOSE infected with retroviral murine c-*Kit*

Late passage MOSE cells were infected with retroviral murine c-*Kit* (MOSE + Kit) and mock infected (MOSE control) and 48 hours later, seeded at a density of 20000 cells/24-well in triplicate in MOSE media supplemented with 4% (A) or 0.2% (B) FCS and cultured for 96 hours. Cell counts were done in duplicate at 24 hour intervals using a Coulter counter. Points represent the mean ± SEM of two experiments done in triplicate. Asterisks (*) indicate statistical significance between groups at that timepoint. Late passage MOSE cells infected with retroviral murine c-*Kit* proliferated significantly more rapidly than cells that were mock infected (control) when cultured in the presence of 0.2% FCS. The significant difference in proliferation rates can be seen as early as 48 hours. There was no effect of Kit evident when cells were cultured in the presence of 4% FCS.

A

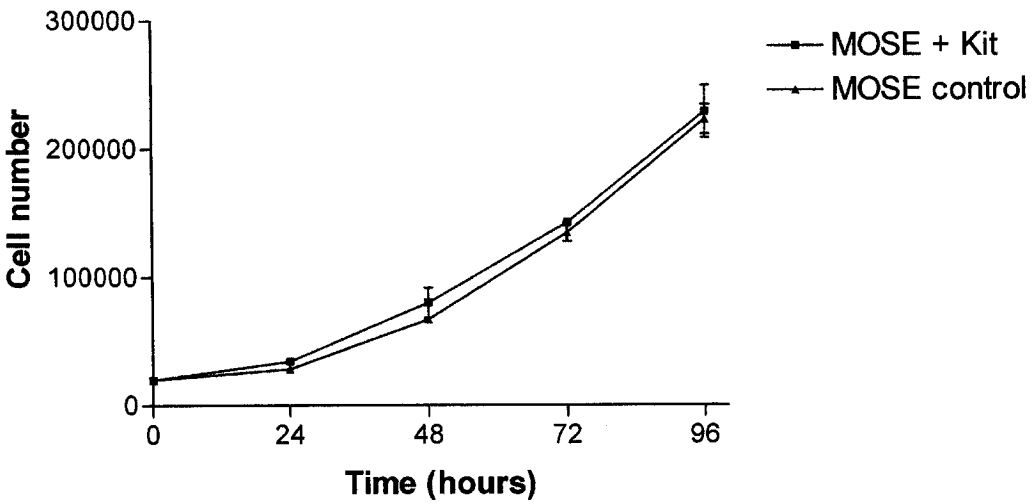
300000
200000
100000
0
Cell number
0
24
48
72
96
Time (hours)
MOSE + Kit
MOSE control

B

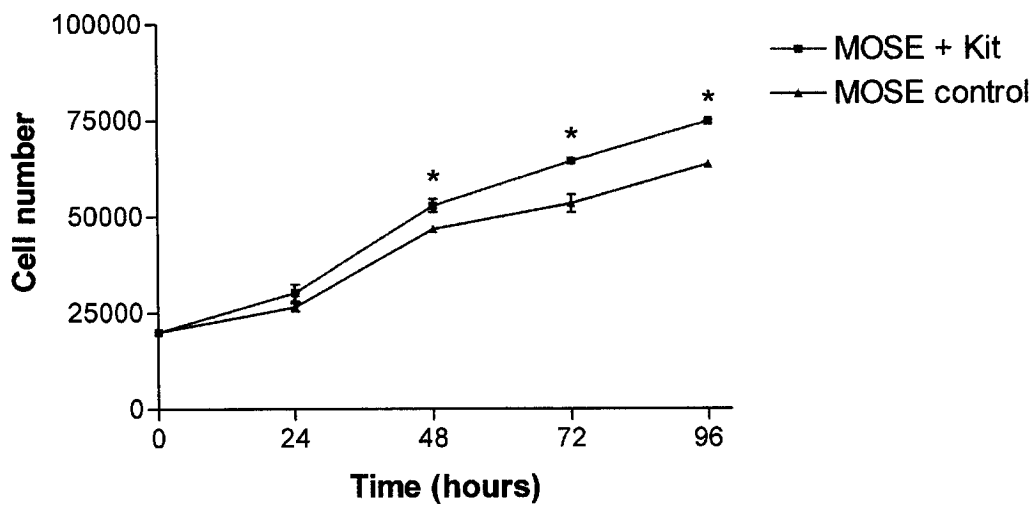
100000
75000
50000
25000
0
Cell number
0
24
48
72
96
Time (hours)
*
*
*
MOSE + Kit
MOSE control

FIGURE 20 – Proliferation of early passage MOSE infected with retroviral murine c-*Kit*

Early passage MOSE cells were infected with retroviral murine c-*Kit* (MOSE + Kit) and mock infected (MOSE control) and 48 hours later, seeded at a density of 20000 cells/24-well in triplicate in MOSE media supplemented with 10% (A) or 1% (B) FCS and cultured for 96 hours. Cell counts were done in duplicate at 24 hour intervals using a Coulter counter. Points represent the mean ± SEM of two experiments done in triplicate. Asterisks (*) indicate statistical significance between groups at that timepoint ($p<0.05$). Early passage MOSE cells infected with retroviral murine c-*Kit* proliferated significantly more rapidly than cells that were mock infected (control) when cultured in the presence of 10% or 1% FCS. The significant difference in proliferation rates can be seen as early as 48 hours.

A

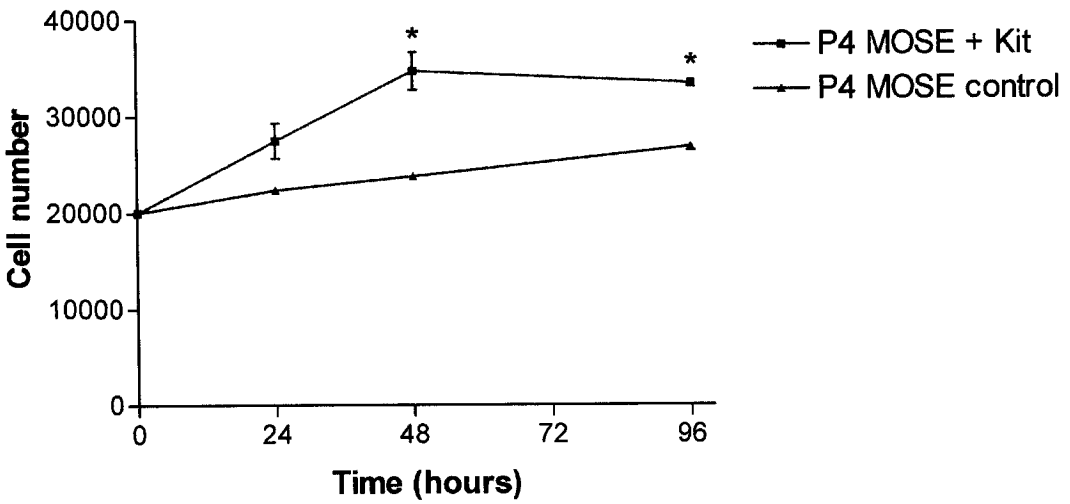
40000
30000
20000
10000
0
Cell number
0
24
48
72
96
Time (hours)
*
*
P4 MOSE + Kit
P4 MOSE control

B

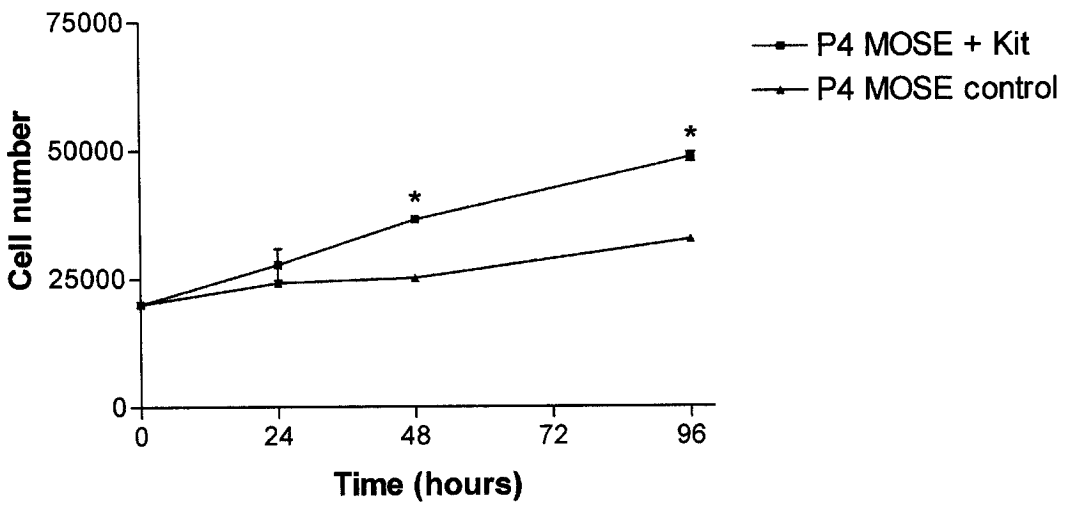
75000
50000
25000
0
Cell number
0
24
48
72
96
Time (hours)
*
*
P4 MOSE + Kit
P4 MOSE control

19. Analysis of ovarian tumours for mutations in the c-*KIT* gene.

Ovarian tumours were analysed for mutations in the c-*KIT* gene by two methods. To investigate the presence of any chromosomal rearrangements or large deletions, DNA was isolated from 10 ovarian tumours, digested with BamHI, and analysed by Southern blot. The blots were probed with a 3kb c-*KIT* probe to detect differences in sizes of bands. Figure 21A provides a view of a representative DNA gel and shows approximate equal loading in all lanes except for lane 7 which appears empty. Figure 21B shows the corresponding blot of 10 tumours digested with BamHI. Identical banding patterns consisting of 3000bp, 6000bp, 12045bp, and 13844bp can be seen in wells 2-11 except for lane 7 which corresponds to the sample with no DNA. Lane 1 and lane 12 are the 1kb and 100bp ladders, respectively.

Direct sequencing of three regions of the c-*KIT* gene was done for 21 tumours. DNA was isolated by Laser Capture Microscopy (11 tumours) or from the entire section on the slide (10 tumous) and amplified by PCR using a high fidelity enzyme. We analysed the juxtamembrane domain in exon 10-11, as well as the SHP-1 binding site and the PI3K binding site in exon 14. Sequences were analysed using Vector NTI and revealed no mutations in the juxtamembrane (exon 10-11) domain and no mutations in exon 14 for all 21 ovarian tumours. Figure 22 shows a sample alignment of the juxtamembrane domain of c-*KIT* from one of the tumours. Panel A shows an alignment similarity of 100% between the tumour and the published c-*KIT* gene sequence (L04143; (Vandenbark, G.R. *et al.*, 1992) while panel B shows the direct sequence alignment between the tumour and exon 10 and 11 of the c-*KIT* gene.

FIGURE 21 – Southern blot analysis of the c-*KIT* gene in ovarian tumours

Genomic DNA was isolated from ovarian tumours, and digested (5μg) with BamHI and separated by agarose gel electrophoresis (A-BamHI). Samples were transferred to a membrane and probed with a [^{32}P]-labelled human c-*KIT* cDNA (B). Lane 1 and lane 12 correspond to the 1kb and 100bp ladder respectively. Lane 2-11 show identical banding patterns ranging from 3000 bp to 13844 bp in length except for lane 7 which appears empty. This is supported by the lack of a DNA smear in A which indicates that there is insufficient DNA in that sample.

A

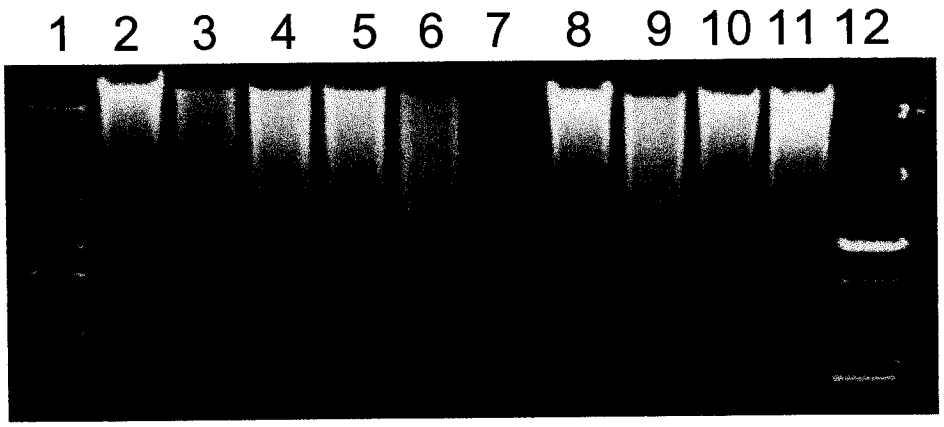
1 2 3 4 5 6 7 8 9 10 11 12

B

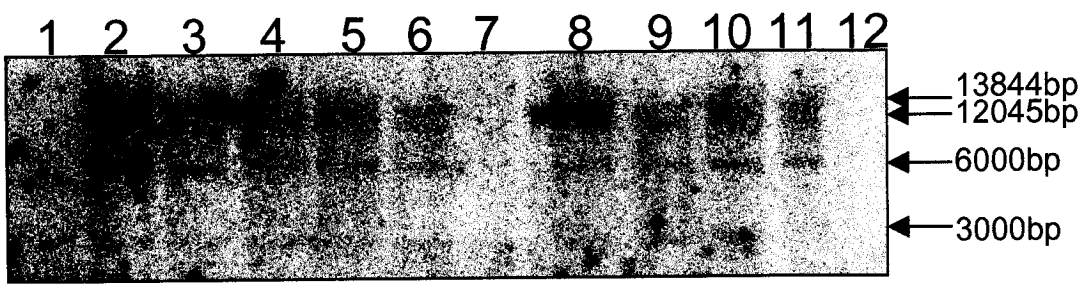
1 2 3 4 5 6 7 8 9 10 11 12
13844bp
12045bp
6000bp
3000bp

FIGURE 22 – Sequence analysis of the juxtamembrane domain of c-*KIT* gene in ovarian tumours.

Genomic DNA was extracted from 21 ovarian tumours and two portions of the c-*KIT* gene were amplified by PCR. The figure shows the alignment of the juxtamembrane domain of c-*KIT* from one of the tumours. The alignment similarity of 100% between the tumour and the published c-*KIT* gene is seen in A and the direct sequence alignment of the tumour and exon 10 and 11 of the c-*KIT* gene is seen in B.

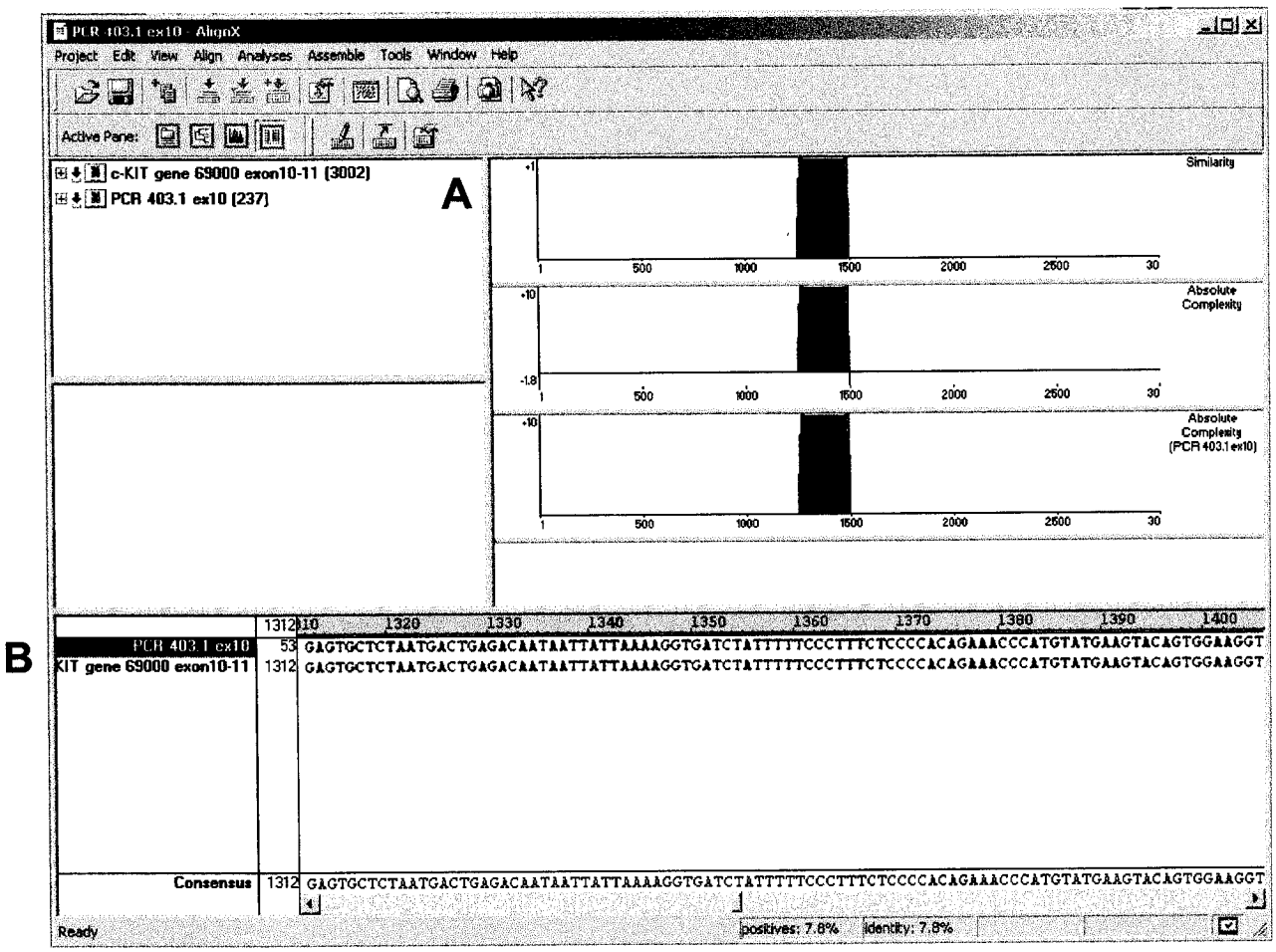
PCR 403.1 ex10 - AlignX
Project Edit View Align Analyses Assemble Tools Window Help
Active Pane:
c-KIT gene 69000 exon10-11 (3002)
PCR 403.1 ex10 (237)
A
Similarity
Absolute Complexity
Absolute Complexity (PCR 403.1 ex10)
B
PCR 403.1 ex10
KIT gene 69000 exon10-11
Consensus
GAGTGCTCTAATGACTGAGACAATAATTATTAAAAGGTGATCTATTTTTCCCTTTCTCCCCACAGAAACCCATGTATGAAGTACAGTGGAAGGT
Ready
positives: 7.8%
identity: 7.8%

DISCUSSION

Ovarian cancer affects 1 in 70 women in the western world. Increased risk of ovarian cancer is associated with uninterrupted ovulation and formation of invaginations and inclusion cysts by the ovarian surface epithelium. During and after ovulation, the OSE are in direct contact with the underlying stromal ECM. Our goal was to investigate whether ECM has any effect on OSE cell morphology, proliferation, or expression of the proto-oncogene c-*KIT*, which is known to be upregulated in the preneoplastic invaginations and inclusion cysts as well as in 70% of ovarian tumours. Culturing ROSE 199 cells on monomeric ECM (collagen I, laminin, fibronectin, and collagen IV) had no effect on morphology or proliferation rate compared to controls (plastic and poly D lysine). Since ROSE 199 express basal levels of c-*Kit* mRNA detectable by RT-PCR, expression of c-*Kit* in cells cultured on ECM was measured using Q-RT-PCR. Analysis revealed no change in expression of c-*Kit*. Mouse OSE cells were also cultured on monomeric collagen I to determine if primary cells were more sensitive to changes in the extracellular matrix. MOSE do not express c-*Kit*, therefore this experiment would indicate if collagen I was capable of inducing expression. Results show that MOSE cells proliferate significantly slower on collagen I; however Q-RT-PCR results indicate that there is no change in the expression level of c-*Kit* mRNA.

This experiment was also repeated on fibrillar collagen I, which is reported to be a better system for simulating the ovarian stroma (Kruk, P.A. *et al.*, 1994). This caused a significant change in morphology of both ROSE 199 and MOSE cells. The cells appeared to transition from an epithelial phenotype to a more mesenchymal phenotype

based on extensive differentiation as referenced in the literature for other cell types such as thyroid follicular cells (Greenburg, G. and Hay, E.D., 1988; Link, R.E. *et al.*, 1990; Hay, E.D., 1995). Culture on fibrillar collagen I also caused a significant decrease in cellular proliferation, yet did not affect expression of c-*Kit*. These experiments suggest that although extracellular matrices can modulate cellular behaviours such as morphology and proliferation, the interaction of OSE cells with the individual components of the basement membrane (laminin and collagen IV) and stromal ECM (collagen I and fibronectin) after ovulation and during wound repair is likely not responsible for induction of KIT in the OSE. The cause of induction of Kit expression within the OSE of invaginations and inclusion cysts is not the cells interaction with single ECM components. OSE cells are rarely in contact with only one matrix component so culturing on a combination of matrices and in the presence of ovarian stromal cells would provide us with a more relevant model. Culturing the cells on Matrigel which consists of a combination of matrices and is often used to simulate the ovarian basement membrane (Kruk, P.A. *et al.*, 1994) would be ideal for this experiment. We could also alter the ratios of each matrix component to try to imitate the environmental changes after ovulation (i.e. high fibronectin/collagen I ratio followed by increasing amounts of collagen III and decreasing amounts of fibronectin, and then increasing amounts of collagen I and fibronectin and low amounts of collagen III). It has also been shown that ROSE 199 can produce their own ECM (Kruk, P.A. *et al.*, 1994). Although this has only been studied in long term cultures, it is possible that we aren't seeing effects on cell behaviour because the cells are compensating for the lack of various ECMs in the culture conditions and are producing their own. It would also be interesting to look at the

differences between MOSE and ROSE 199. ROSE 199 cells are spontaneously immortalized cells and express basal levels of Kit, while primary MOSE cells are Kit negative. The presence of Kit in the immortalized ROSE 199 could be some evidence that induction of Kit expression is associated with the early events of transformation.

Another objective of this study was to determine if cellular density affected expression of KIT. OSE cells on the surface of the ovary are single layered and usually quiescent. In contrast, the OSE cells that form the preneoplastic lesions are often multi-layered and proliferating more rapidly which increases the cellular density. Perhaps, when cells are at a higher density, expression of KIT is induced. To study this we cultured ROSE 199 cells at increasing densities and analysed expression of c-*Kit* mRNA by Q-RT-PCR and Kit protein by western blot. Both experiments showed that expression of c-*Kit* can be modulated by confluency in culture. C-*Kit* mRNA and Kit protein progressively increased in abundance as ROSE 199 cells became more confluent. This is interesting because a similar study showed that when ROSE 199 are cultured at high densities, they produce abundant quantities of ECM components such as collagen I and fibronectin (Kruk, P.A. *et al.*, 1994). Although earlier *in vitro* studies don't support this, the increase in ECM components in the culture environment could be upregulating expression of Kit in the cells. ROSE 199 cells can produce KL, therefore at a higher density, more ligand could be produced which could be upregulating the KIT receptor. Although this hasn't been shown in OSE cells, the potential for autocrine growth stimulation between KIT and KL is possible.

Another possibility is that when cells are more confluent, there are more cell-cell interactions and this regulates expression of KIT. One of the factors that may mediate the cell-cell interaction is E-cadherin, a cell-adhesion molecule that is not expressed in surface epithelium but is expressed in the OSE lining the invaginations and inclusion cysts (Kruk, P.A. and Auersperg, N., 1994; Cruet, S. *et al.*, 1999). E-cadherin has a pattern of expression that is identical to KIT's expression in the OSE. To investigate this further, we transfected ImmortoMOSE cells with E-cadherin. Western blot analysis of these transfected cells revealed that expression of E-cadherin was not capable of inducing expression of Kit. These density studies require further research since cell density appears to be one of the few regulators of KIT expression. Future studies could involve culturing ROSE 199 and MOSE cells in spheroid cultures to simulate the cellular interaction in an invagination or inclusion cyst as well as looking at other cell-adhesion molecules that could be involved in cellular density such as catenins and other cadherins. Also, some signalling molecules (notably cAMP) have been shown to upregulate KIT expression and it would be interesting to determine if cAMP has this effect on OSE cells. These results are also interesting because it is the opposite of what is seen in the ovarian cancer cell line HEY, in which KIT expression decreases as cellular density increases (Tonary, A; Ph.D. Thesis, 2001). However, density regulation of KIT expression is not universal, as the ovarian cancer cell line 429 shows no change in expression of KIT with changes in density. MOSE cells are distinct from cancer cells because they do not express Kit. This means that we require induction of Kit expression as well as regulation, which potentially involves many more players. It is possible that there are factors

regulating the Kit promoter that would make expression impossible when only one factor is altered. This would need to be investigated in future experiments with MOSE cells.

Very few studies have shown which ECM components are expressed in the human ovary. Most studies have looked at expression of ECM within the follicle or the corpus luteum (Huet, C. *et al.*, 1997; Rodgers, R.J. *et al.*, 1999; Silvester, L.M. and Luck, M.R., 1999; Rodgers, R.J. *et al.*, 2003). In this study, we analysed normal human pre- and post-menopausal ovaries for expression of collagen I, laminin, fibronectin, collagen III and collagen IV. Specifically, we looked at the expression of ECM surrounding the OSE lining the invaginations and inclusion cysts and compared it to expression of KIT within the cells. To ensure that we were analysing inclusion cysts and not collapsed follicles or follicular cysts, all sections were also stained with α-inhibin and structures that were positive were excluded from the study. Over 50% of invaginations and inclusion cysts found in pre- and post-menopausal ovaries expressed KIT and there was no apparent difference between the number of inclusion cysts or invaginations and menopausal state. This was not the expected result as there are some reports of increased abnormal OSE structures within the ovaries of post-menopausal women (Nicosia, S.V., 1987; Clow, O.L. *et al.*, 2002). However, since only two post-menopausal ovaries were examined in this study, any significant differences may not be detected. It is also important to note that although the pre-menopausal ovaries used in this study are normal, they have been removed from patients as young as 25 years of age for preventative measures or for other reproductive diseases. It is therefore possible that the number of

invaginations and inclusion cysts in theses ovaries are higher than healthy ovaries that are not surgically removed.

The immunohistochemical results from this study indicated 88% of invaginations and inclusion cysts express collagen I, 7% express laminin, 80% express fibronectin, 15% express collagen III, and 15% express collagen IV. It is not surprising that collagen I and fibronectin are highly expressed in these structures, as this corresponds to what is reported in the literature, where collagen I and fibronectin are often co-expressed in tissue undergoing wound repair (Grinnell, F. *et al.*, 1981; Sottile, J. and Hocking, D.C., 2002). Correlation of ECM and KIT expression in the OSE structures revealed that approximately 65% of the structures that express collagen I, fibronectin, or collagen III express KIT. Chi-squared tests of the number of structures that express each individual ECM and/or KIT revealed that there is a positive association ($p<0.005$) between KIT and collagen I and between KIT and fibronectin expression, but not between KIT and expression of laminin, collagen III, or collagen IV. This strengthens our hypothesis that OSE on the surface of the ovary when in contact with the basement membrane (composed of collagen IV and laminin) do not express KIT, while the OSE in the invaginations and inclusion cysts that interact with the ovarian stroma (composed of collagen I and fibronectin) have induced expression of KIT. These results indicate that KIT expression is associated with changes in the ovarian ECM.

This relationship between c-*KIT* and ECM is not replicable *in vitro*. From the experiments presented above, it is clear that individual ECM components alone such as collagen I are unable to induce or regulate expression of KIT in these cells under the conditions used in these experiments. The *in vivo* expression of ECM components

suggests that MOSE or ROSE 199 should be cultured on a combination of collagen I and fibronectin since they correlated most strongly with KIT expression. In these studies, we have only tried to further test the hypothesis that changes in the ECM in the formation of invaginations and inclusion cysts are regulating KIT expression. As well, all *in vitro* work was done in the absence of hormones. Additional experiments to investigate the relationship between KIT and ECM components could include the culture of OSE cells on matrices in the presence of growth factors or hormones known to be present in the ovarian microenvironment. Growth factors such as TGF-β have been shown to regulate KIT expression in hematopoietic cells (Dubois, C.M. *et al.*, 1994). It is also known that degrading ECM can release growth factors into the local cellular environment and it may be the combination of these factors and ECM changes that can affect KIT expression.

The possibility also exists that KIT expression can have an impact on OSE cell production of ECM. Previous studies have shown that OSE cells are able to produce ECM components such as collagen I, fibronectin, and collagen III (Kruk, P.A. *et al.*, 1994), so perhaps KIT expression can regulate production of ECM. In this study, of the structures that expressed KIT, 94% co-expressed collagen I and 89% co-expressed fibronectin. KIT expression was rarely associated (<10%) with expression of collagen IV or laminin; which are the main components of the basement membrane and are continually in contact with the OSE. KIT co-expressed with collagen III in approximately 15% of the structures analysed. Collagen III is only expressed immediately following wounding and is quickly replaced with collagen I (Gay, S. *et al.*, 1978; Grinnell, F. *et al.*, 1981), therefore the lack of collagen III expression in the ovaries

is not surprising. A recent study showed that Akt and PKC can regulate expression of ECM components such as laminin and collagen IV (Li, X. *et al.*, 2001). Since KIT has been shown to signal via Akt and PKC, this suggests that KIT may affect changes in the ECM and this warrants further investigation. Future experiments to examine this could involve modulating KIT expression and signalling within OSE cells and studying the ECM production. The MOSE cells infected with c-*Kit* in this study could be a useful tool for that investigation.

Expression of KIT is not seen in OSE cells on the ovarian surface but expression is detected in the OSE that migrate into the stroma to form invaginations and can seal off to form inclusion cysts. As a reliable mechanism to induce Kit expression in OSE cells could not be identified, we used retroviral infection to force expression of murine c-*Kit* in MOSE cells and analysed the effect on cellular proliferation. NIH 3T3 cells as well as late passage (P20) and early passage MOSE (P4), were infected and all cell types proliferated faster when infected with c-*Kit* compared to control infected cells. This effect was amplified when the cells were put under the stress of low serum concentrations. The increase in proliferation was significant in all three cell types as early as 48 hours. These results support the concepts that c-*Kit* can promote proliferation and survival. Future experiments will determine if the cells have transformed and gained tumourigenic capabilities. Caruana *et al.* (1998) reported changes to NIH 3T3 cells with ectopic expression of c-*Kit* such as gain of anchorage-independent growth and formation of tumours in nude mice. We can conclude that ectopic expression of KIT is sufficient to enhance OSE cell proliferation. Although no morphological changes were observed in

the MOSE cells, it would be interesting to see if the cells display phenotypic changes characteristic of transformation such as forming colonies in soft agar and tumour formation in immuno-deficient mice. As well, determining the expression of E-cadherin in these KIT expressing cells could reveal a link between KIT expression and induction of E-cadherin expression in the preneoplastic structures. These cells also provide a good opportunity to study the ECM production associated with KIT-expressing OSE cells. This could perhaps answer questions about the activity of the KIT expression OSE cells in the invaginations and inclusion cysts *in vivo*.

KIT expression is found in a variety of cancers, including mast cell leukemia, gastrointestinal stromal tumours and ovarian cancers (Wang, C. *et al.*, 1989; Ikeda, H. *et al.*, 1991; Hassan, S. *et al.*, 1998; Shinomura, Y., 2000; Tonary, A.M. *et al.*, 2000). In some mast cell leukemia and GISTs, KIT has been shown to be constitutively active due to mutations in the gene. A purpose of this research project was to analyse the c-*KIT* gene in ovarian tumours for similar mutations. Tumours from the Ottawa Ovarian Cancer Tissue Bank were analysed for large mutations such as insertions or deletions in the c-*KIT* gene. Preliminary results from the restriction digest and Southern blot analysis indicate that no such mutations are found in ovarian tumours and this is similar to the report by Singer *et al.* (2003).

This project corresponded with the beginning of a Phase II clinical trial testing Gleevec on patients with primary peritoneal or recurrent ovarian cancer. Tumour samples from the trial were analysed for mutations in three regions of the c-*KIT* gene commonly mutated in CML and GIST patients. To ensure isolation of DNA specifically

from the tumour cells, laser capture microscopy was performed and samples were PCR amplified and sequenced. Sequences revealed no activating mutations in the juxtamembrane domain or the SHP-1 or PI3K binding sites of the c-*KIT* gene of the tumours. For some samples, obtaining sufficient quantities of DNA from laser capture microscopy was impossible and tissue from the whole section was used. Sequences were carefully examined to ensure that no contaminants were present. Again, analysis revealed that no mutations were found in any of the three regions. A recent study has reported that a mutation in the ATP binding pocket of the c-*KIT* gene of GISTs renders the tumour resistant to the targeted therapeutic Gleevec (Tamborini, E. *et al.*, 2004). In our study, this region was not analyzed for mutations and this should be done.

The results of these experiments have suggested that during the formation of normal invaginations and inclusion cysts, OSE cells invade into the ovarian stroma and are in contact with stromal ECM components such as collagen I and fibronectin. We've shown that collagen I decreases proliferation of OSE cells suggesting that perhaps collagen I plays a role in inhibiting proliferation of OSE cells within invaginations and inclusion cysts. These structures remain quiescent within the ovary or eventually degrade. We propose that during formation of premalignant invaginations and inclusion cysts, the OSE cells gain expression of KIT. The invading cells have increased proliferation due to KIT expression and are therefore less responsive to collagen I. As well, the OSE cells may be capable of producing or modulating the ECM to form an environment more condusive to tumour growth (Figure 23). As well, the expression of KIT (a known survival factor; (Abrahamson, J.L. *et al.*, 1995; Carson, J.P. *et al.*, 1999; Johnson, M.D. *et al.*, 2002)) within the OSE may promote survival of these cells, causing

FIGURE 23 – Model depicting formation of invaginations and inclusion cysts and interaction with ECM.

Following ovulation, OSE cells can invade into the ovarian stroma to form invaginations and inclusion cysts. The OSE cells forming these structures are in contact with ECM components such as collagen I and fibronectin. Normally, these structures remain quiescent within the ovary or eventually degrade. We propose that during formation of premalignant invaginations and inclusion cysts, the OSE cells gain expression of KIT, which causes an increase in cellular proliferation, survival, and a change in the cells production or modulation of ECM. This results in more aggressive cells and an environment that is more condusive to tumour growth.

Normal Invaginations and Inclusion Cysts

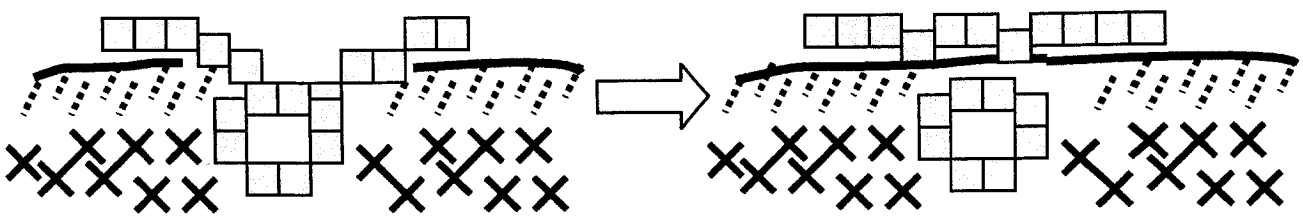

stromal ECM

- collagen I and fibronectin

decreased proliferation

- structure eventually degrades

Precursor Lesions

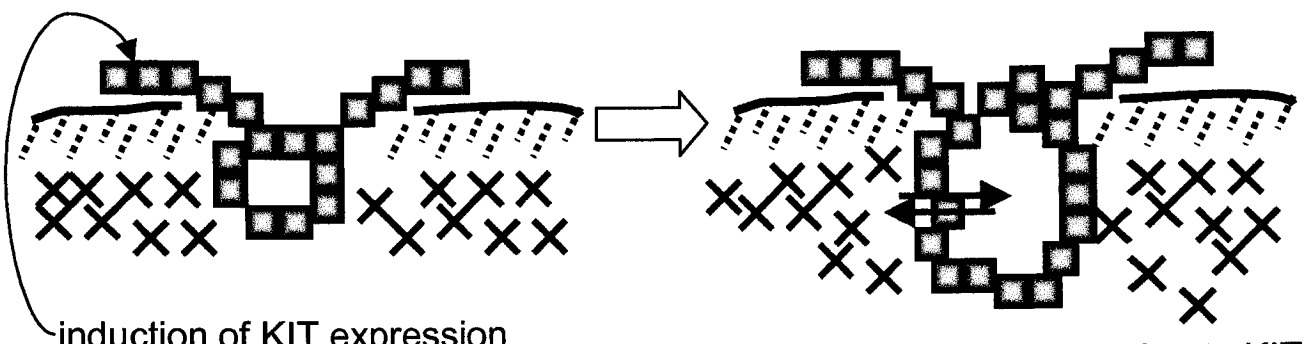

induction of KIT expression

increased proliferation due to KIT

- less responsive to collagen I?
- KIT modulates ECM?

them to escape the nomal mechanism of degradation and give them a propensity to remain in the ovary longer than normal increasing the risk of tumour formation.

In conclusion, we determined that no individual ECM component enables the expression of Kit in ROSE 199 or early passage MOSE cells *in vitro*, however *in vivo* data reveals a high correlation between KIT, collagen I, and fibronectin expression in invaginations and inclusion cysts. Increased density of ROSE 199 can upregulate the expression of Kit and transfection of c-*Kit* into MOSE cells increases proliferation and survival. Unlike other KIT expressing tumours, ovarian tumours do not have any mutations in the c-*KIT* gene. In conclusion, these experiments have increased our understanding of some elements of KIT expression in OSE cells, and have perhaps provided some clues as to the appropriate directions to follow in future experiments.

REFERENCES

Abrahamson, J. L., Lee, J. M., and Bernstein, A. (1995). Regulation of p53-mediated apoptosis and cell cycle arrest by Steel factor. *Mol.Cell Biol* 15(12): 6953-6960.

Ackerman, R. C. and Murdoch, W. J. (1993). Prostaglandin-induced apoptosis of ovarian surface epithelial cells. *Prostaglandins* 45(5): 475-485.

Adams, A. T. and Auersperg, N. (1985). A cell line, ROSE 199, derived from normal rat ovarian surface epithelium. *Exp.Cell Biol.* 53(4): 181-188.

Aoki, Y., Kawada, N., and Tanaka, K. (2000). Early form of ovarian cancer originating in inclusion cysts. A case report. *J.Reprod.Med.* 45(2): 159-161.

Assoian, R. K. and Marcantonio, E. E. (1996). The extracellular matrix as a cell cycle control element in atherosclerosis and restenosis. *J.Clin.Invest* 98(11): 2436-2439.

Auersperg, N., Maines-Bandiera, S. L., Dyck, H. G., and Kruk, P. A. (1994). Characterization of cultured human ovarian surface epithelial cells: phenotypic plasticity and premalignant changes. *Lab Invest* 71(4): 510-518.

Auersperg, N., Pan, J., Grove, B. D., Peterson, T., Fisher, J., Maines-Bandiera, S., Somasiri, A., and Roskelley, C. D. (1999). E-cadherin induces mesenchymal-to-epithelial transition in human ovarian surface epithelium. *Proc Natl.Acad.Sci.U.S.A* 96(11): 6249-6254.

Auersperg, N., Siemens, C. H., and Myrdal, S. E. (1984). Human ovarian surface epithelium in primary culture. *In Vitro* 20(10): 743-755.

Auersperg, N., Wong, A. S., Choi, K. C., Kang, S. K., and Leung, P. C. (2001). Ovarian surface epithelium: biology, endocrinology, and pathology. *Endocr.Rev.* 22(2): 255-288.

Bailey, A. J., Sims, T. J., Le, Lous, and Bazin, S. (1975). Collagen polymorphism in experimental granulation tissue. *Biochem.Biophys.Res.Commun.* 66(4): 1160-1165.

Baldi, A., Santini, D., Battista, T., Dragonetti, E., Ferranti, G., Petitti, T., Groeger, A. M., Angelini, A., Rossiello, R., Baldi, F., Natali, P. G., and Paggi, M. G. (2001).

Expression of AP-2 transcription factor and of its downstream target genes c-kit, E-cadherin and p21 in human cutaneous melanoma. *J.Cell Biochem.* 83(3): 364-372.

Besmer, P., Murphy, J. E., George, P. C., Qiu, F. H., Bergold, P. J., Lederman, L., Snyder, H. W., Jr., Brodeur, D., Zuckerman, E. E., and Hardy, W. D. (1986). A new acute transforming feline retrovirus and relationship of its oncogene v-kit with the protein kinase gene family. *Nature* 320(6061): 415-421.

Biskind, M. and Biskind, G. (1944). Development of tumors in the rat ovary after transplantation into the spleen. *Proc Soc Exp Biol Med* 55: 176-179.

Bjersing, L. and Cajander, S. (1974). Ovulation and the mechanism of follicle rupture. V. Ultrastructure of tunica albuginea and theca externa of rabbit graafian follicles prior to induced ovulation. *Cell Tissue Res.* 153(1): 15-30.

Blaustein, A. and Lee, H. (1979). Surface cells of the ovary and pelvic peritoneum: a histochemical and ultrastructure comparison. *Gynecol.Oncol.* 8(1): 34-43.

Blume-Jensen, P., Ronnstrand, L., Gout, I., Waterfield, M. D., and Heldin, C. H. (1994). Modulation of Kit/stem cell factor receptor-induced signaling by protein kinase C. *J.Biol.Chem.* 269(34): 21793-21802.

Blume-Jensen, P., Siegbahn, A., Stabel, S., Heldin, C. H., and Ronnstrand, L. (1993). Increased Kit/SCF receptor induced mitogenicity but abolished cell motility after inhibition of protein kinase C. *EMBO J.* 12(11): 4199-4209.

Brown, N. H., Gregory, S. L., and Martin-Bermudo, M. D. (2000). Integrins as mediators of morphogenesis in Drosophila. *Dev.Biol.* 223(1): 1-16.

Burmeister, L. and Healy, D. L. (1998). Ovarian cancer in infertility patients. *Ann.Med.* 30(6): 525-528.

Capo-chichi, C. D., Smith, E. R., Yang, D. H., Roland, I. H., Vanderveer, L., Cohen, C., Hamilton, T. C., Godwin, A. K., and Xu, X. X. (2002). Dynamic alterations of the extracellular environment of ovarian surface epithelial cells in premalignant transformation, tumorigenicity, and metastasis. *Cancer* 95(8): 1802-1815.

Carson, J. P., Kulik, G., and Weber, M. J. (1999). Antiapoptotic signaling in LNCaP prostate cancer cells: a survival signaling pathway independent of phosphatidylinositol 3'-kinase and Akt/protein kinase B. *Cancer Res.* 59(7): 1449-1453.

Caruana, G., Cambareri, A. C., Gonda, T. J., and Ashman, L. K. (1998). Transformation of NIH3T3 fibroblasts by the c-Kit receptor tyrosine kinase: effect of receptor density and ligand-requirement. *Oncogene* 16(2): 179-190.

Chabot, B., Stephenson, D. A., Chapman, V. M., Besmer, P., and Bernstein, A. (1988). The proto-oncogene c-kit encoding a transmembrane tyrosine kinase receptor maps to the mouse W locus. *Nature* 335(6185): 88-89.

Chen, Y., Wu, P. C., Lang, J. H., Ge, W. J., Hartge, P., and Brinton, L. A. (1992). Risk factors for epithelial ovarian cancer in Beijing, China. *Int.J.Epidemiol.* 21(1): 23-29.

Chian, R., Young, S., nilkovitch-Miagkova, A., Ronnstrand, L., Leonard, E., Ferrao, P., Ashman, L., and Linnekin, D. (2001). Phosphatidylinositol 3 kinase contributes to the transformation of hematopoietic cells by the D816V c-Kit mutant. *Blood* 98(5): 1365-1373.

Clow, O. L., Hurst, P. R., and Fleming, J. S. (2002). Changes in the mouse ovarian surface epithelium with age and ovulation number. *Mol.Cell Endocrinol.* 191(1): 105-111.

Colgin, D. C. and Murdoch, W. J. (1997). Evidence for a role of the ovarian surface epithelium in the ovulatory mechanism of the sheep: secretion of urokinase-type plasminogen activator. *Anim Reprod.Sci.* 47(3): 197-204.

Cramer, D. W. and Welch, W. R. (1983). Determinants of ovarian cancer risk. II. Inferences regarding pathogenesis. *J.Natl.Cancer Inst.* 71(4): 717-721.

Cramer, D. W., Welch, W. R., Cassells, S., and Scully, R. E. (1983). Mumps, menarche, menopause, and ovarian cancer. *Am.J.Obstet.Gynecol.* 147(1): 1-6.

Croom, K. F. and Perry, C. M. (2003). Imatinib mesylate: in the treatment of gastrointestinal stromal tumours. *Drugs* 63(5): 513-522.

Cruet, S., Salamanca, C., Mitchell, G. W., and Auersperg, N. (1999). alphavbeta3 and vitronectin expression by normal ovarian surface epithelial cells: role in cell adhesion and cell proliferation. *Gynecol.Oncol.* 75(2): 254-260.

Czernobilsky, B., Moll, R., Levy, R., and Franke, W. W. (1985). Co-expression of cytokeratin and vimentin filaments in mesothelial, granulosa and rete ovarii cells of the human ovary. *Eur.J.Cell Biol.* 37: 175-190.

Dahlen, D. D., Lin, N. L., Liu, Y. C., and Broudy, V. C. (2001). Soluble Kit receptor blocks stem cell factor bioactivity in vitro. *Leuk.Res.* 25(5): 413-421.

Damsky, C. H. and Werb, Z. (1992). Signal transduction by integrin receptors for extracellular matrix: cooperative processing of extracellular information. *Curr.Opin.Cell Biol.* 4(5): 772-781.

Danilovich, N., Roy, I., and Sairam, M. R. (2001). Ovarian pathology and high incidence of sex cord tumors in follitropin receptor knockout (FORKO) mice. *Endocrinology* 142(8): 3673-3684.

Davies, B. R., Worsley, S. D., and Ponder, B. A. (1998). Expression of E-cadherin, alpha-catenin and beta-catenin in normal ovarian surface epithelium and epithelial ovarian cancers. *Histopathology* 32(1): 69-80.

Driancourt, M. A., Reynaud, K., Cortvrindt, R., and Smitz, J. (2000). Roles of KIT and KIT LIGAND in ovarian function. *Rev.Reprod.* 5(3): 143-152.

Dubois, C. M., Ruscetti, F. W., Stankova, J., and Keller, J. R. (1994). Transforming growth factor-beta regulates c-kit message stability and cell-surface protein expression in hematopoietic progenitors. *Blood* 83(11): 3138-3145.

Duronio, V., Welham, M. J., Abraham, S., Dryden, P., and Schrader, J. W. (1992). p21ras activation via hemopoietin receptors and c-kit requires tyrosine kinase activity but not tyrosine phosphorylation of p21ras GTPase-activating protein. *Proc.Natl.Acad.Sci.U.S.A* 89(5): 1587-1591.

Dyck, H. G., Hamilton, T. C., Godwin, A. K., Lynch, H. T., Maines-Bandiera, S., and Auersperg, N. (1996). Autonomy of the epithelial phenotype in human ovarian surface epithelium: changes with neoplastic progression and with a family history of ovarian cancer. *Int.J.Cancer* 69(6): 429-436.

Eisenberg, B. L. (2003). Imatinib mesylate: a molecularly targeted therapy for gastrointestinal stromal tumors. *Oncology (Huntingt)* 17(11): 1615-1620.

Espey, L. L. (1980). Ovulation as an inflammatory reaction--a hypothesis. *Biol.Reprod.* 22(1): 73-106.

Espey, L. L., Bellinger, A. S., and Healy, J. A. (2004). Ovulation: An Infammatory Cascade of Gene Expression. In: Leung, P. C. and Adashi, E. Y (eds.), The Ovary. San Diego, CA: Elsevier Academic Press, pp. 145-165.

Fathalla, M. F. (1971). Incessant ovulation--a factor in ovarian neoplasia? *Lancet* 2(7716): 163

Flanagan, J. G., Chan, D. C., and Leder, P. (1991). Transmembrane form of the kit ligand growth factor is determined by alternative splicing and is missing in the Sld mutant. *Cell* 64(5): 1025-1035.

Flesken-Nikitin, A., Choi, K. C., Eng, J. P., Shmidt, E. N., and Nikitin, A. Y. (2003). Induction of carcinogenesis by concurrent inactivation of p53 and Rb1 in the mouse ovarian surface epithelium. *Cancer Res.* 63(13): 3459-3463.

Fredrickson, T. N. (1987). Ovarian tumors of the hen. *Environ.Health Perspect.* 73: 35-51.

Furitsu, T., Tsujimura, T., Tono, T., Ikeda, H., Kitayama, H., Koshimizu, U., Sugahara, H., Butterfield, J. H., Ashman, L. K., Kanayama, Y., and . (1993). Identification of mutations in the coding sequence of the proto-oncogene c-kit in a human mast cell leukemia cell line causing ligand-independent activation of c-kit product. *J.Clin.Invest* 92(4): 1736-1744.

Gay, S., Vijanto, J., Raekallio, J., and Penttinen, R. (1978). Collagen types in early phases of wound healing in children. *Acta Chir Scand.* 144(4): 205-211.

Geissler, E. N., Liao, M., Brook, J. D., Martin, F. H., Zsebo, K. M., Housman, D. E., and Galli, S. J. (1991). Stem cell factor (SCF), a novel hematopoietic growth factor and ligand for c-kit tyrosine kinase receptor, maps on human chromosome 12 between 12q14.3 and 12qter. *Somat.Cell Mol.Genet.* 17(2): 207-214.

Ghahremani, M., Foghi, A., and Dorrington, J. H. (1999). Etiology of ovarian cancer: a proposed mechanism. *Med.Hypotheses* 52(1): 23-26.

Giebel, L. B., Strunk, K. M., Holmes, S. A., and Spritz, R. A. (1992). Organization and nucleotide sequence of the human KIT (mast/stem cell growth factor receptor) proto-oncogene. *Oncogene* 7(11): 2207-2217.

Godin, I., Deed, R., Cooke, J., Zsebo, K., Dexter, M., and Wylie, C. C. (1991). Effects of the steel gene product on mouse primordial germ cells in culture. *Nature* 352(6338): 807-809.

Greenburg, G. and Hay, E. D. (1988). Cytoskeleton and thyroglobulin expression change during transformation of thyroid epithelium to mesenchyme-like cells. *Development* 102(3): 605-622.

Grinnell, F., Billingham, R. E., and Burgess, L. (1981). Distribution of fibronectin during wound healing in vivo. *J.Invest Dermatol.* 76(3): 181-189.

Gross, T. P. and Schlesselman, J. J. (1994). The estimated effect of oral contraceptive use on the cumulative risk of epithelial ovarian cancer. *Obstet Gynecol* 83(3): 419-424.

Gumbiner, B. M. (1996). Cell adhesion: the molecular basis of tissue architecture and morphogenesis. *Cell* 84(3): 345-357.

Hall, J. A., Meisterling, E. M., Benoit, A. M., Cooper, D. A., Coleman, D. A., Lerner, S. P., Lewis, P. E., and Dailey, R. A. (1993). Factors contributing to the formation of experimentally-induced ovarian cysts in prepubertal gilts. *Domest.Anim Endocrinol.* 10(2): 141-155.

Hamilton, T. C. (1992). Ovarian cancer, Part I: Biology. *Curr.Probl.Cancer* 16(1): 1-57.

Hankinson, S. E., Hunter, D. J., Colditz, G. A., Willett, W. C., Stampfer, M. J., Rosner, B., Hennekens, C. H., and Speizer, F. E. (1993). Tubal ligation, hysterectomy, and risk of ovarian cancer. A prospective study. *JAMA* 270(23): 2813-2818.

Hassan, S., Kinoshita, Y., Kawanami, C., Kishi, K., Matsushima, Y., Ohashi, A., Funasaka, Y., Okada, A., Maekawa, T., He-Yao, W., and Chiba, T. (1998).

Expression of protooncogene c-kit and its ligand stem cell factor (SCF) in gastric carcinoma cell lines. *Dig.Dis.Sci.* 43(1): 8-14.

Hay, E. D. (1995). An overview of epithelio-mesenchymal transformation. *Acta Anat.(Basel)* 154(1): 8-20.

Heinrich, M. C., Corless, C. L., Duensing, A., McGreevey, L., Chen, C. J., Joseph, N., Singer, S., Griffith, D. J., Haley, A., Town, A., Demetri, G. D., Fletcher, C. D., and Fletcher, J. A. (2003). PDGFRA activating mutations in gastrointestinal stromal tumors. *Science* 299(5607): 708-710.

Herbst, R., Lammers, R., Schlessinger, J., and Ullrich, A. (1991). Substrate phosphorylation specificity of the human c-kit receptor tyrosine kinase. *J.Biol.Chem.* 266(30): 19908-19916.

Hibi, K., Takahashi, T., Sekido, Y., Ueda, R., Hida, T., Ariyoshi, Y., Takagi, H., and Takahashi, T. (1991). Coexpression of the stem cell factor and the c-kit genes in small-cell lung cancer. *Oncogene* 6(12): 2291-2296.

Hines, S. J., Litz, J. S., and Krystal, G. W. (1999). Coexpression of c-kit and stem cell factor in breast cancer results in enhanced sensitivity to members of the EGF family of growth factors. *Breast Cancer Res.Treat.* 58(1): 1-10.

Hines, S. J., Organ, C., Kornstein, M. J., and Krystal, G. W. (1995). Coexpression of the c-kit and stem cell factor genes in breast carcinomas. *Cell Growth Differ.* 6(6): 769-779.

Hirota, S., Isozaki, K., Moriyama, Y., Hashimoto, K., Nishida, T., Ishiguro, S., Kawano, K., Hanada, M., Kurata, A., Takeda, M., Muhammad, Tunio G., Matsuzawa, Y., Kanakura, Y., Shinomura, Y., and Kitamura, Y. (1998). Gain-of-function mutations of c-kit in human gastrointestinal stromal tumors. *Science* 279(5350): 577-580.

Horie, K., Fujita, J., Takakura, K., Kanzaki, H., Suginami, H., Iwai, M., Nakayama, H., and Mori, T. (1993). The expression of c-kit protein in human adult and fetal tissues. *Hum.Reprod.* 8(11): 1955-1962.

Huang, E., Nocka, K., Beier, D. R., Chu, T. Y., Buck, J., Lahm, H. W., Wellner, D., Leder, P., and Besmer, P. (1990). The hematopoietic growth factor KL is encoded by

the Sl locus and is the ligand of the c-kit receptor, the gene product of the W locus. *Cell* 63(1): 225-233.

Huet, C., Monget, P., Pisselet, C., and Monniaux, D. (1997). Changes in extracellular matrix components and steroidogenic enzymes during growth and atresia of antral ovarian follicles in the sheep. *Biol.Reprod.* 56(4): 1025-1034.

Hutson, R., Ramsdale, J., and Wells, M. (1995). p53 protein expression in putative precursor lesions of epithelial ovarian cancer. *Histopathology* 27: 367-371.

Ikeda, H., Kanakura, Y., Tamaki, T., Kuriu, A., Kitayama, H., Ishikawa, J., Kanayama, Y., Yonezawa, T., Tarui, S., and Griffin, J. D. (1991). Expression and functional role of the proto-oncogene c-kit in acute myeloblastic leukemia cells. *Blood* 78(11): 2962-2968.

Ingber, D. E. and Folkman, J. (1989). Mechanochemical switching between growth and differentiation during fibroblast growth factor-stimulated angiogenesis in vitro: role of extracellular matrix. *J.Cell Biol.* 109(1): 317-330.

Inoue, M., Kyo, S., Fujita, M., Enomoto, T., and Kondoh, G. (1994). Coexpression of the c-kit receptor and the stem cell factor in gynecological tumors. *Cancer Res.* 54(11): 3049-3053.

Ismail, R. S., Cada, M., and Vanderhyden, B. C. (1999). Transforming growth factor-beta regulates Kit ligand expression in rat ovarian surface epithelial cells. *Oncogene* 18(33): 4734-4741.

Ismail, R. S., Dube, M., and Vanderhyden, B. C. (1997). Hormonally regulated expression and alternative splicing of kit ligand may regulate kit-induced inhibition of meiosis in rat oocytes. *Dev.Biol.* 184(2): 333-342.

Ismail, R. S., Okawara, Y., Fryer, J. N., and Vanderhyden, B. C. (1996). Hormonal regulation of the ligand for c-kit in the rat ovary and its effects on spontaneous oocyte meiotic maturation. *Mol.Reprod.Dev.* 43(4): 458-469.

Isola, J., Kallioniemi, O. P., Korte, J. M., Wahlstrom, T., Aine, R., Helle, M., and Helin, H. (1990). Steroid receptors and Ki-67 reactivity in ovarian cancer and in normal ovary: correlation with DNA flow cytometry, biochemical receptor assay, and patient survival. *J.Pathol.* 162(4): 295-301.

Jat, P. S., Noble, M. D., Ataliotis, P., Tanaka, Y., Yannoutsos, N., Larsen, L., and Kioussis, D. (1991). Direct derivation of conditionally immortal cell lines from an H-2Kb-tsA58 transgenic mouse. *Proc.Natl.Acad.Sci.U.S.A* 88(12): 5096-5100.

Jiang, F., Saunders, B. O., Haller, E., Livingston, S., Nicosia, S. V., and Bai, W. (2003). Conditionally immortal ovarian cell lines for investigating the influence of ovarian stroma on the estrogen sensitivity and tumorigenicity of ovarian surface epithelial cells. *In Vitro Cell Dev.Biol.Anim* 39(7): 304-312.

Jiang, H., Chen, S. S., Jiang, B., Jiang, Q., and Lu, D. P. (2003). [Treatment of 54 chronic myelogenous leukemia with Gleevec]. *Zhonghua Xue.Ye.Xue.Za Zhi.* 24(6): 281-285.

Jindal, S. K., Snoey, D. M., Lobb, D. K., and Dorrington, J. H. (1994). Transforming growth factor α localization and role in surface epithelium of normal human ovaries and in ovarian carcinoma cells. *Gynecol.Oncol.* 53(1): 17-23.

Joensuu, H. (2002). Treatment of inoperable gastrointestinal stromal tumor (GIST) with Imatinib (Glivec, Gleevec). *Med.Klin.(Munich)* 97 Suppl 1: 28-30.

Johnson, M. D., Okedli, E., Woodard, A., Toms, S. A., and Allen, G. S. (2002). Evidence for phosphatidylinositol 3-kinase-Akt-p7S6K pathway activation and transduction of mitogenic signals by platelet-derived growth factor in meningioma cells. *J.Neurosurg.* 97(3): 668-675.

Juliano, R. L. and Haskill, S. (1993). Signal transduction from the extracellular matrix. *J.Cell Biol.* 120(3): 577-585.

Karlan, B. Y., Jones, J., Greenwald, M., and Lagasse, L. D. (1995). Steroid hormone effects on the proliferation of human ovarian surface epithelium in vitro. *Am.J.Obstet.Gynecol.* 173(1): 97-104.

Keri, R. A., Lozada, K. L., bdul-Karim, F. W., Nadeau, J. H., and Nilson, J. H. (2000). Luteinizing hormone induction of ovarian tumors: oligogenic differences between mouse strains dictates tumor disposition. *Proc Natl.Acad.Sci.U.S.A* 97(1): 383-387.

Khoury, E., Andre, C., Pontvert-Delucq, S., Drenou, B., Baillou, C., Guigon, M., Najman, A., and Lemoine, F. M. (1994). Tumor necrosis factor alpha (TNF alpha) downregulates c-kit proto-oncogene product expression in normal and acute myeloid leukemia CD34+ cells via p55 TNF alpha receptors. *Blood* 84(8): 2506-2514.

Kissel, H., Timokhina, I., Hardy, M. P., Rothschild, G., Tajima, Y., Soares, V., Angeles, M., Whitlow, S. R., Manova, K., and Besmer, P. (2000). Point mutation in kit receptor tyrosine kinase reveals essential roles for kit signaling in spermatogenesis and oogenesis without affecting other kit responses. *EMBO J.* 19(6): 1312-1326.

Kozlowski, M., Larose, L., Lee, F., Le, D. M., Rottapel, R., and Siminovitch, K. A. (1998). SHP-1 binds and negatively modulates the c-Kit receptor by interaction with tyrosine 569 in the c-Kit juxtamembrane domain. *Mol.Cell Biol.* 18(4): 2089-2099.

Kruk, P. A. and Auersperg, N. (1994). A line of rat ovarian surface epithelium provides a continuous source of complex extracellular matrix. *In Vitro Cell Dev.Biol.Anim* 30A(4): 217-225.

Kruk, P. A. and Auersperg, N. (1992). Human ovarian surface epithelial cells are capable of physically restructuring extracellular matrix. *Am.J.Obstet.Gynecol.* 167(5): 1437-1443.

Kruk, P. A., Uitto, V. J., Firth, J. D., Dedhar, S., and Auersperg, N. (1994). Reciprocal interactions between human ovarian surface epithelial cells and adjacent extracellular matrix. *Exp.Cell Res.* 215(1): 97-108.

Laitinen, M., Rutanen, E. M., and Ritvos, O. (1995). Expression of c-kit ligand messenger ribonucleic acids in human ovaries and regulation of their steady state levels by gonadotropins in cultured granulosa-luteal cells. *Endocrinology* 136(10): 4407-4414.

Lammie, A., Drobnjak, M., Gerald, W., Saad, A., Cote, R., and Cordon-Cardo, C. (1994). Expression of c-kit and kit ligand proteins in normal human tissues. *J.Histochem.Cytochem.* 42(11): 1417-1425.

Lancaster, J. M., Wooster, R., Mangion, J., Phelan, C. M., Cochran, C., Gumbs, C., Seal, S., Barfoot, R., Collins, N., Bignell, G., Patel, S., Hamoudi, R., Larsson, C., Wiseman, R. W., Berchuck, A., Iglehart, J. D., Marks, J. R., Ashworth, A., Stratton, M. R., and Futreal, P. A. (1996). BRCA2 mutations in primary breast and ovarian cancers. *Nat.Genet.* 13(2): 238-240.

Landis, S. H., Murray, T., Bolden, S., and Wingo, P. A. (1998). Cancer statistics, 1998 [published errata appear in CA Cancer J Clin 1998 May-Jun;48(3):192 and 1998 Nov-Dec;48(6):329]. *CA Cancer J.Clin.* 48(1): 6-29.

Lennartsson, J., Blume-Jensen, P., Hermanson, M., Ponten, E., Carlberg, M., and Ronnstrand, L. (1999). Phosphorylation of Shc by Src family kinases is necessary for stem cell factor receptor/c-kit mediated activation of the Ras/MAP kinase pathway and c-fos induction. *Oncogene* 18(40): 5546-5553.

Lev, S., Givol, D., and Yarden, Y. (1991). A specific combination of substrates is involved in signal transduction by the kit-encoded receptor. *EMBO J.* 10(3): 647-654.

Lev, S., Givol, D., and Yarden, Y. (1992). Interkinase domain of kit contains the binding site for phosphatidylinositol 3' kinase. *Proc.Natl.Acad.Sci.U.S.A* 89(2): 678-682.

Lev, S., Yarden, Y., and Givol, D. (1990). Receptor functions and ligand-dependent transforming potential of a chimeric kit proto-oncogene. *Mol.Cell Biol.* 10(11): 6064-6068.

Li, X., Talts, U., Talts, J. F., Arman, E., Ekblom, P., and Lonai, P. (2001). Akt/PKB regulates laminin and collagen IV isotypes of the basement membrane. *Proc.Natl.Acad.Sci.U.S.A* 98(25): 14416-14421.

Lin, C. Q. and Bissell, M. J. (1993). Multi-faceted regulation of cell differentiation by extracellular matrix. *FASEB J.* 7(9): 737-743.

Link, R. E., Paus, R., Stenn, K. S., Kuklinska, E., and Moellmann, G. (1990). Epithelial growth by rat vibrissae follicles in vitro requires mesenchymal contact via native extracellular matrix. *J.Invest Dermatol.* 95(2): 202-207.

Logan, A. and Hill, D. J. (1992). Bioavailability: is this a key event in regulating the actions of peptide growth factors? *J.Endocrinol.* 134(2): 157-161.

Maines-Bandiera, S. L. and Auersperg, N. (1997). Increased E-cadherin expression in ovarian surface epithelium: an early step in metaplasia and dysplasia? *Int.J.Gynecol.Pathol.* 16(3): 250-255.

Manova, K., Huang, E. J., Angeles, M., De, Leon, V, Sanchez, S., Pronovost, S. M., Besmer, P., and Bachvarova, R. F. (1993). The expression pattern of the c-kit ligand in gonads of mice supports a role for the c-kit receptor in oocyte growth and in proliferation of spermatogonia. *Dev.Biol.* 157(1): 85-99.

Manova, K., Nocka, K., Besmer, P., and Bachvarova, R. F. (1990). Gonadal expression of c-kit encoded at the W locus of the mouse. *Development* 110(4): 1057-1069.

Matei, D., Chang, D. D., and Jeng, M. H. (2004). Imatinib mesylate (Gleevec) inhibits ovarian cancer cell growth through a mechanism dependent on platelet-derived growth factor receptor alpha and Akt inactivation. *Clin.Cancer Res.* 10(2): 681-690.

Matsuda, R., Takahashi, T., Nakamura, S., Sekido, Y., Nishida, K., Seto, M., Seito, T., Sugiura, T., Ariyoshi, Y., and Takahashi, T. (1993). Expression of the c-kit protein in human solid tumors and in corresponding fetal and adult normal tissues. *Am.J.Pathol.* 142(1): 339-346.

Matsui, Y., Toksoz, D., Nishikawa, S., Nishikawa, S., Williams, D., Zsebo, K., and Hogan, B. L. (1991). Effect of Steel factor and leukaemia inhibitory factor on murine primordial germ cells in culture. *Nature* 353(6346): 750-752.

Matsushima, T., Fukuda, Y., Tsukada, K., and Yamanaka, N. (1996). The extracellular matrices and vascularization of the developing corpus luteum in rats. *J.Submicrosc.Cytol.Pathol.* 28(4): 441-455.

Matzuk, M. M., Finegold, M. J., Su, J. G., Hsueh, A. J., and Bradley, A. (1992). Alpha-inhibin is a tumour-suppressor gene with gonadal specificity in mice. *Nature* 360(6402): 313-319.

Metcalf, D. and Nicola, N. A. (1991). Direct proliferative actions of stem cell factor on murine bone marrow cells in vitro: effects of combination with colony-stimulating factors. *Proc.Natl.Acad.Sci.U.S.A* 88(14): 6239-6243.

Mirmonsef, P., Shelburne, C. P., Fitzhugh, Yeatman C., Chong, H. J., and Ryan, J. J. (1999). Inhibition of Kit expression by IL-4 and IL-10 in murine mast cells: role of STAT6 and phosphatidylinositol 3'-kinase. *J.Immunol.* 163(5): 2530-2539.

Moore, K. L. (1992). The pelvis and perineum. In: Satterfield, T. S., Napora, L, and Lumpkin, K. (eds.), Clinically oriented anatomy. Baltimore: Williams & Williams, pp. 281-289.

Murdoch, W. J. (1996). Ovarian surface epithelium, ovulation and carcinogenesis. *Biol.Rev.Camb.Philos.Soc.* 71(4): 529-543.

Murdoch, W. J., Townsend, R. S., and McDonnel, A. C. (2001). Ovulation-induced DNA damage in ovarian surface epithelial cells of ewes: prospective regulatory mechanisms of repair/survival and apoptosis. *Biol.Reprod.* 65(5): 1417-1424.

Nagai, R., Tanaka, N., Fukumatsu, Y., Katabuchi, H., and Okamura, H. (1998). Spatio-temporal changes of prolyl 4-hydroxylase in granulosa cells during ovulation in eCG-hCG-treated immature rat ovaries. *J.Reprod.Fertil.* 113(2): 349-354.

Naora, H., Montz, F. J., Chai, C. Y., and Roden, R. B. (2001). Aberrant expression of homeobox gene HOXA7 is associated with mullerian-like differentiation of epithelial ovarian tumors and the generation of a specific autologous antibody response. *Proc.Natl.Acad.Sci.U.S.A* 98(26): 15209-15214.

Narod, S. A., Sun, P., Ghadirian, P., Lynch, H., Isaacs, C., Garber, J., Weber, B., Karlan, B., Fishman, D., Rosen, B., Tung, N., and Neuhausen, S. L. (2001). Tubal ligation and risk of ovarian cancer in carriers of BRCA1 or BRCA2 mutations: a case-control study. *Lancet* 357(9267): 1467-1470.

National Cancer Institute of Canada: Canadian Cancer Statistics (2004) Toronto, Canada.

Neta, R., Oppenheim, J. J., Wang, J. M., Snapper, C. M., Moorman, M. A., and Dubois, C. M. (1994). Synergy of IL-1 and stem cell factor in radioprotection of mice is associated with IL-1 up-regulation of mRNA and protein expression for c-kit on bone marrow cells. *J.Immunol.* 153(4): 1536-1543.

Nicosia, S. V. (1987). The aging ovary. *Med.Clin.North Am.* 71(1): 1-9.

Nicosia, S. V., Saunders, B. O., Acevedo-Duncan, M. E., Setrakian, S., and Degregorio, R. (2004). Biopathology of ovarian mesothelium. In: Familiari, S. M. and Motta, P. M. (eds.), Ultrastructure of the Ovary. Boston, MA: Kluwer Academic Publishers, pp. 287-310.

Nilson, J. H., Abbud, R. A., Keri, R. A., and Quirk, C. C. (2000). Chronic hypersecretion of luteinizing hormone in transgenic mice disrupts both ovarian and pituitary function, with some effects modified by the genetic background. *Recent Prog.Horm.Res.* 55: 69-89.

Obermair, A., Jirecek, S., and Leodolter, S. (1998). [Epidemiologic considerations on the significance of hormones in carcinogenesis]. *Gynakol.Geburtshilfliche Rundsch.* 38(2): 73-79.

Ogawa, K., Takeda, Y., Tashima, M., Sawai, H., Toi, T., Okazaki, T., Sawada, H., Maruyama, Y., and Okuma, M. (1995). High expression of c-kit in K562YO cells due to the prolonged half-life of its mRNA: the effects of modification with serine/threonine kinase signals. *Blood* 85(6): 1496-1503.

Ong, A., Maines-Bandiera, S. L., Roskelley, C. D., and Auersperg, N. (2000). An ovarian adenocarcinoma line derived from SV40/E-cadherin-transfected normal human ovarian surface epithelium. *Int.J.Cancer* 85(3): 430-437.

Osterholzer, H. O., Johnson, J. H., and Nicosia, S. V. (1985). An autoradiographic study of rabbit ovarian surface epithelium before and after ovulation. *Biol.Reprod.* 33(3): 729-738.

Papadaki, L. and Beilby, J. O. (1971). The fine structure of the surface epithelium of the human ovary. *J.Cell Sci.* 8(2): 445-465.

Papadimitriou, C. A., Topp, M. S., Serve, H., Oelmann, E., Koenigsmann, M., Maurer, J., Oberberg, D., Reufi, B., Thiel, E., and Berdel, W. E. (1995). Recombinant human stem cell factor does exert minor stimulation of growth in small cell lung cancer and melanoma cell lines. *Eur.J.Cancer* 31A(13-14): 2371-2378.

Parrott, J. A., Doraiswamy, V., Kim, G., Mosher, R., and Skinner, M. K. (2001). Expression and actions of both the follicle stimulating hormone receptor and the luteinizing hormone receptor in normal ovarian surface epithelium and ovarian cancer. *Mol.Cell Endocrinol.* 172(1-2): 213-222.

Parrott, J. A., Kim, G., Mosher, R., and Skinner, M. K. (2000a). Expression and action of keratinocyte growth factor (KGF) in normal ovarian surface epithelium and ovarian cancer. *Mol.Cell Endocrinol.* 167(1-2): 77-87.

Parrott, J. A., Kim, G., and Skinner, M. K. (2000b). Expression and action of kit ligand/stem cell factor in normal human and bovine ovarian surface epithelium and ovarian cancer. *Biol.Reprod.* 62(6): 1600-1609.

Parrott, J. A. and Skinner, M. K. (2000). Expression and action of hepatocyte growth factor in human and bovine normal ovarian surface epithelium and ovarian cancer. *Biol.Reprod.* 62(3): 491-500.

Paulson, R. F., Vesely, S., Siminovitch, K. A., and Bernstein, A. (1996). Signalling by the W/Kit receptor tyrosine kinase is negatively regulated in vivo by the protein tyrosine phosphatase Shp1. *Nat.Genet.* 13(3): 309-315.

Prevost, M. (1999). The role of steroid hormones and growth factors on rat ovarian surface epithelial cells. *MSc.Thesis, University of Ottawa* :

Pupa, S. M., Menard, S., Forti, S., and Tagliabue, E. (2002). New insights into the role of extracellular matrix during tumor onset and progression. *J.Cell Physiol* 192(3): 259-267.

Quirk, S. M., Cowan, R. G., and Huber, S. H. (1997). Fas antigen-mediated apoptosis of ovarian surface epithelial cells. *Endocrinology* 138(11): 4558-4566.

Radford, I. R. (2002). Imatinib. Novartis. *Curr.Opin.Investig.Drugs* 3(3): 492-499.

Reith, A. D., Ellis, C., Lyman, S. D., Anderson, D. M., Williams, D. E., Bernstein, A., and Pawson, T. (1991). Signal transduction by normal isoforms and W mutant variants of the Kit receptor tyrosine kinase. *EMBO J.* 10(9): 2451-2459.

Reynaud, K., Cortvrindt, R., Smitz, J., and Driancourt, M. A. (2000). Effects of Kit Ligand and anti-Kit antibody on growth of cultured mouse preantral follicles. *Mol.Reprod.Dev.* 56(4): 483-494.

Roby, K. F., Taylor, C. C., Sweetwood, J. P., Cheng, Y., Pace, J. L., Tawfik, O., Persons, D. L., Smith, P. G., and Terranova, P. F. (2000). Development of a syngeneic mouse model for events related to ovarian cancer. *Carcinogenesis* 21(4): 585-591.

Rodgers, R. J. and Irving Rodgers, H. F. (2002). Extracellular matrix of the bovine ovarian membrana granulosa. *Mol.Cell Endocrinol.* 191(1): 57-64.

Rodgers, R. J., Irving-Rodgers, H. F., and Russell, D. L. (2003). Extracellular matrix of the developing ovarian follicle. *Reproduction.* 126(4): 415-424.

Rodgers, R. J., van, Wezel, I, Irving-Rodgers, H. F., Lavranos, T. C., Irvine, C. M., and Krupa, M. (1999). Roles of extracellular matrix in follicular development. *J.Reprod.Fertil.Suppl* 54: 343-352.

Rodriguez, G. C., Berchuck, A., Whitaker, R. S., Schlossman, D., Clarke-Pearson, D. L., and Bast, R. C. Jr (1991). Epidermal growth factor receptor expression in normal ovarian epithelium and ovarian cancer. II. Relationship between receptor expression and response to epidermal growth factor. *Am.J.Obstet.Gynecol.* 164(3): 745-750.

Rusten, L. S., Smeland, E. B., Jacobsen, F. W., Lien, E., Lesslauer, W., Loetscher, H., Dubois, C. M., and Jacobsen, S. E. (1994). Tumor necrosis factor-alpha inhibits stem cell factor-induced proliferation of human bone marrow progenitor cells in vitro. Role of p55 and p75 tumor necrosis factor receptors. *J.Clin.Invest* 94(1): 165-172.

Salazar, H., Godwin, A. K., Daly, M. B., Laub, P. B., Hogan, W. M., Rosenblum, N., Boente, M. P., Lynch, H. T., and Hamilton, T. C. (1996). Microscopic benign and invasive malignant neoplasms and a cancer-prone phenotype in prophylactic oophorectomies [see comments]. *J.Natl.Cancer Inst.* 88(24): 1810-1820.

Schuetz, A. W. and Lessman, C. (1982). Evidence for follicle wall involvement in ovulation and progesterone production by frog (Rana pipiens) follicles in vitro. *Differentiation* 22(2): 79-84.

Schwartz, M. A. and Ginsberg, M. H. (2002). Networks and crosstalk: integrin signalling spreads. *Nat.Cell Biol.* 4(4): E65-E68.

Shattil, S. J. and Newman, P. J. (2004). Integrins: dynamic scaffolds for adhesion and signaling in platelets. *Blood* 104(6): 1606-1615.

Shaw, T. J., Keszthelyi, E. J., Tonary, A. M., Cada, M., and Vanderhyden, B. C. (2002). Cyclic AMP in ovarian cancer cells both inhibits proliferation and increases c-KIT expression. *Exp Cell Res.* 273(1): 95-106.

Shaw, T. J. and Vanderhyden, B. C. (submitted 2005). Gleevec decreases proliferation and survival of ovarian cancer cell lines in vitro but does not improve the outcome of xenograft models.

Shinomura, Y. (2000). Expression of c-kit in gastrointestinal stromal tumors. *Intern.Med.* 39(11): 869-870.

Siemens, C. H. and Auersperg, N. (1988). Serial propagation of human ovarian surface epithelium in tissue culture. *J.Cell Physiol.* 134(3): 347-356.

Silvester, L. M. and Luck, M. R. (1999). Distribution of extracellular matrix components in the developing ruminant corpus luteum: a wound repair hypothesis for luteinization. *J.Reprod.Fertil.* 116(1): 187-198.

Singer, G., Schraml, P., Belgard, C., Raggi, A., Dirnhofer, S., Went, P., Mihatsch, M. J., and Moch, H. (2003). KIT in ovarian carcinoma: disillusion about a potential therapeutic target. *J.Natl.Cancer Inst.* 95(13): 1009-1010.

Smith, M. F., Ricke, W. A., Bakke, L. J., Dow, M. P., and Smith, G. W. (2002). Ovarian tissue remodeling: role of matrix metalloproteinases and their inhibitors. *Mol.Cell Endocrinol.* 191(1): 45-56.

Sottile, J. and Hocking, D. C. (2002). Fibronectin polymerization regulates the composition and stability of extracellular matrix fibrils and cell-matrix adhesions. *Mol.Biol.Cell* 13(10): 3546-3559.

Sundfeldt, K., Piontkewitz, Y., Ivarsson, K., Nilsson, O., Hellberg, P., Brannstrom, M., Janson, P. O., Enerback, S., and Hedin, L. (1997). E-cadherin expression in human epithelial ovarian cancer and normal ovary. *Int.J.Cancer* 74(3): 275-280.

Tajima, Y., Onoue, H., Kitamura, Y., and Nishimune, Y. (1991). Biologically active kit ligand growth factor is produced by mouse Sertoli cells and is defective in SId mutant mice. *Development* 113(3): 1031-1035.

Takahashi, H., Behbakht, K., McGovern, P. E., Chiu, H. C., Couch, F. J., Weber, B. L., Friedman, L. S., King, M. C., Furusato, M., and LiVolsi, V. A. (1995). Mutation analysis of the BRCA1 gene in ovarian cancers. *Cancer Res.* 55(14): 2998-3002.

Tamborini, E., Bonadiman, L., Greco, A., Albertini, V., Negri, T., Gronchi, A., Bertulli, R., Colecchia, M., Casali, P. G., Pierotti, M. A., and Pilotti, S. (2004). A new mutation in the KIT ATP pocket causes acquired resistance to imatinib in a gastrointestinal stromal tumor patient. *Gastroenterology* 127(1): 294-299.

Teneriello, M. G. and Park, R. C. (1995). Early detection of ovarian cancer. *CA Cancer J.Clin.* 45(2): 71-87.

Testa, J. R., Getts, L. A., Salazar, H., Liu, Z., Handel, L. M., Godwin, A. K., and Hamilton, T. C. (1994). Spontaneous transformation of rat ovarian surface epithelial cells results in well to poorly differentiated tumors with a parallel range of cytogenetic complexity. *Cancer Res.* 54(10): 2778-2784.

Thomas, F. H., Ethier, J. F., Shimasaki, S., and Vanderhyden, B. C. (2004). Follicle-Stimulating Hormone regulates oocyte growth by modulation of expression of oocyte and granulosa cell factors. *Endocrinology* :

Tomeczkowski, J., Frick, D., Schwinzer, B., Wittner, N., Ludwig, W. D., Reiter, A., Welte, K., and Sykora, K. W. (1998). Expression and regulation of c-kit receptor and response to stem cell factor in childhood malignant T-lymphoblastic cells. *Leukemia* 12(8): 1221-1229.

Tonary, A. M., Macdonald, E. A., Faught, W., Senterman, M. K., and Vanderhyden, B. C. (2000). Lack of expression of c-KIT in ovarian cancers is associated with poor prognosis. *Int.J.Cancer* 89(3): 242-250.

Tsai, M., Takeishi, T., Thompson, H., Langley, K. E., Zsebo, K. M., Metcalfe, D. D., Geissler, E. N., and Galli, S. J. (1991). Induction of mast cell proliferation, maturation, and heparin synthesis by the rat c-kit ligand, stem cell factor. *Proc.Natl.Acad.Sci.U.S.A* 88(14): 6382-6386.

Turner, A. M., Bennett, L. G., Lin, N. L., Wypych, J., Bartley, T. D., Hunt, R. W., Atkins, H. L., Langley, K. E., Parker, V., and Martin, F. (1995). Identification and characterization of a soluble c-kit receptor produced by human hematopoietic cell lines. *Blood* 85(8): 2052-2058.

Vandenbark, G. R., deCastro, C. M., Taylor, H., Dew-Knight, S., and Kaufman, R. E. (1992). Cloning and structural analysis of the human c-kit gene. *Oncogene* 7(7): 1259-1266.

Vessey, M. P. and Painter, R. (1995). Endometrial and ovarian cancer and oral contraceptives--findings in a large cohort study. *Br.J.Cancer* 71(6): 1340-1342.

Wang, C., Curtis, J. E., Geissler, E. N., McCulloch, E. A., and Minden, M. D. (1989). The expression of the proto-oncogene C-kit in the blast cells of acute myeloblastic leukemia. *Leukemia* 3(10): 699-702.

Weiss, N. S., Homonchuk, T., and Young, J. L., Jr. (1977). Incidence of the histologic types of ovarian cancer: the U.S. Third National Cancer Survey, 1969-1971. *Gynecol.Oncol.* 5(2): 161-167.

Wong, A. S., Maines-Bandiera, S. L., Rosen, B., Wheelock, M. J., Johnson, K. R., Leung, P. C., Roskelley, C. D., and Auersperg, N. (1999). Constitutive and conditional cadherin expression in cultured human ovarian surface epithelium: influence of family history of ovarian cancer. *Int.J.Cancer* 81(2): 180-188.

Xiong, J. P., Stehle, T., Zhang, R., Joachimiak, A., Frech, M., Goodman, S. L., and Arnaout, M. A. (2002). Crystal structure of the extracellular segment of integrin alpha Vbeta3 in complex with an Arg-Gly-Asp ligand. *Science* 296(5565): 151-155.

Yarden, Y., Kuang, W. J., Yang-Feng, T., Coussens, L., Munemitsu, S., Dull, T. J., Chen, E., Schlessinger, J., Francke, U., and Ullrich, A. (1987). Human proto-oncogene c-kit: a new cell surface receptor tyrosine kinase for an unidentified ligand. *EMBO J.* 6(11): 3341-3351.

Yarden, Y. and Ullrich, A. (1988). Molecular analysis of signal transduction by growth factors. *Biochemistry* 27(9): 3113-3119.

Young, R. H., Clement, P. B., and Scully, R. E. (1989). In: Sternberg, S. S. (eds.), Diagnostic Surgical Pathology. New York: Raven Press, pp. 165-173.

Yurchenco, P. D. and Schittny, J. C. (1990). Molecular architecture of basement membranes. *FASEB J.* 4(6): 1577-1590.